

Scientific challenges expected from future balloon-borne experiments

P. de Bernardis

Sapienza Università di Roma - Italy

From Planck to the future of CMB

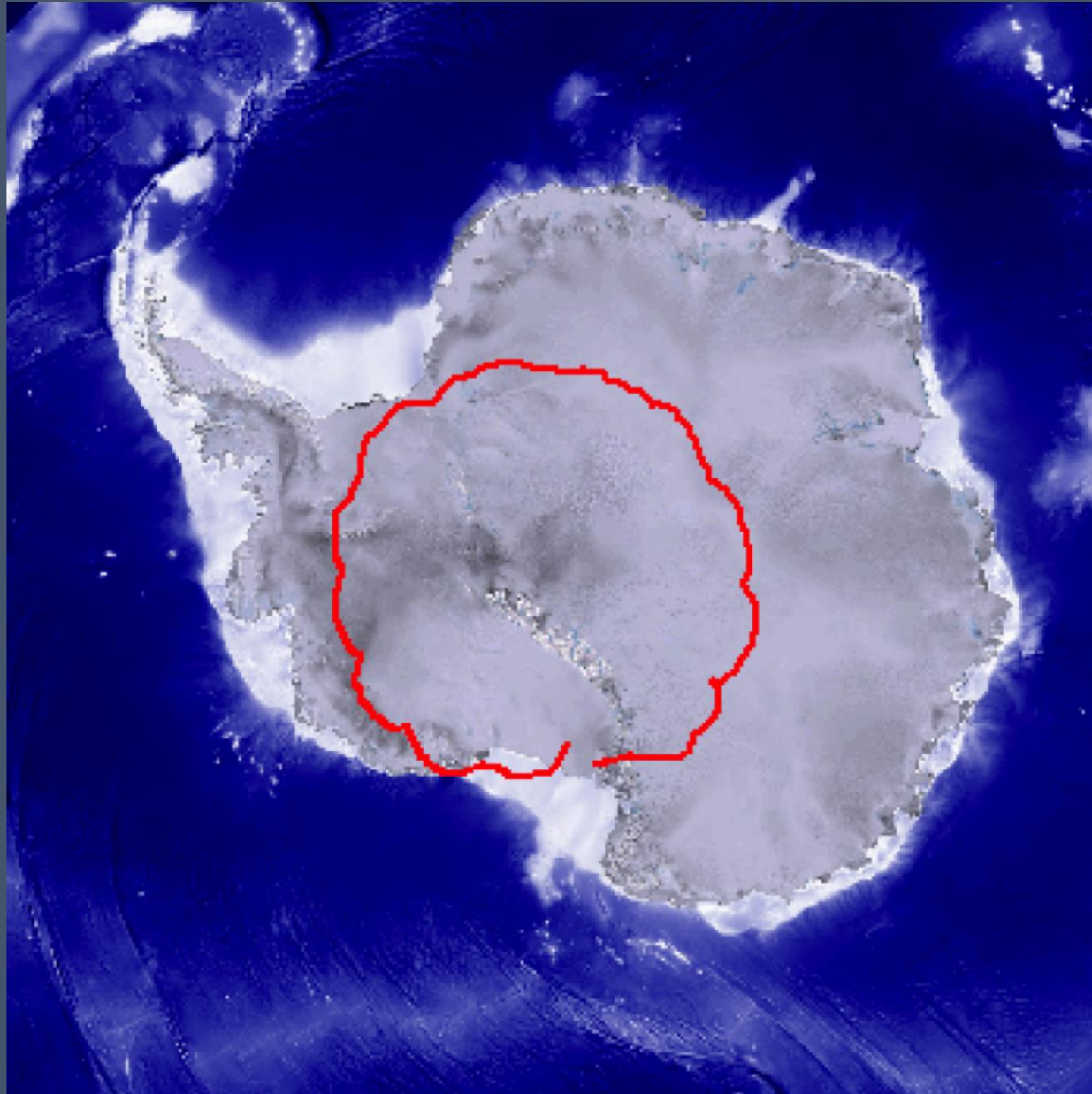
Ferrara - June 23rd, 2022



Stratospheric Balloons:



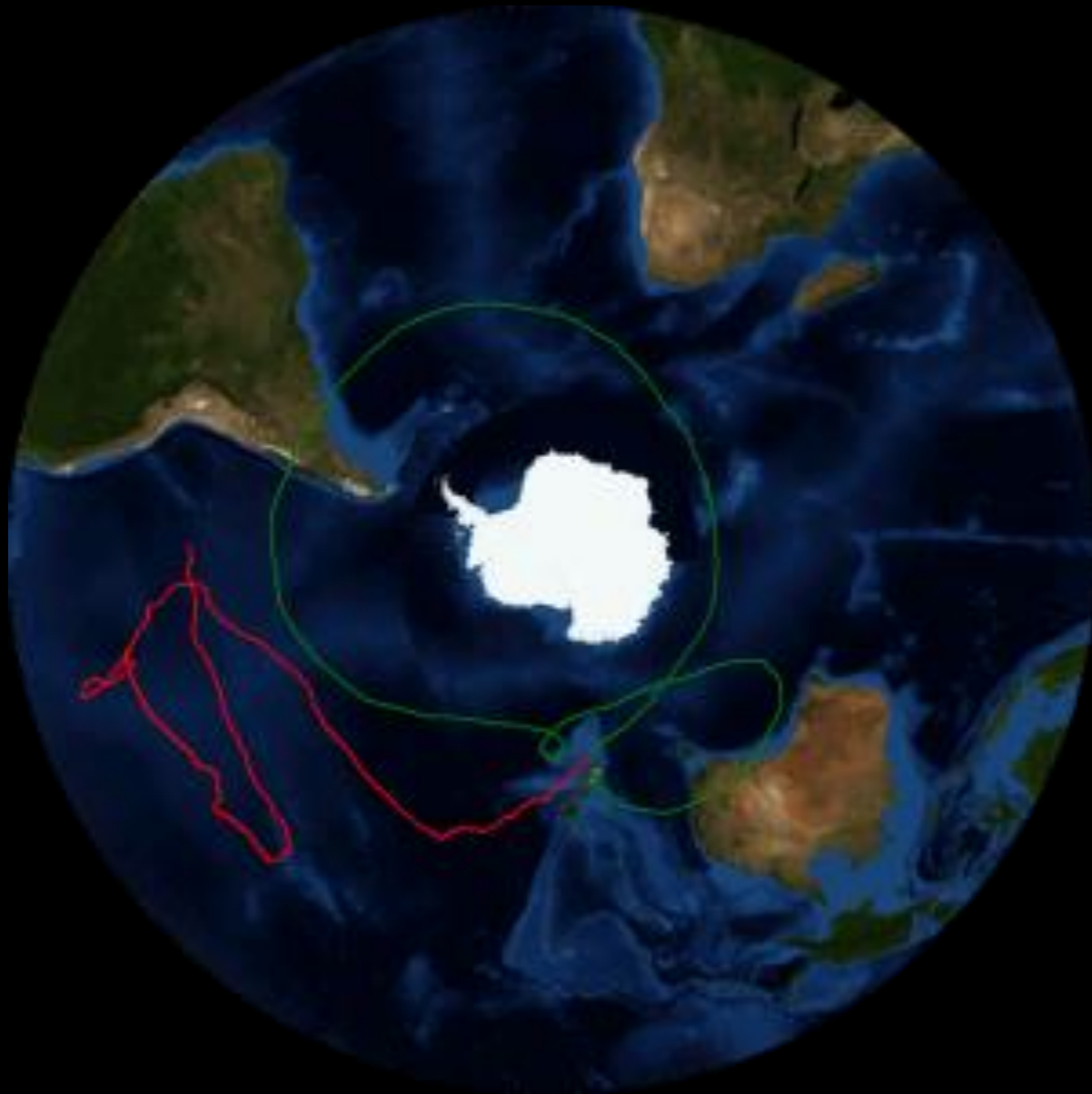
- Near-space carriers able to:
 - Reach ~ 40 km (~ 3 mbar)
 - Stay there for up to 40 days (LDB) and more (ULDB)
 - Lift heavy (2 tons) large payloads (even larger than what we can reasonably fly on satellites)
 - Cost roughly 1/100 of a satellite mission
 - Allow for recovery and reflly of the payload
- Important for the CMB community:
 - To carry out sensitive observations at
 - high frequency,
 - high resolution,
 - at the largest angular scales
 - To qualify instrumentation in preparation of satellite missions
 - To educate young experimentalists !



Long-duration circumpolar flights
(2-4 weeks) for 1-2 tons
payloads at 38-40 km
altitude

NASA-CSBF :
well established
launch facility
near McMurdo, Antarctica

Typical ground-path of a LDB summer flight

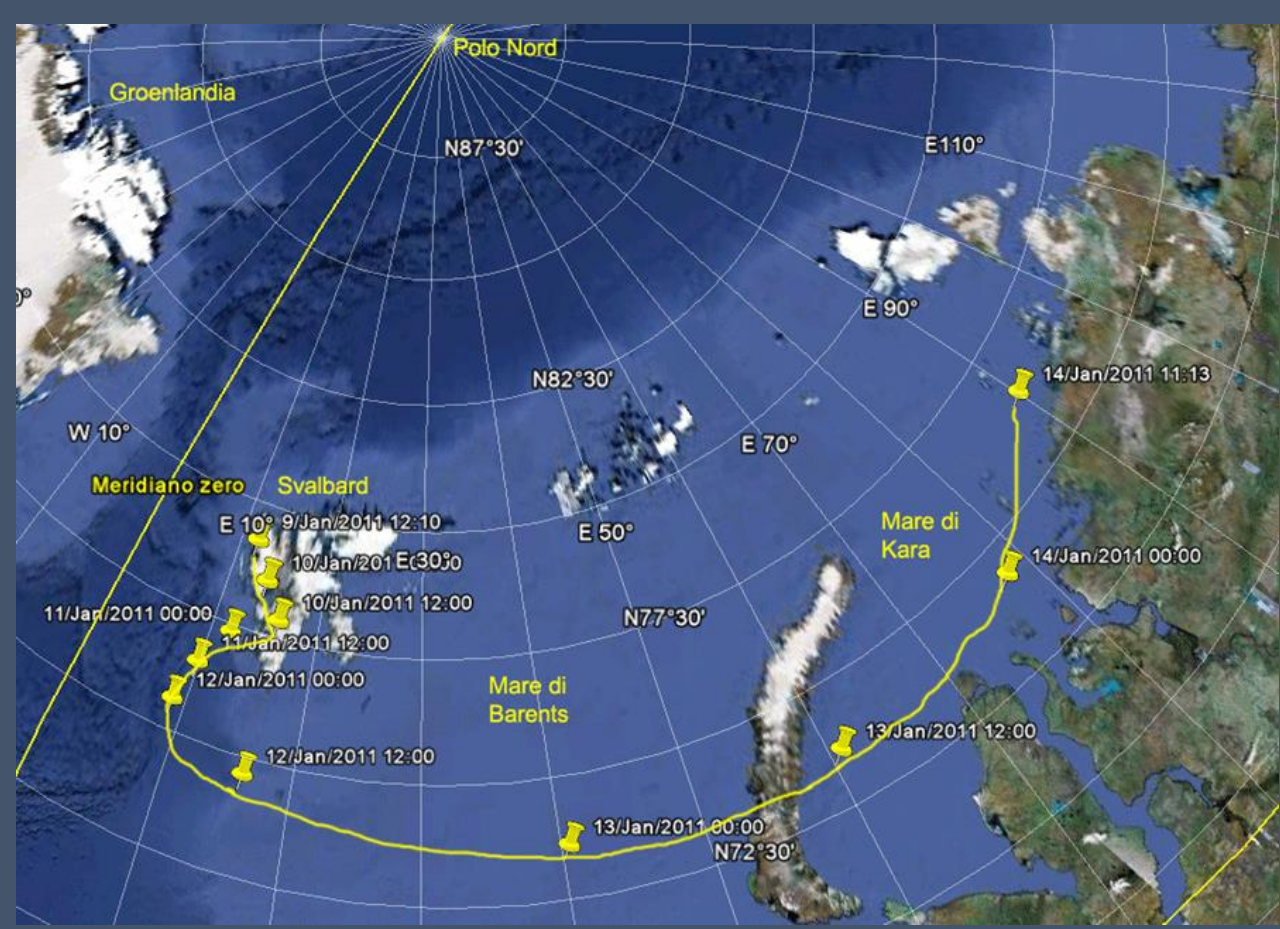


Great progress with super-pressure balloons: COSI payload flown by CSBF in may 2016 for 47 days at altitudes between 33 km and 21 km, with a with a 0.5Mm^3 SPB

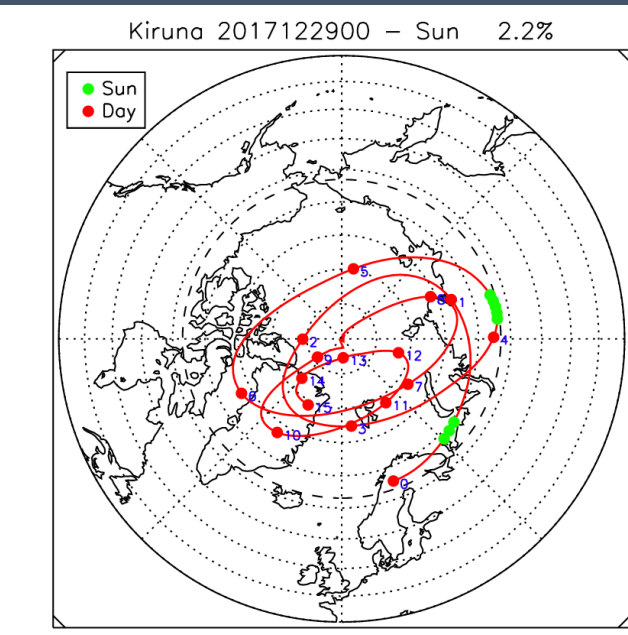
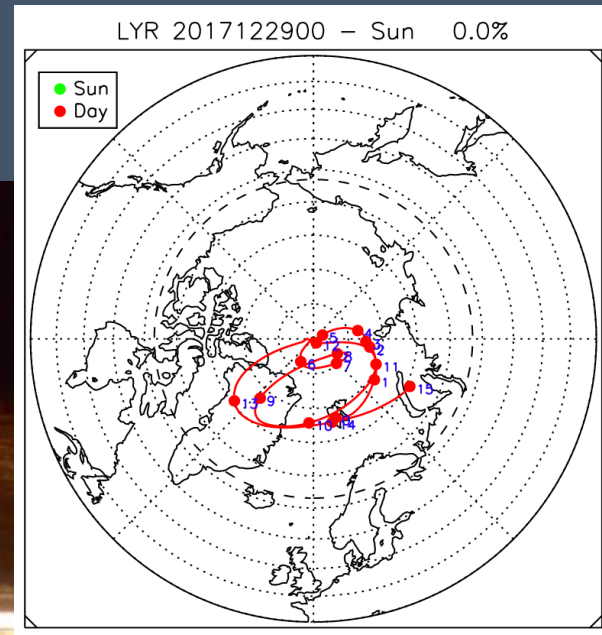
ULDB: 30-100 days, 1 ton

<https://blogs.nasa.gov/superpressureballoon/>

Polar Night Flights



10-20 days winter flights in the Arctic, in total darkness

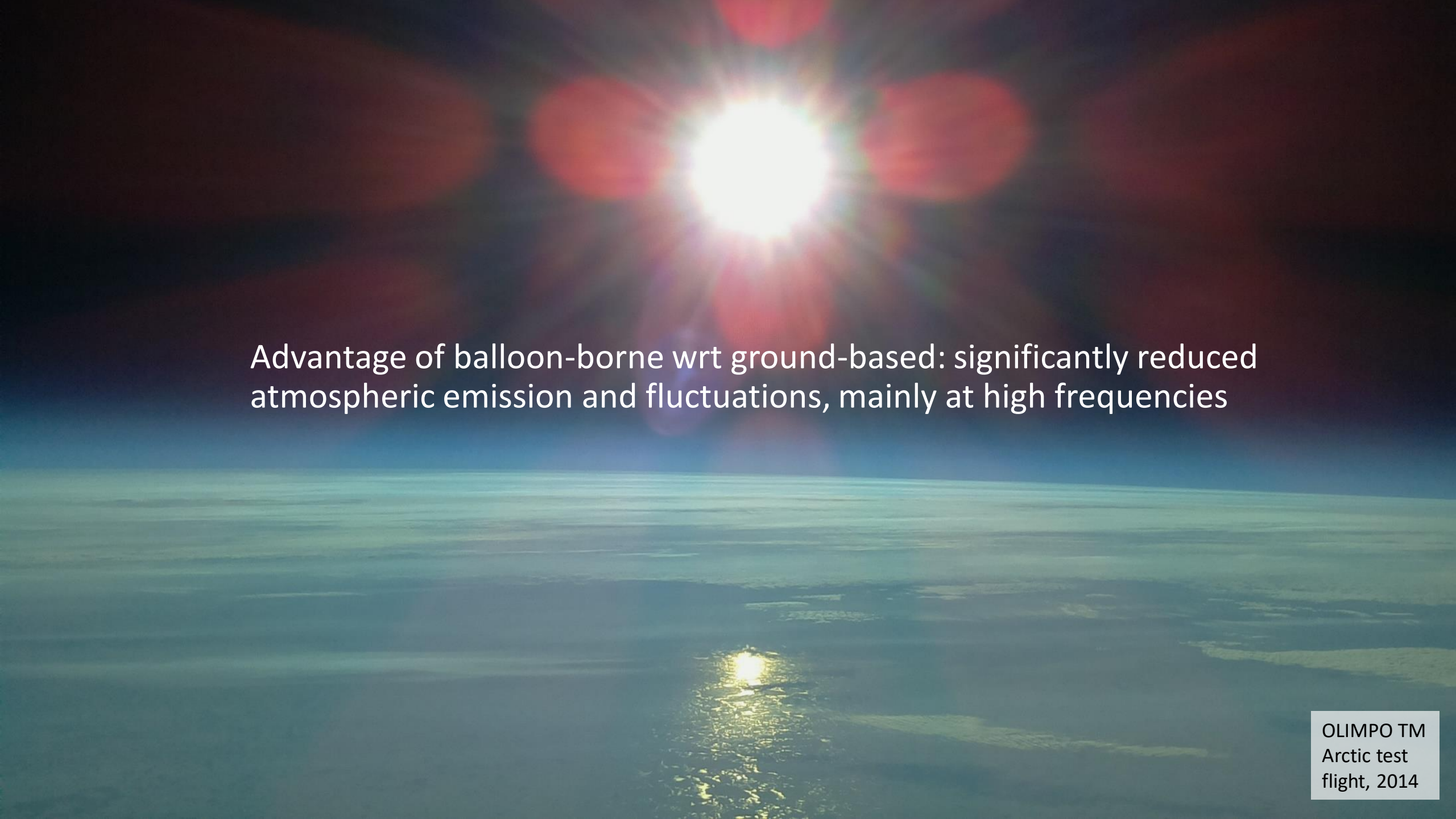


Stratospheric Balloons:



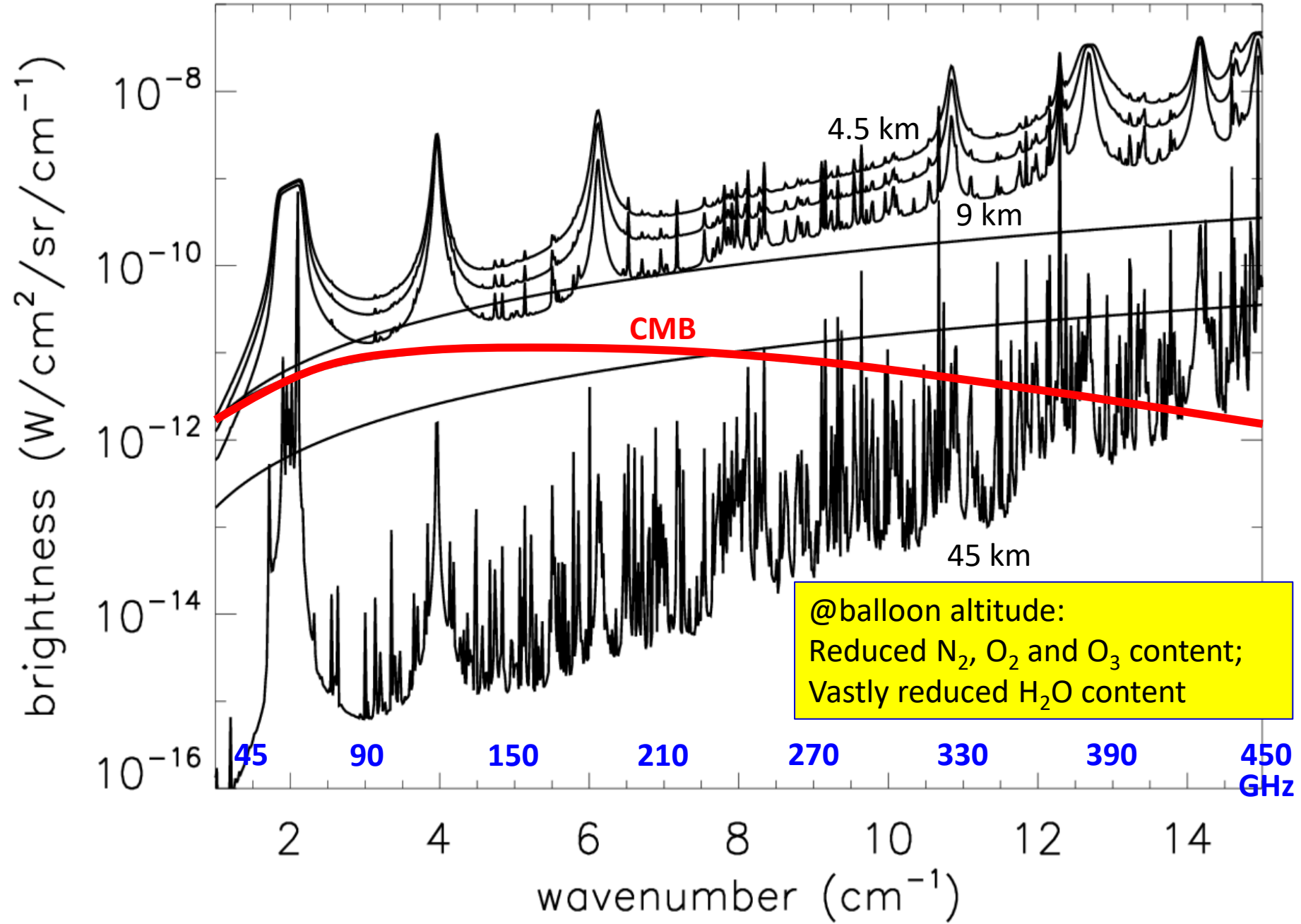
Disadvantages:

- Stringent limits on mass, power
- Complexity of automation
- Insane integration schedule
- Narrow, and scarce, flight windows: expect many failed launch attempts
- Risky recovery

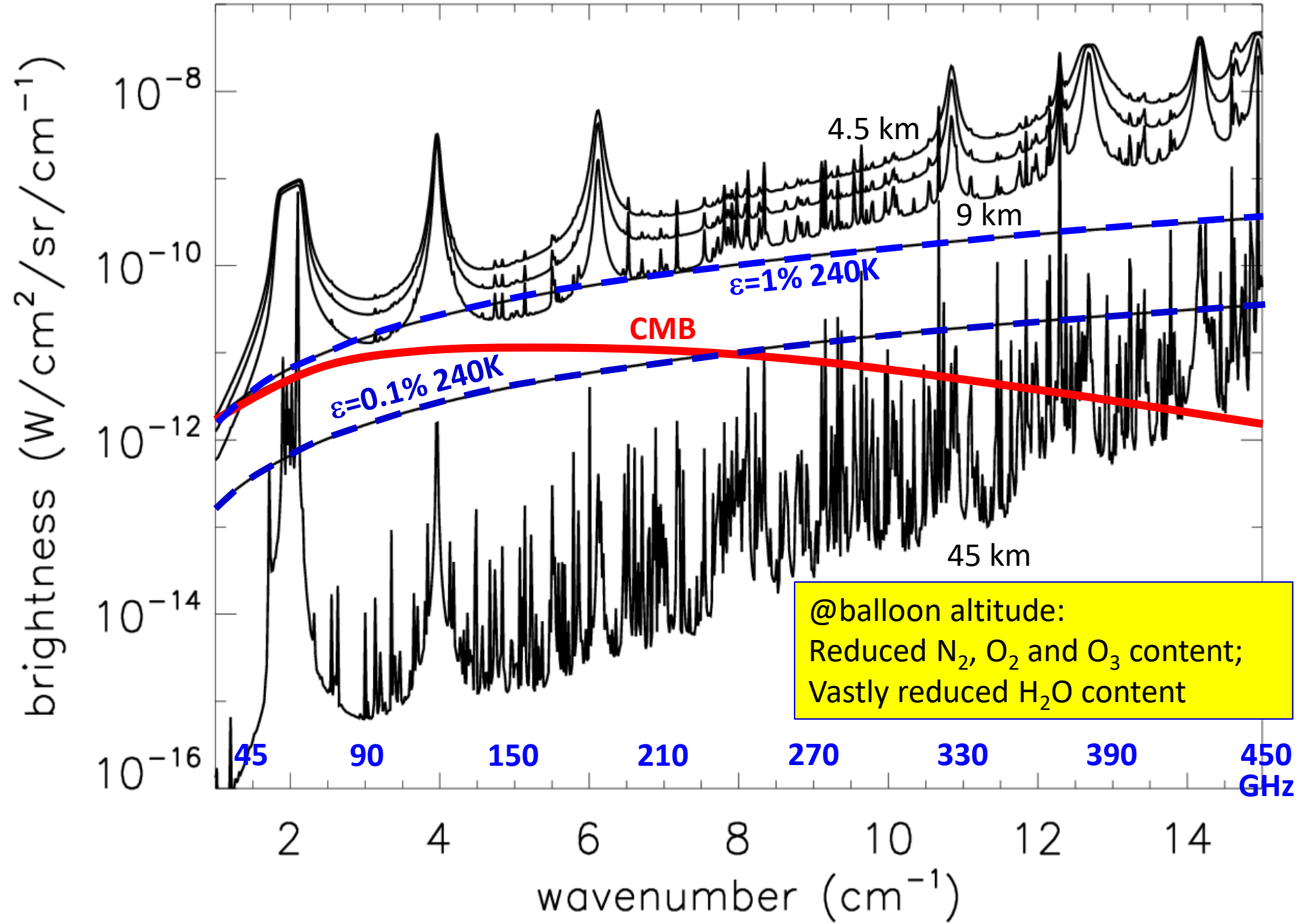


Advantage of balloon-borne wrt ground-based: significantly reduced atmospheric emission and fluctuations, mainly at high frequencies

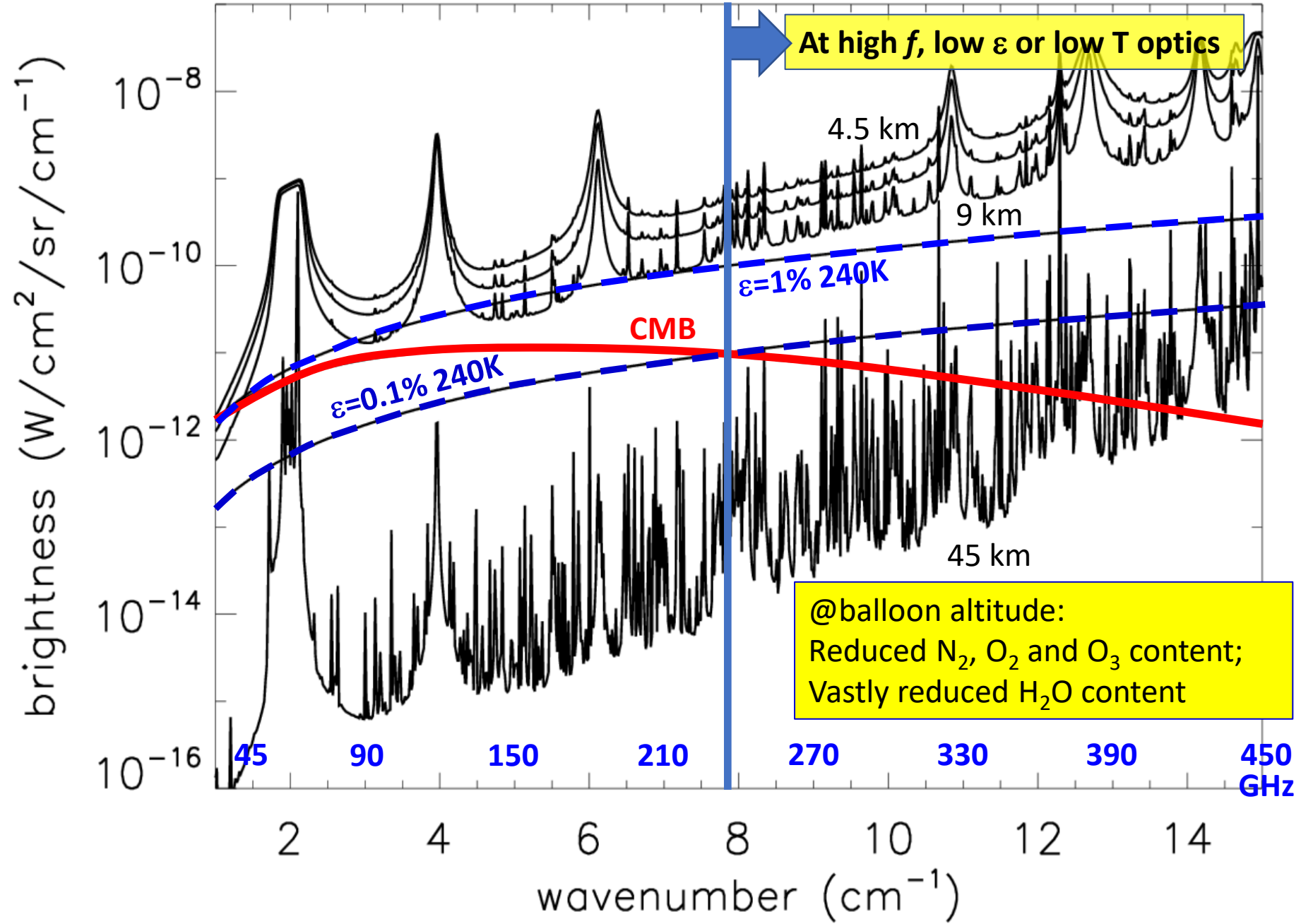
Atmospheric Emission at different altitudes



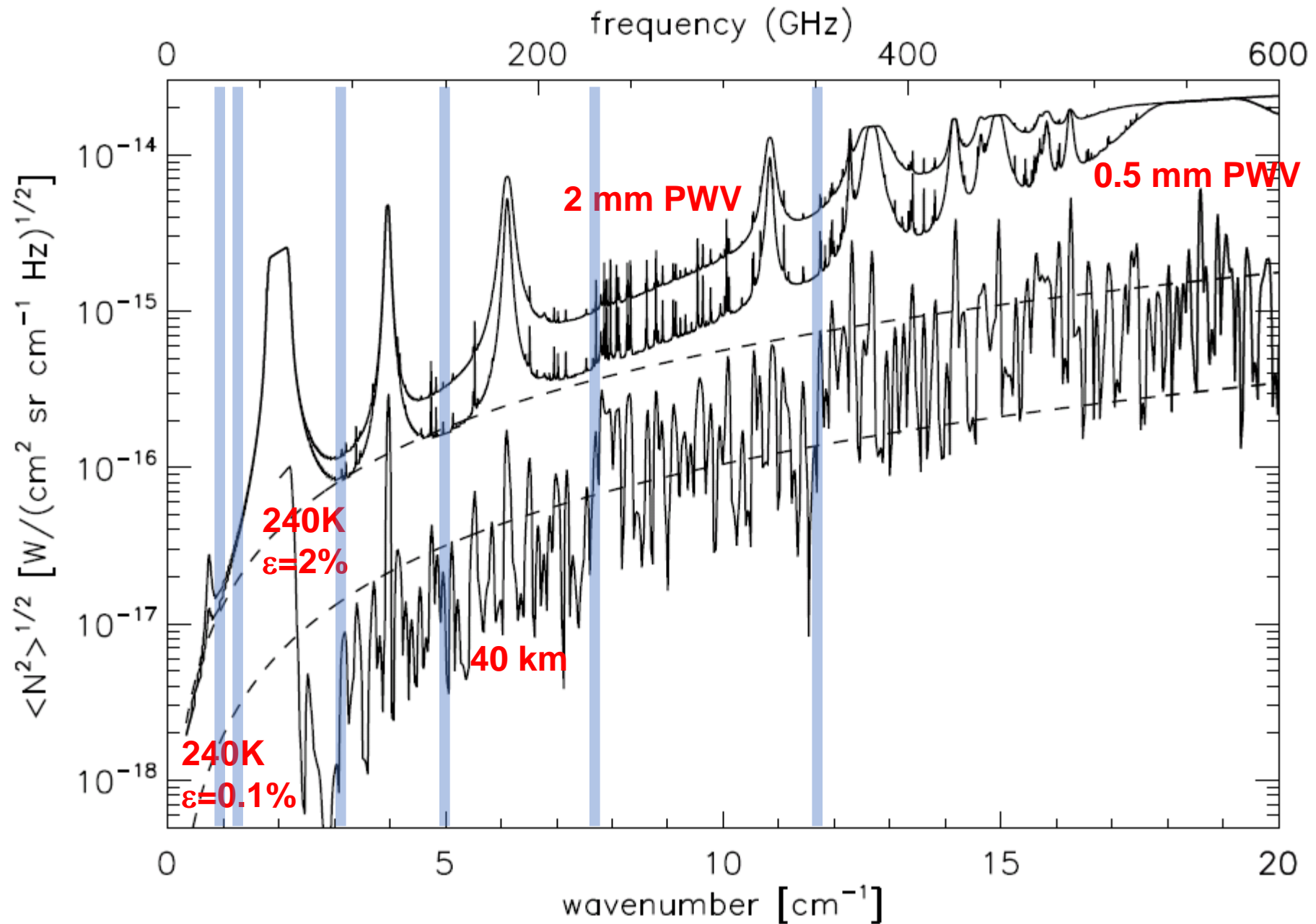
Atmospheric Emission at different altitudes



Atmospheric Emission at different altitudes



Photon noise from the local environment for CMB observations



@150 GHz : One day on a balloon ...

	GHz	GHz	BKG 4.5km e=0.01	BKG 6.0km e=0.01	BKG 9.0km e=0.01	BKG 45km e=0.001	Space,40K	CMB
0	34	45	2.63	2.14	1.57	0.57	0.53	0.52
1	82	105	5.58	4.39	3.12	0.80	0.70	0.68
2	132	168	8.35	5.95	4.03	0.75	0.59	0.55
3	187	253	26.39	17.08	10.28	0.78	0.47	0.41
4	229	310	39.81	25.70	15.33	0.74	0.33	0.25
5	336	364	27.28	15.65	7.66	0.22	0.05	0.03

pW

	GHz	GHz	NEP 4.5km e=0.01	NEP 6.0km e=0.01	NEP 9.0km e=0.01	NEP 45km e=0.001	Space,40K	CMB
0	34	45	1.06E-017	1.06E-017	7.49E-018	5.51E-018	5.29E-018	5.24E-018
1	82	105	2.57E-017	2.30E-017	1.99E-017	1.00E-017	9.35E-018	9.19E-018
2	132	168	4.10E-017	3.55E-017	2.90E-017	1.22E-017	1.08E-017	1.05E-017
3	187	253	8.78E-017	7.02E-017	5.55E-017	1.51E-017	1.17E-017	1.09E-017
4	229	310	1.20E-016	9.53E-017	7.53E-017	1.63E-017	1.08E-017	9.50E-018
5	336	364	1.13E-016	8.58E-017	5.86E-017	1.02E-017	4.90E-018	3.55E-018

W/\sqrt{Hz}

... is like >16 days at the best site
on the ground ...

@150 GHz : One day on a balloon ...

	GHz	GHz	BKG 4.5km e=0.01	BKG 6.0km e=0.01	BKG 9.0km e=0.01	BKG 45km e=0.001	Space,40K	CMB
0	34	45	2.63	2.14	1.57	0.57	0.53	0.52
1	82	105	5.58	4.39	3.12	0.80	0.70	0.68
2	132	168	8.35	5.95	4.03	0.75	0.59	0.55
3	187	253	26.39	17.08	10.28	0.78	0.47	0.41
4	229	310	39.81	25.70	15.33	0.74	0.33	0.25
5	336	364	27.28	15.65	7.66	0.22	0.05	0.03

pW

	GHz	GHz	NEP 4.5km e=0.01	NEP 6.0km e=0.01	NEP 9.0km e=0.01	NEP 45km e=0.001	Space,40K	CMB
0	34	45	1.06E-017	1.06E-017	7.49E-018	5.51E-018	5.29E-018	5.24E-018
1	82	105	2.57E-017	2.30E-017	1.99E-017	1.00E-017	9.35E-018	9.19E-018
2	132	168	4.10E-017	3.55E-017	2.90E-017	1.22E-017	1.08E-017	1.05E-017
3	187	253	8.78E-017	7.02E-017	5.55E-017	1.51E-017	1.17E-017	1.09E-017
4	229	310	1.20E-016	9.53E-017	7.53E-017	1.63E-017	1.08E-017	9.50E-018
5	336	364	1.13E-016	8.58E-017	5.86E-017	1.02E-017	4.90E-018	3.55E-018

W/\sqrt{Hz}

... is close to one day in deep space

@350 GHz : One day on a balloon ...

	GHz	GHz	BKG 4.5km e=0.01	BKG 6.0km e=0.01	BKG 9.0km e=0.01	BKG 45km e=0.001	Space,40K	CMB
0	34	45	2.63	2.14	1.57	0.57	0.53	0.52
1	82	105	5.58	4.39	3.12	0.80	0.70	0.68
2	132	168	8.35	5.95	4.03	0.75	0.59	0.55
3	187	253	26.39	17.08	10.28	0.78	0.47	0.41
4	229	310	39.81	25.70	15.33	0.74	0.33	0.25
5	336	364	27.28	15.65	7.66	0.22	0.05	0.03

pW

	GHz	GHz	NEP 4.5km e=0.01	NEP 6.0km e=0.01	NEP 9.0km e=0.01	NEP 45km e=0.001	Space,40K	CMB
0	34	45	1.06E-017	1.06E-017	7.49E-018	5.51E-018	5.29E-018	5.24E-018
1	82	105	2.57E-017	2.30E-017	1.99E-017	1.00E-017	9.35E-018	9.19E-018
2	132	168	4.10E-017	3.55E-017	2.90E-017	1.22E-017	1.08E-017	1.05E-017
3	187	253	8.78E-017	7.02E-017	5.55E-017	1.51E-017	1.17E-017	1.09E-017
4	229	310	1.20E-016	9.53E-017	7.53E-017	1.63E-017	1.08E-017	9.50E-018
5	336	364	1.13E-016	8.58E-017	5.86E-017	1.02E-017	4.90E-018	3.55E-018

W/\sqrt{Hz}

... is like >100 days at the best site on the ground ...

@350 GHz : One day on a balloon ...

	GHz	GHz	BKG 4.5km e=0.01	BKG 6.0km e=0.01	BKG 9.0km e=0.01	BKG 45km e=0.001	Space,40K	CMB
0	34	45	2.63	2.14	1.57	0.57	0.53	0.52
1	82	105	5.58	4.39	3.12	0.80	0.70	0.68
2	132	168	8.35	5.95	4.03	0.75	0.59	0.55
3	187	253	26.39	17.08	10.28	0.78	0.47	0.41
4	229	310	39.81	25.70	15.33	0.74	0.33	0.25
5	336	364	27.28	15.65	7.66	0.22	0.05	0.03

pW

	GHz	GHz	NEP 4.5km e=0.01	NEP 6.0km e=0.01	NEP 9.0km e=0.01	NEP 45km e=0.001	Space,40K	CMB
0	34	45	1.06E-017	1.06E-017	7.49E-018	5.51E-018	5.29E-018	5.24E-018
1	82	105	2.57E-017	2.30E-017	1.99E-017	1.00E-017	9.35E-018	9.19E-018
2	132	168	4.10E-017	3.55E-017	2.90E-017	1.22E-017	1.08E-017	1.05E-017
3	187	253	8.78E-017	7.02E-017	5.55E-017	1.51E-017	1.17E-017	1.09E-017
4	229	310	1.20E-016	9.53E-017	7.53E-017	1.63E-017	1.08E-017	9.50E-018
5	336	364	1.13E-016	8.58E-017	5.86E-017	1.02E-017	4.90E-018	3.55E-018

W/\sqrt{Hz}

... is like 0.25-0.1 days in deep space

@420 GHz : One day on a balloon ...

GHz	GHz	BKG 4.5km e=0.01	BKG 6.0km e=0.01	BKG 9.0km e=0.01	BKG 45km e=0.001	Space,40K	CMB
0	34 45	2.63	2.14	1.57	0.57	0.53	0.52
1	82 105	5.58	4.39	3.12	0.80	0.70	0.68
2	132 168	8.35	5.95	4.03	0.75	0.59	0.55
3	187 253	26.39	17.08	10.28	0.78	0.47	0.41
4	229 310	39.81	25.70	15.33	0.74	0.33	0.25
5	336 364	27.28	15.65	7.66	0.22	0.05	0.03
6	405 435	80.57	57.50	35.28	0.33	0.04	0.01

pW

GHz	GHz	NEP 4.5km e=0.01	NEP 6.0km e=0.01	NEP 9.0km e=0.01	NEP 45km e=0.001	Space,40K	CMB
0	34 45	1.06E-017	1.06E-017	7.49E-018	5.51E-018	5.29E-018	5.24E-018
1	82 105	2.57E-017	2.30E-017	1.99E-017	1.00E-017	9.35E-018	9.19E-018
2	132 168	4.10E-017	3.55E-017	2.90E-017	1.22E-017	1.08E-017	1.05E-017
3	187 253	8.78E-017	7.02E-017	5.55E-017	1.51E-017	1.17E-017	1.09E-017
4	229 310	1.20E-016	9.53E-017	7.53E-017	1.63E-017	1.08E-017	9.50E-018
5	336 364	1.13E-016	8.58E-017	5.86E-017	1.02E-017	4.90E-018	3.55E-018
6	405 435	2.11E-016	1.78E-016	1.39E-016	1.35E-017	4.44E-018	2.38E-018

W/\sqrt{Hz}

... is like >250 days at the best site on the ground ...

@420 GHz : One day on a balloon ...

GHz	GHz	BKG 4.5km e=0.01	BKG 6.0km e=0.01	BKG 9.0km e=0.01	BKG 45km e=0.001	Space,40K	CMB
0	34 45	2.63	2.14	1.57	0.57	0.53	0.52
1	82 105	5.58	4.39	3.12	0.80	0.70	0.68
2	132 168	8.35	5.95	4.03	0.75	0.59	0.55
3	187 253	26.39	17.08	10.28	0.78	0.47	0.41
4	229 310	39.81	25.70	15.33	0.74	0.33	0.25
5	336 364	27.28	15.65	7.66	0.22	0.05	0.03
6	405 435	80.57	57.50	35.28	0.33	0.04	0.01

pW

GHz	GHz	NEP 4.5km e=0.01	NEP 6.0km e=0.01	NEP 9.0km e=0.01	NEP 45km e=0.001	Space,40K	CMB
0	34 45	1.06E-017	1.06E-017	7.49E-018	5.51E-018	5.29E-018	5.24E-018
1	82 105	2.57E-017	2.30E-017	1.99E-017	1.00E-017	9.35E-018	9.19E-018
2	132 168	4.10E-017	3.55E-017	2.90E-017	1.22E-017	1.08E-017	1.05E-017
3	187 253	8.78E-017	7.02E-017	5.55E-017	1.51E-017	1.17E-017	1.09E-017
4	229 310	1.20E-016	9.53E-017	7.53E-017	1.63E-017	1.08E-017	9.50E-018
5	336 364	1.13E-016	8.58E-017	5.86E-017	1.02E-017	4.90E-018	3.55E-018
6	405 435	2.11E-016	1.78E-016	1.39E-016	1.35E-017	4.44E-018	2.38E-018

W/\sqrt{Hz}

... is like 0.1-0.03 days in deep space
(unless you make a better window)

Additional Considerations

- Atmospheric turbulence increases the advantage of balloons wrt ground
- Space missions longer than LDB and ULDB
- Ground-based measurements also longer (but with lower efficiency)
- Cost for a LDB: way smaller than for a space mission
 - Cost per kg : can use large cryostats, large cold optical systems
 - Cost per m³: use large shields, large aperture telescopes
- Balloons can have very large ground shields and use the Earth as a giant Sun shield
- Excellent test platforms for new technologies, to be flown later in deep space (examples: BOOMERanG & Archeops vs Panck HFI)

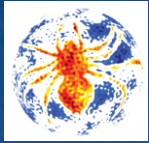
CMB-related science from stratospheric balloons

with large advantage wrt ground-based experiments:

- Polarization measurements at large scales and high frequencies (dust and CMB), instrumental for
 - tau measurements
 - inflationary and lensing B-modes
- Spectral measurements of the SZ effect
 - Cover the high frequency branch of the spectrum
 - 3m dish @350 GHz on a balloon \leftrightarrow 10m dish @ 150 GHz on the ground
- Spectral measurements of CIB anisotropy
- Measurements of spectral distortions of the CMB (in selected frequency bands)
- ...

Science Case 1 : Dust polarization at large scales

- $f=270, 350, 420$ GHz and up basically cannot be done, at the required level of precision, from the ground, especially at large scales.
- 350 GHz is the highest frequency polarized channel of Planck.
- Rough comparison, at 350 GHz:
 - ULDB has shorter observing time than Planck (by a factor 10) \rightarrow 0.33 penalty
 - ULDB has higher photon noise than Planck \rightarrow 0.3 penalty
 - ULDB can have 500 times more detectors than Planck \rightarrow 20 gain
 - ULDB can focus on the cleanest regions of the sky \rightarrow 3.3 gain if 10% of the sky
- So ULDB can be $\sim 3.3 \times 20 \times 0.3 \times 0.33 \sim 6$ *times more sensitive than Planck* in a selected clean region at 350 GHz.
- In addition, **and probably most important**, ULDB can use a **polarization modulator**, which was not present on Planck, potentially improving the control of systematic effects and the final accuracy.
- Also, ULDB can provide the missing polarization information at $f > 350$ GHz.

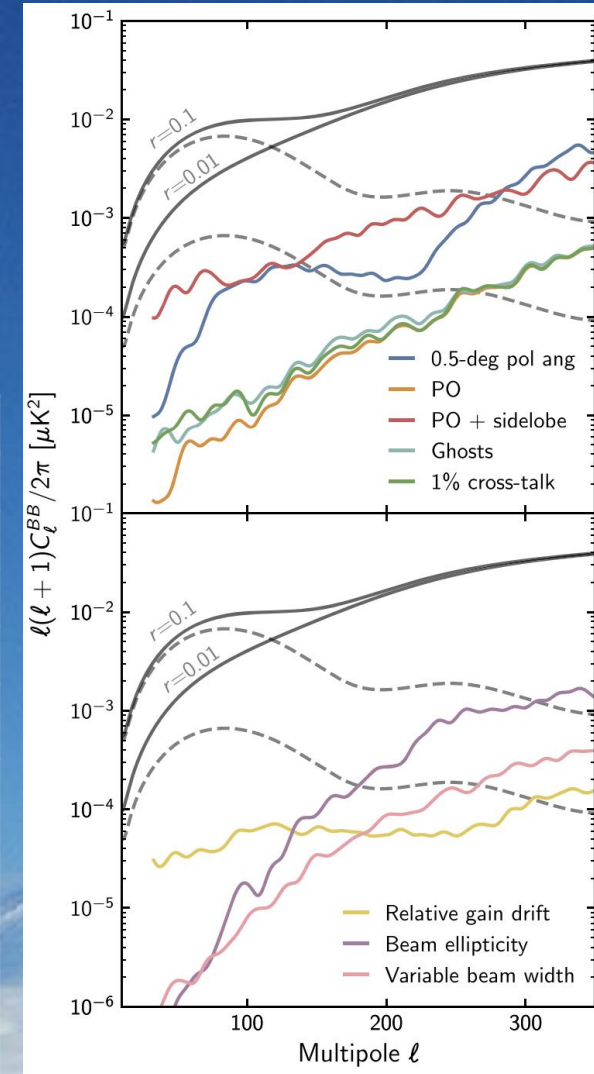


SPIDER

2015 LDB flight with 94 and 150 GHz telescopes

2015 flight	Frequency [GHz]	
	94	150
Telescopes	3	3
Bandwidth [GHz]	22	36
Optical efficiency	30-45%	30-50%
Angular resolution* [arcmin]	42	28
Number of detectors [†]	652 (816)	1030 (1488)
Optical background [‡] [pW]	≤ 0.25	≤ 0.35
Instrument NET [†] [μK·rts]	6.5	5.1

*FWHM. [†]Only counting those currently used in analysis
[‡]Including sleeve, window, and baffle



THE ASTROPHYSICAL JOURNAL, 927:174 (26pp), 2022 March 10

© 2022. The American Astronomical Society. All rights reserved.

OPEN ACCESS

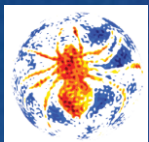
<https://doi.org/10.3847/1538-4357/ac20df>



CrossMark

A Constraint on Primordial *B*-modes from the First Flight of the SPIDER Balloon-borne Telescope

P. A. R. Ade¹, M. Amiri², S. J. Benton³, A. S. Bergman³, R. Bihary⁴, J. J. Bock^{5,6}, J. R. Bond⁷, J. A. Bonetti⁶, S. A. Bryan⁸, H. C. Chiang^{9,10}, C. R. Contaldi¹¹, O. Dore^{5,6}, A. J. Duivenvoorden^{3,12}, H. K. Eriksen¹³, M. Farhang^{7,14,15}

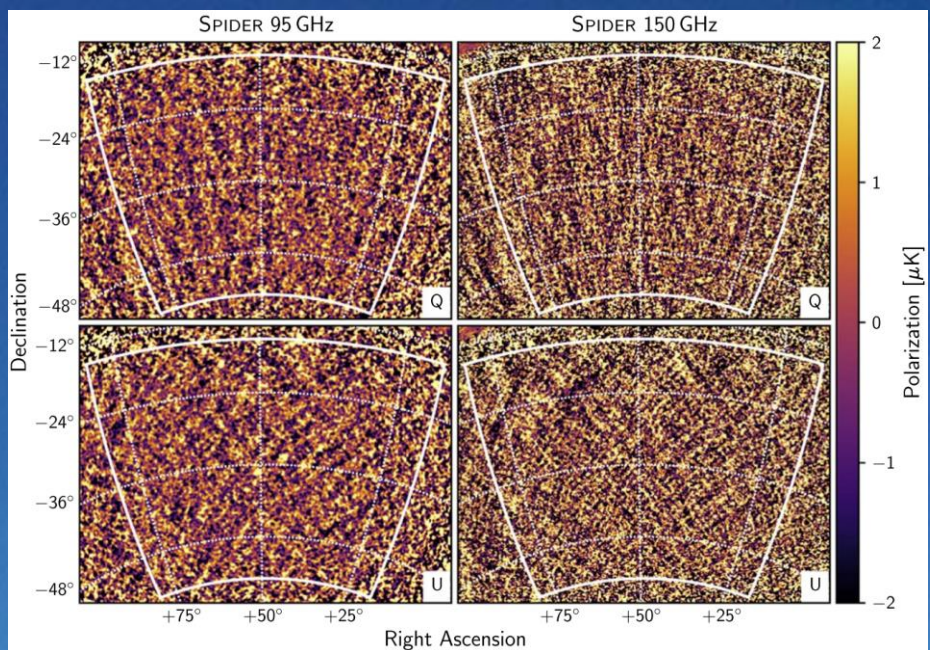


SPIDER

$r < 0.11$ - 95% C.L.

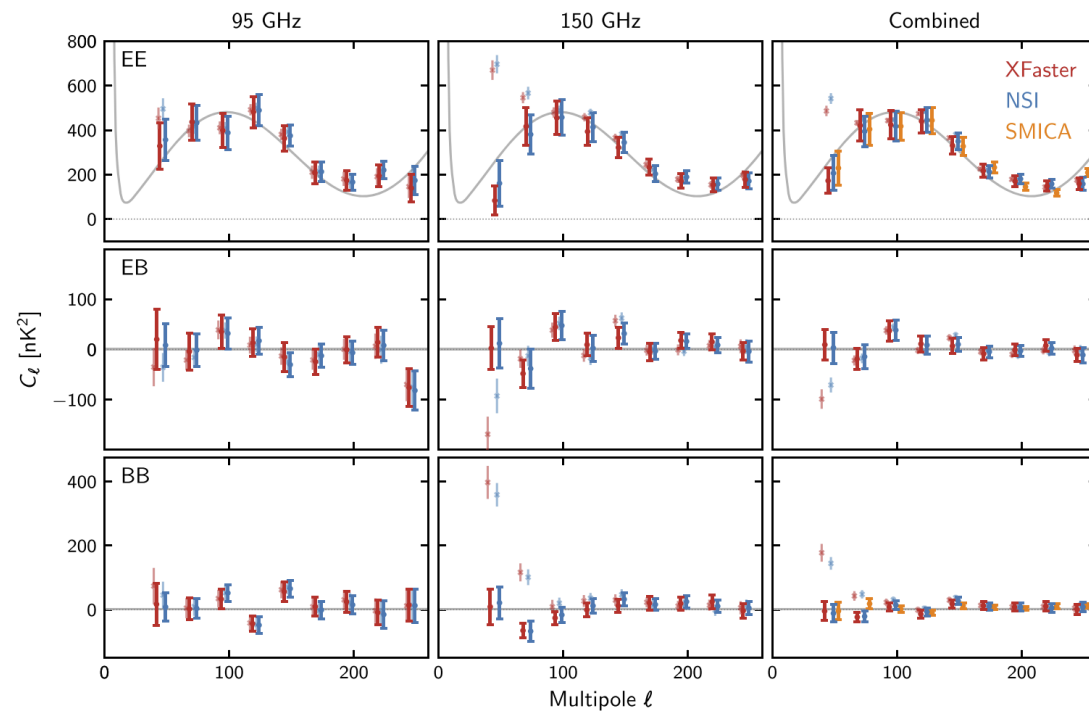
Removing polarized foregrounds was the largest challenge.

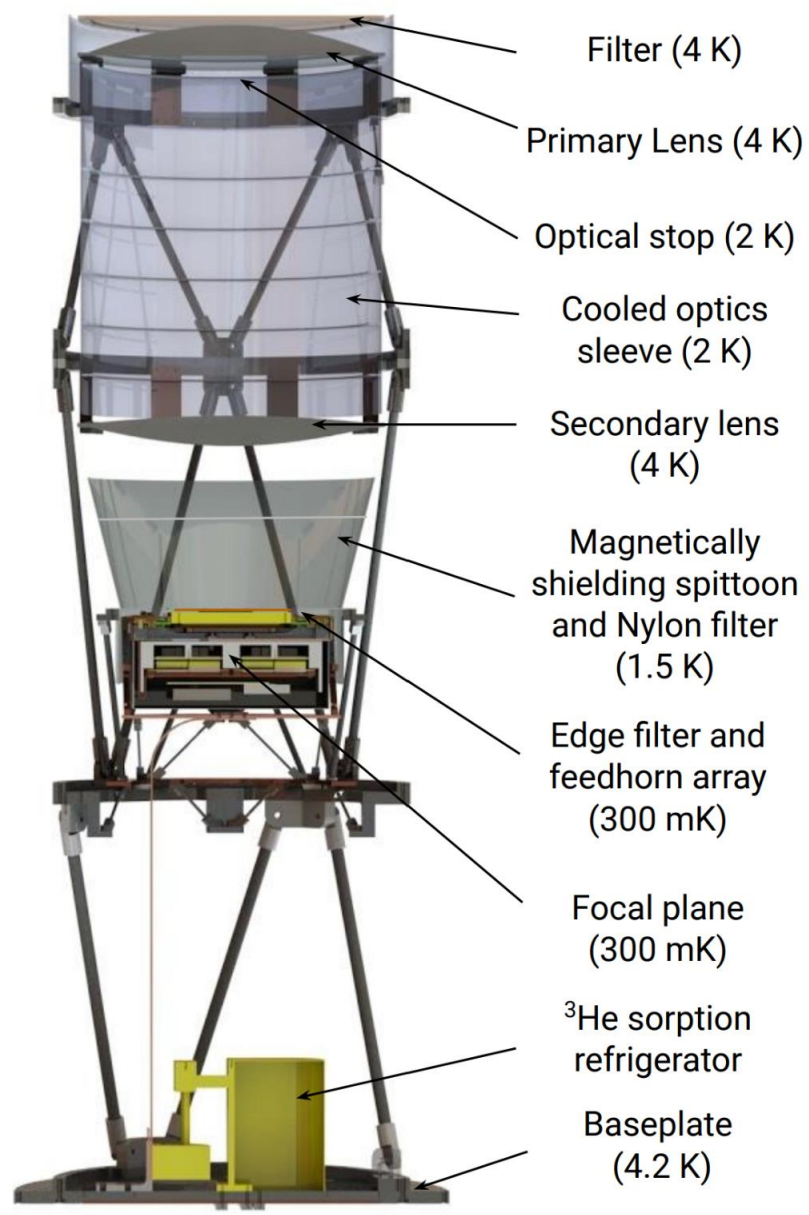
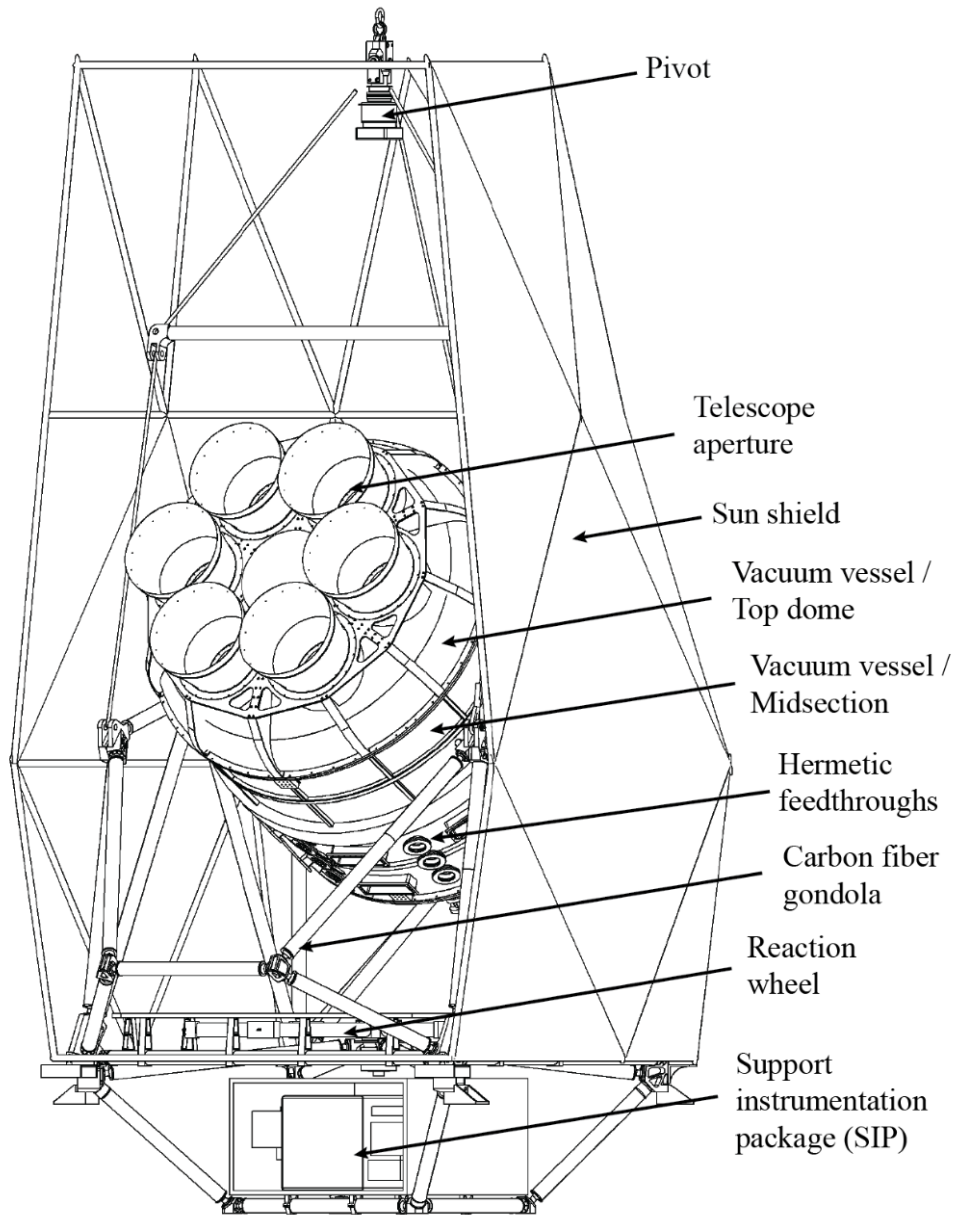
New flight with 3 telescopes total 1530 PSBs @285 GHz. Shipped to Palestine (TX) for an attempt the upcoming Antarctic season.

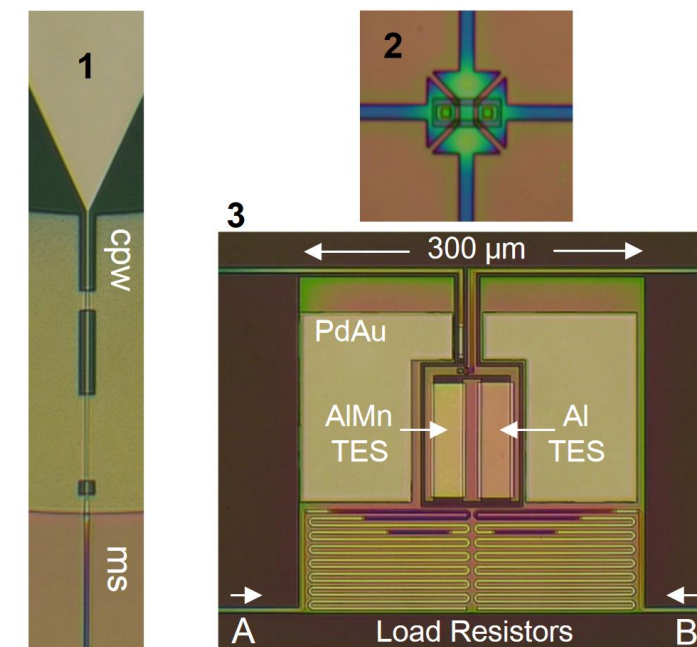
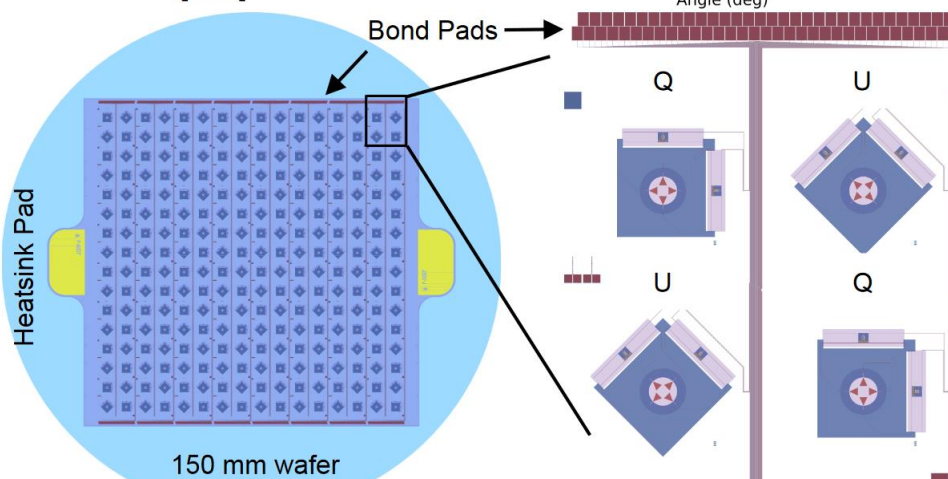
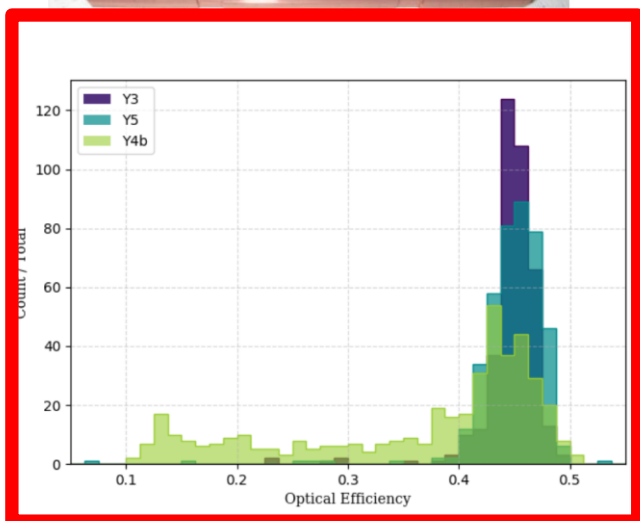
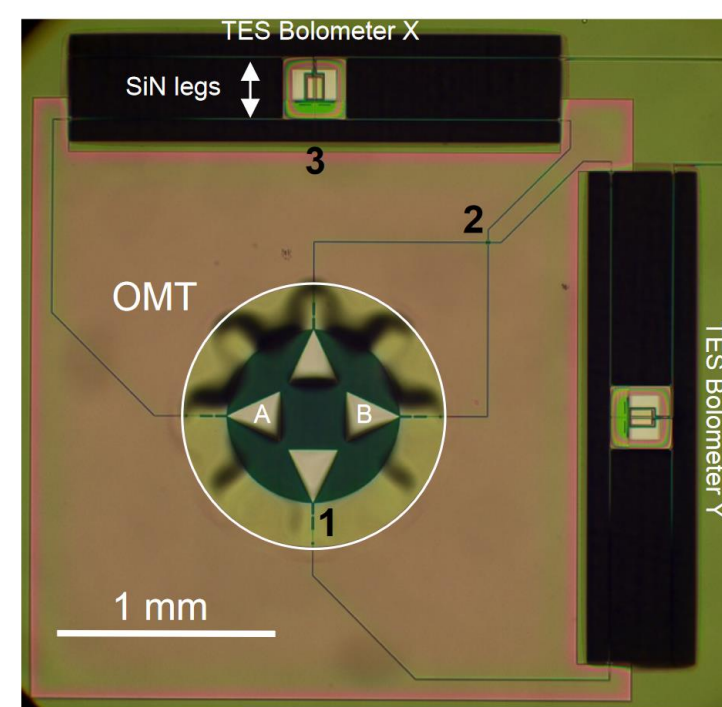
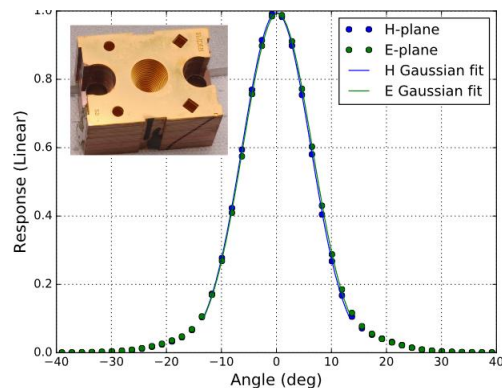
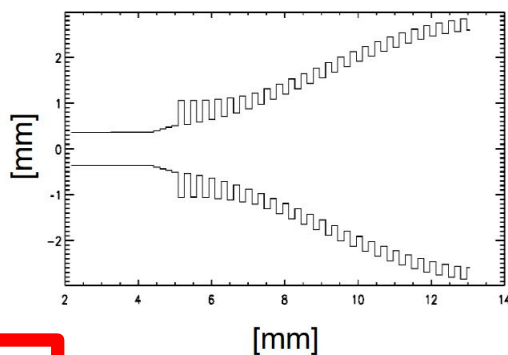
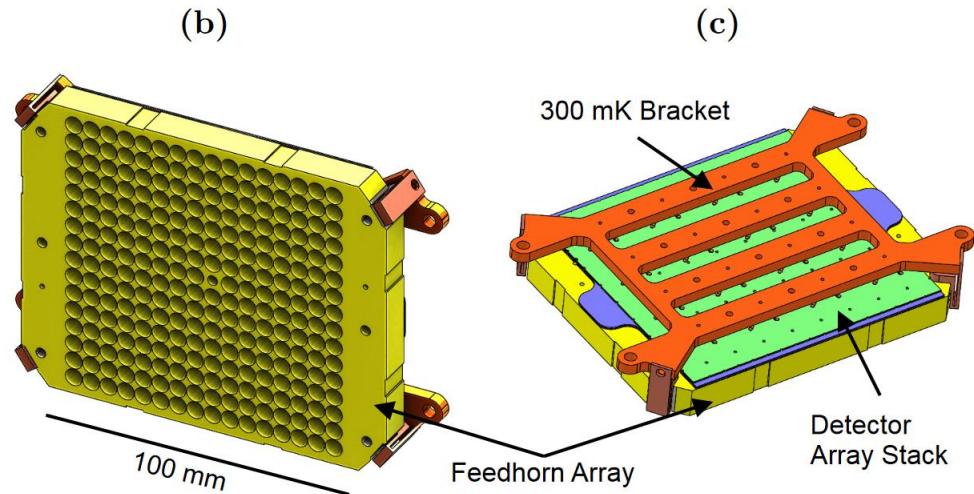
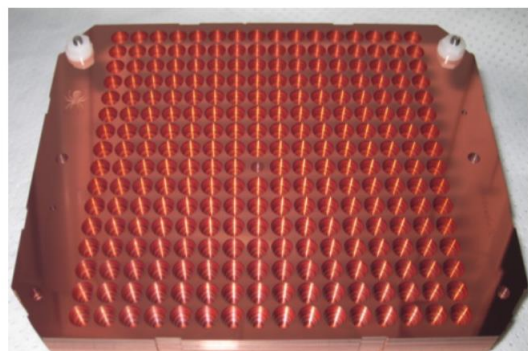
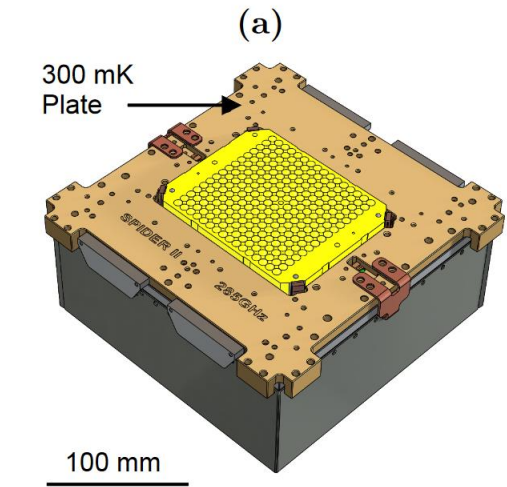


THE ASTROPHYSICAL JOURNAL, 927:174 (26pp), 2022 March 10

SPIDER Collaboration

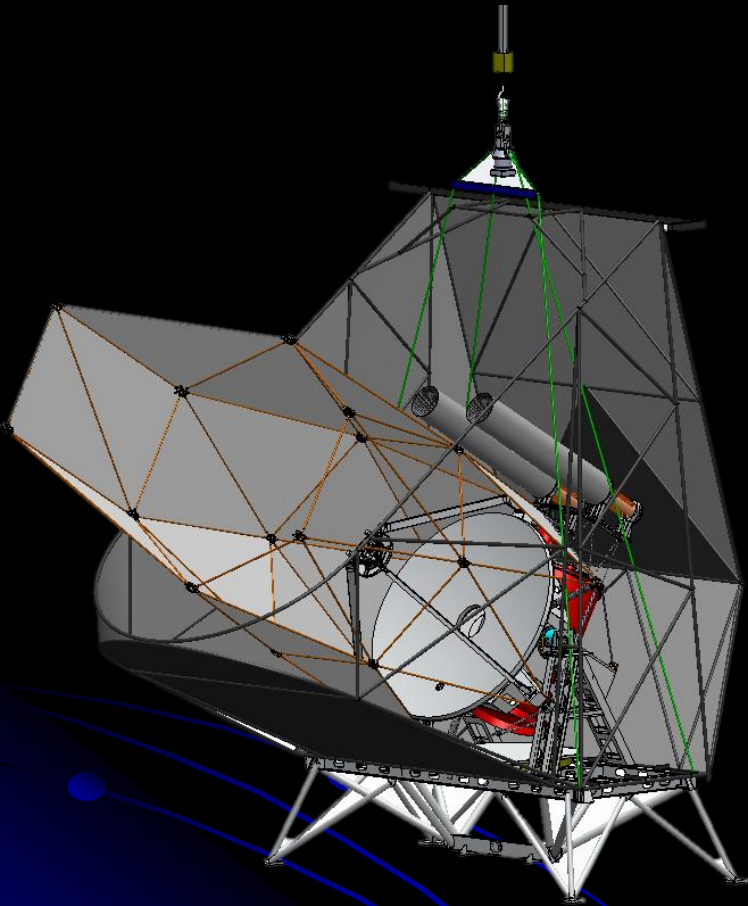




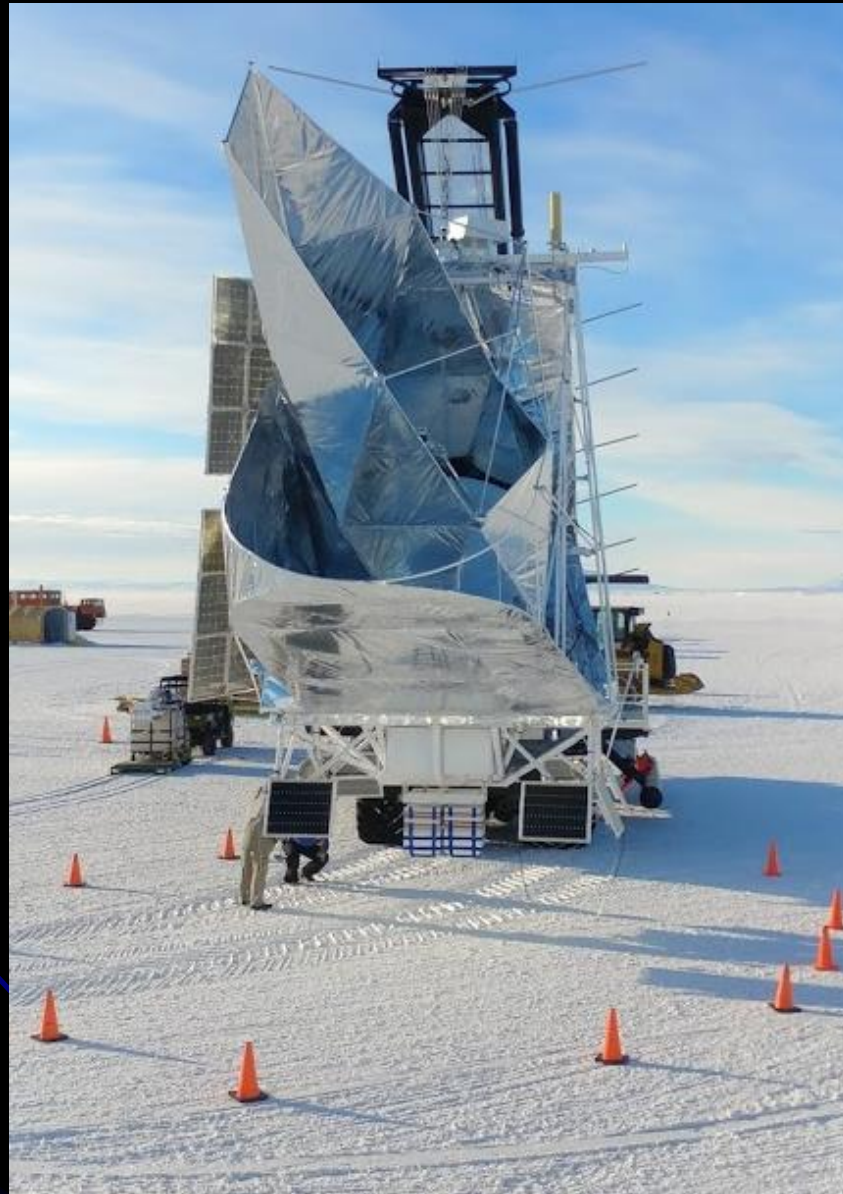


Design of 280 GHz feedhorn-coupled TES arrays for the balloon-borne polarimeter SPIDER - <https://arxiv.org/abs/1606.09396>

The Balloon-borne Large Aperture Submillimeter Telescope BLAST



Flight from Antarctica:
December 2019



PI Marc Devlin (UPenn)

<https://sites.northwestern.edu/blast/>

SPECIFICATIONS:

- 2.5 meter Carbon Fiber Mirror
- **2200 KID detectors**
 - 250, 350 and 500 μm
 - Polarization Sensitive
 - 280 mK
- 22 arcsec resolution at 250 μm
- 28 day flight!

Science:

- Polarized dust emission in **star forming regions** in our Galaxy.
- Polarized dust emission in low dust regions for CMB polarization foregrounds.

Polarized Instrument for Long-wavelength Observation of the Tenuous interstellar medium

PILOT

PI J.P. Bernard
(IRAP Toulouse)

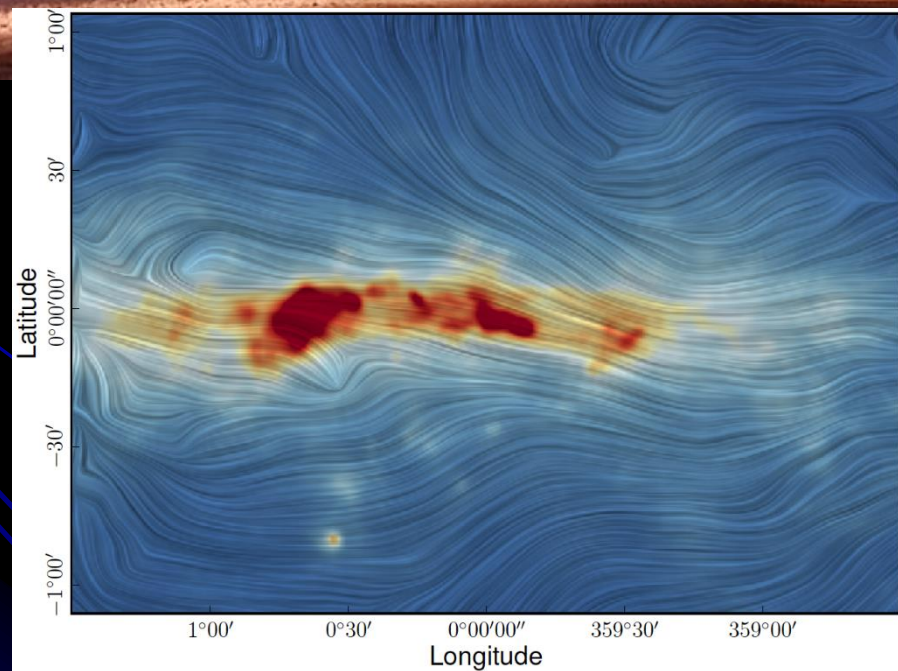
http://pilot.irap.omp.eu/PAGE_PILOT/index.html/

SPECIFICATIONS:

- 0.9 meter aperture telescope
- **2048 bolometers**
 - 240 and 550 μm
 - Polarization Sensitive with cryogenic HWP
 - 280 mK
- 1.9' resolution at 250 μm
- See Mangilli et al. Astro-ph/1804.05645
- Flown by CNES (Timmins)

Science:

- a balloon-borne experiment to study the polarized emission arising from dust grains present in the diffuse interstellar medium in our Galaxy.
- See Mangilli et al. (2019) arXiv:1901.06196 for first science results.



Science case 1b : tau

- The optical depth to recombination (τ) is related to the physics of reionization. The integral measurement of the amount of scattering from free electrons is an important parameter in reionization models. Its effect on $\langle EE \rangle$ is important at low multipoles: large angular scales difficult to measure from the ground due to atmospheric and ground spillover effects.
- A balloon-borne survey at large scales overcomes atmospheric effects and can implement large ground shields to mitigate ground spillover. Changing the ground footprint during the flight, important null tests can be carried out.

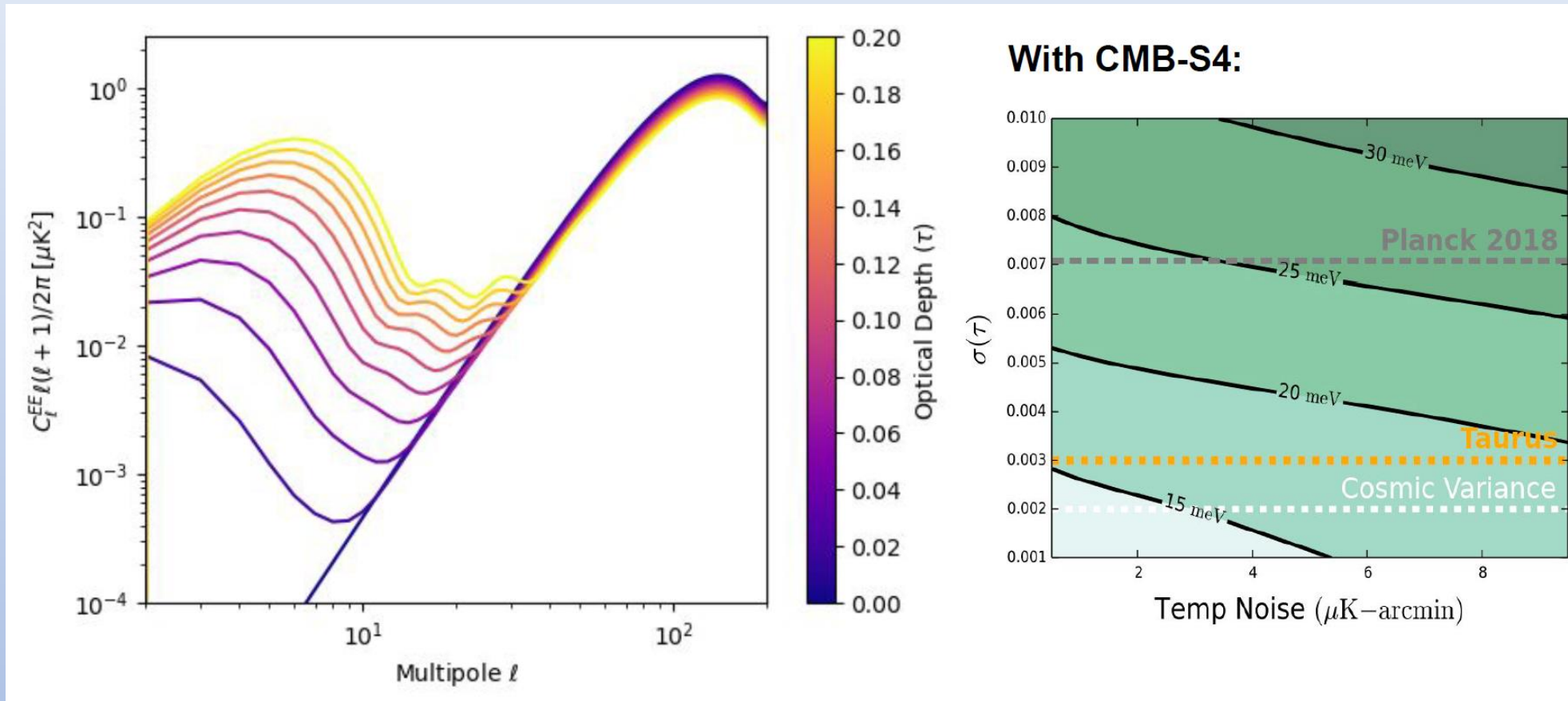
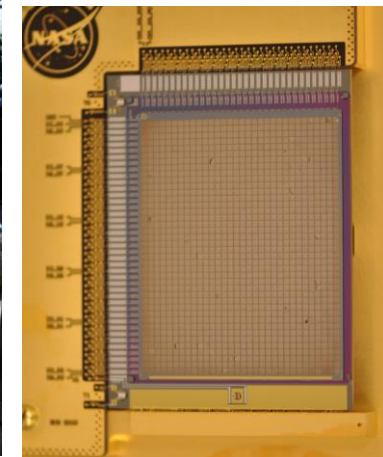
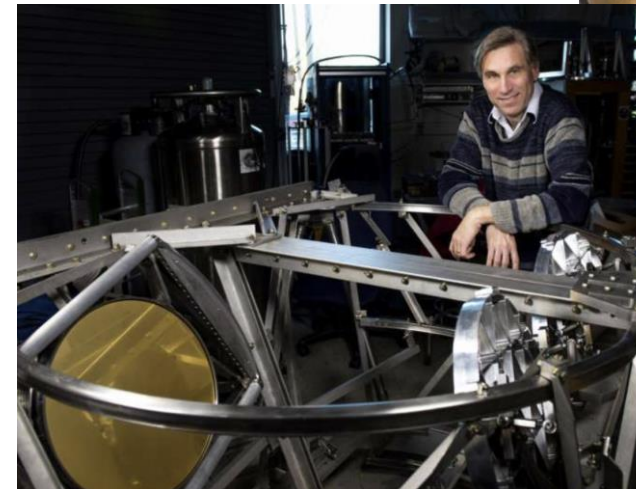
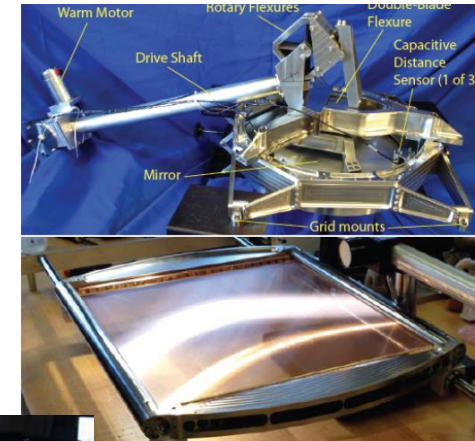
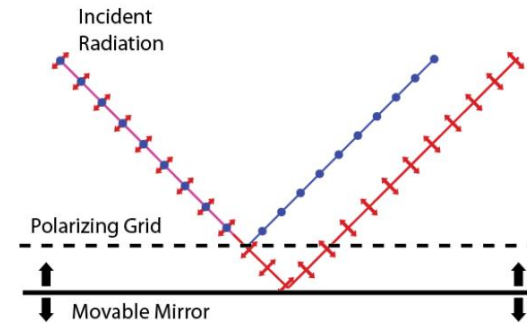
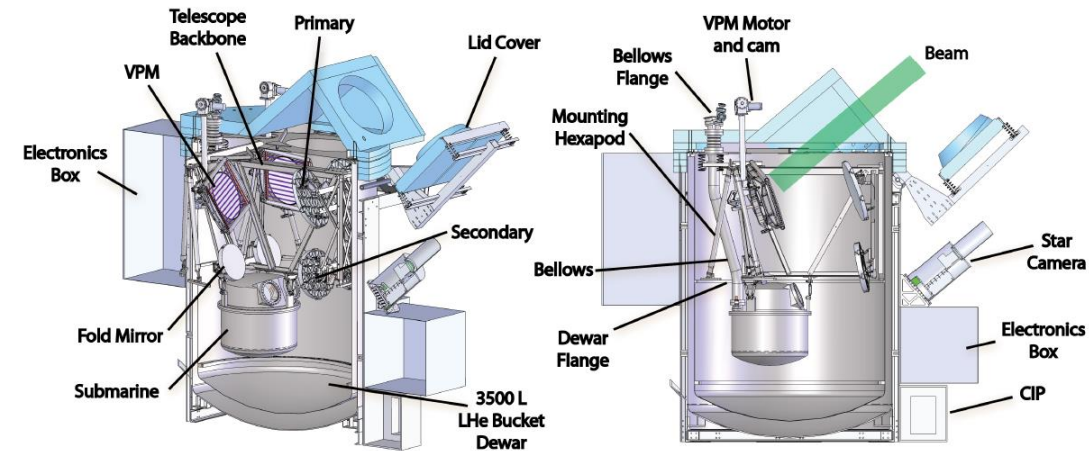


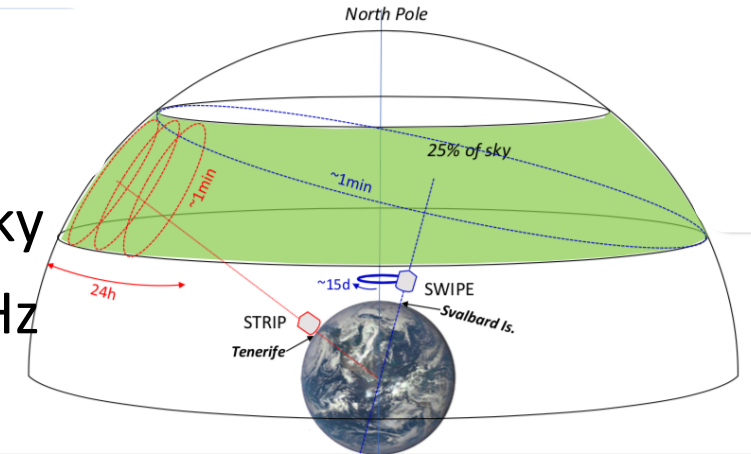
Figure from S. Benton

PIPER

- The **Primordial Inflation Polarization Explorer (PIPER)** consists of two identical telescopes cooled to 1.5 K within a large (3500-liter capacity) liquid helium bucket dewar.
- There are no windows between the LHe-cooled telescope and the ambient environment. The unusual cryogenic design provides very high mapping, allowing PIPER to achieve sensitivities with over-night balloon flights from New Mexico that would otherwise require 10-day flights from Antarctica.
- Each of PIPER's twin telescopes illuminates a pair of 32×40 element transition-edge superconducting detector arrays for a total of **5120 detectors**. In 8 flights, PIPER will map 85% of the sky in both linear and circular polarization, at wavelengths of 1500, 1100, 850, and 500 mm (frequencies 200, 270, 350, and 600 GHz) complementary to ground-based.
- A Variable-Delay Polarization Modulator (VPM) injects a time-dependent phase delay between orthogonal linear polarizations to cleanly separate polarized from unpolarized radiation.
- The combination of background-limited detectors with fast polarization modulation allows PIPER to rapidly scan large areas of the sky. PIPER is capable of observing on angular scales larger than 20° , where the inflationary signal is expected to be largest.
- Engineering flight in 2017 OK - <https://doi.org/10.1117/12.2313874>
- <https://asd.gsfc.nasa.gov/piper/>

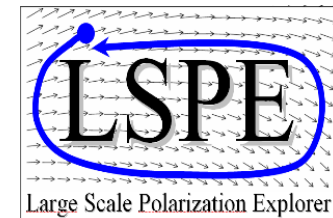


- The Large-Scale Polarization Explorer is an experiment **to measure the polarization of the CMB and interstellar dust at large angular scales.**
- Frequency coverage: 40 – 250 GHz (5 bands)
- 2 instruments: **STRIP** & **SWIPE** covering the same northern sky
- **STRIP** is a ground-based instrument working at 44 and 90 GHz
- **SWIPE** works at 140, 220, 240 GHz
 - collects 8800 radiation modes
 - uses *a spinning stratospheric balloon payload* to avoid atmospheric noise, flying *long-duration, in the arctic polar night*
 - uses *a polarization modulator* to achieve high stability
 - Uses a large polarizer to define an accurate polarization direction reference
 - Angular resolution: 1.3° FWHM
 - Sky coverage: 20-25% of the sky per flight / year
 - Combined sensitivity: $10 \mu\text{K arcmin}$ per flight
- See astro-ph/1208.0298, 1208.0281, 1208.0164 and 2008.11049

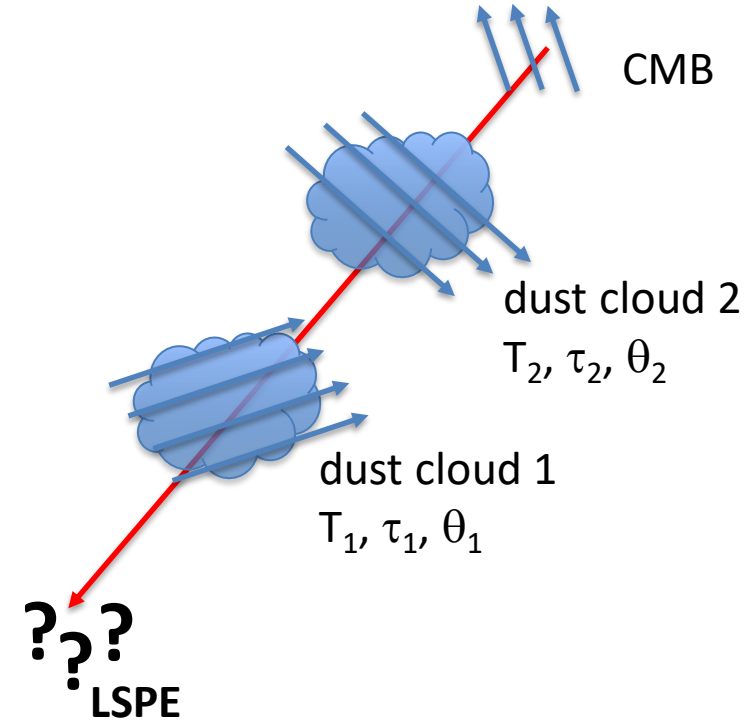
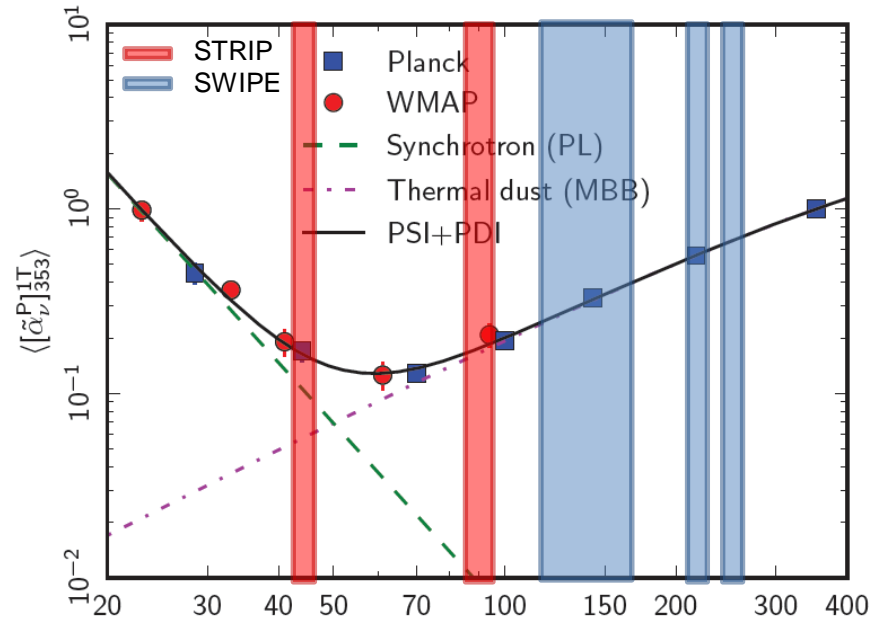


The LSPE-SWIPE Collaboration

Peter	Ade	Dept. Of Phys. And Astronomy, Cardiff Univ. (UK)			
Giorgio	Amico	Phys. Dep. Sapienza Roma & INFN Roma	Marco	Incagli	INFN Pisa
Alessandro	Baldini	INFN Pisa	Luca	Lamagna	Phys. Dep. Sapienza Roma & INFN Roma
Elia	Battistelli	Phys. Dep. Sapienza Roma & INFN Roma	Massimiliano	Lattanzi	Dipartimento di Fisica e Scienze della Terra, Università di Ferrara and INFN, Sez. Di Ferrara
Michele	Biasotti	Phys. Dep. Genova & INFN Genova	Margherita	Lebo	Dipartimento di Fisica e Scienze della Terra, Università di Ferrara and INFN, Sez. Di Ferrara
Corrado	Boragno	Phys. Dep. Genova & INFN Genova	Matteo	Lorenzini	Phys. Dep. Tor Vergata Roma & INFN Roma 2
Andrea	Boscaleri	IFAC CNR Firenze	Vladimir	Lukovich	Phys. Dep. Tor Vergata Roma & INFN Roma 2
Alessandro	Buzzelli	Phys. Dep. Tor Vergata Roma & INFN Roma 2	Tommaso	Marchetti	Phys. Dep. Sapienza Roma & INFN Roma
Paolo	Cabella	Phys. Dep. Tor Vergata Roma & INFN Roma 2	Lorenzo	Martinis	Phys. Dep. Univ. of Manchester (UK)
Fabrizio	Cei	INFN Pisa	Silvia	Masi	Phys. Dep. Sapienza Roma & INFN Roma
Valentina	Ceriale	Phys. Dep. Genova & INFN Genova	Andrew	May	Phys. Dep. Univ. of Manchester (UK)
Elisabetta	Cesarini	Phys. Dep. Tor Vergata Roma & INFN Roma 2	Mark	McCulloch	Phys. Dep. Univ. of Manchester (UK)
Stefano	Chiozzi	Dipartimento di Fisica e Scienze della Terra, Università di Ferrara and INFN, Sez. Di Ferrara	Simon	Melhuish	Phys. Dep. Univ. of Manchester (UK)
Eugenio	Coccia	Phys. Dep. Tor Vergata Roma & INFN Roma 2	Marina	Migliaccio	Dipartimento di Fisica e Scienze della Terra, Università di Ferrara and INFN, Sez. Di Ferrara
Fabio	Columbro	Phys. Dep. Sapienza Roma & INFN Roma	Andrea	Moggi	INFN Pisa
Gabriele	Coppi	Phys. Dep. Sapienza Roma & INFN Roma	Diego	Molinari	Dipartimento di Fisica e Scienze della Terra, Università di Ferrara and INFN, Sez. Di Ferrara
Gabriele	Coppi	Phys. Dep. Univ. of Manchester (UK)	Umberto	Natale	Dipartimento di Fisica e Scienze della Terra, Università di Ferrara and INFN, Sez. Di Ferrara
Alessandro	Coppolecchia	Phys. Dep. Sapienza Roma & INFN Roma	Paolo	Natoli	Dipartimento di Fisica e Scienze della Terra, Università di Ferrara and INFN, Sez. Di Ferrara
Dario	Corsini	Phys. Dep. Genova & INFN Genova	Donato	Nicolò	INFN Pisa
Angelo	Cotta Ramusino	Dipartimento di Fisica e Scienze della Terra, Università di Ferrara and INFN, Sez. Di Ferrara	Luca	Pagano	IAS Orsay
Giuseppe	D'Alessandro	Phys. Dep. Sapienza Roma & INFN Roma	Alessandro	Paiella	Phys. Dep. Sapienza Roma & INFN Roma
Sabrina	D'Antonio	Phys. Dep. Tor Vergata Roma & INFN Roma 2	Francesco	Piacentini	Phys. Dep. Sapienza Roma & INFN Roma
Paolo	de Bernardis	Phys. Dep. Sapienza Roma & INFN Roma	Lucio	Piccirillo	Phys. Dep. Univ. of Manchester (UK)
Giancarlo	De Gasperis	Phys. Dep. Tor Vergata Roma & INFN Roma 2	Marco	Piendibene	INFN Pisa
Viviana	Fafone	Phys. Dep. Tor Vergata Roma & INFN Roma 2	Giampaolo	Pisano	Dept. Of Phys. And Astronomy, Cardiff Univ. (UK)
Flavio	Fontanelli	Phys. Dep. Genova & INFN Genova	Linda	Polastri	Dipartimento di Fisica e Scienze della Terra, Università di Ferrara and INFN, Sez. Di Ferrara
Francesco	Forastieri	Dipartimento di Fisica e Scienze della Terra, Università di Ferrara and INFN, Sez. Di Ferrara	Gianluca	Polenta	Agenzia Spaziale Italiana
Elisa	Fumagalli	Phys. Dep. Genova & INFN Genova	Alessio	Rocchi	Phys. Dep. Tor Vergata Roma & INFN Roma 2
Luca	Galli	INFN Pisa	Alessandro	Schillaci	Phys. Dep. Sapienza Roma & Caltech
Flavio	Gatti	Phys. Dep. Genova & INFN Genova	Giovanni	Signorelli	INFN Pisa
Mauro	Giovannini	Phys. Dep. Genova & INFN Genova	Franco	Spinella	INFN Pisa
Marco	Grassi	INFN Pisa	Elisabetta	Tommasi	Agenzia Spaziale Italiana
Daniele	Grosso	Phys. Dep. Genova & INFN Genova	Carole	Tucker	Dept. Of Phys. And Astronomy, Cardiff Univ. (UK)
Alessandro	Gruppuso	Dipartimento di Fisica e Scienze della Terra, Università di Ferrara and INFN, Sez. Di Ferrara	Davide	Vaccaro	INFN Pisa
Sandeep	Haridasu Balakrishna	Phys. Dep. Tor Vergata Roma & INFN Roma 2	Nicola	Vittorio	Phys. Dep. Tor Vergata Roma & INFN Roma 2
Giuseppe	Iacobellis	Dipartimento di Fisica e Scienze della Terra, Università di Ferrara and INFN, Sez. Di Ferrara	Angela	Volpe	Agenzia Spaziale Italiana
			Guido	Zavattini	Dipartimento di Fisica e Scienze della Terra, Università di Ferrara and INFN, Sez. Di Ferrara



LSPE : Foregrounds cleaning strategy



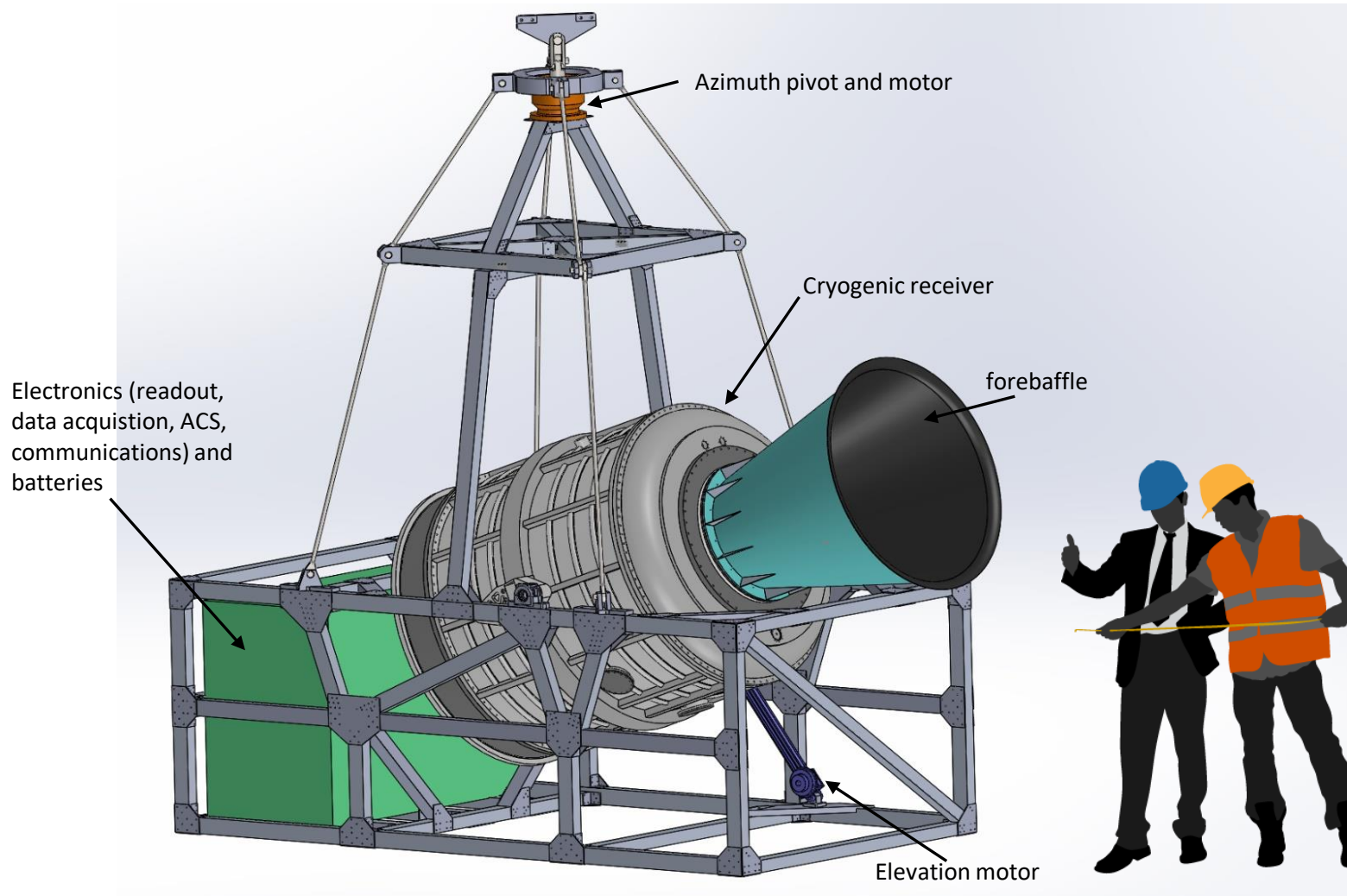
44 GHz - STRIP
Monitor polarized synchrotron

90 GHz - STRIP
Atmospheric monitor

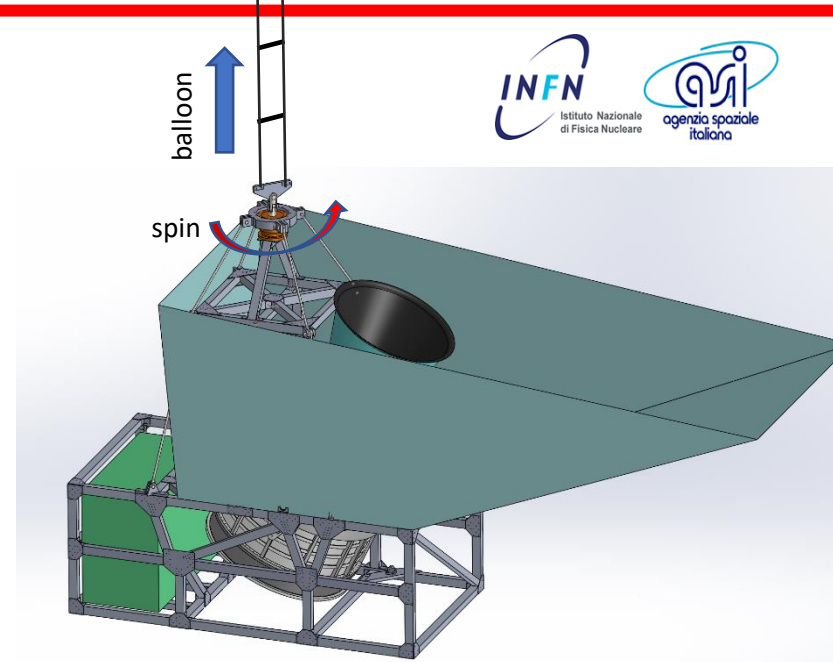
140 GHz - SWIPE
Main CMB channel

220 + 240 GHz - SWIPE
Monitor **level, slope and possible rotation** of polarized dust emission.
To date - extrapolated from 350 GHz

LSPE/SWIPE



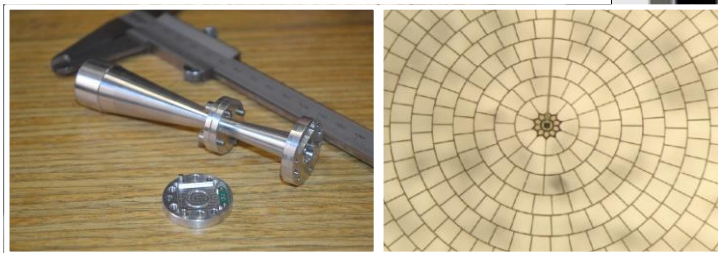
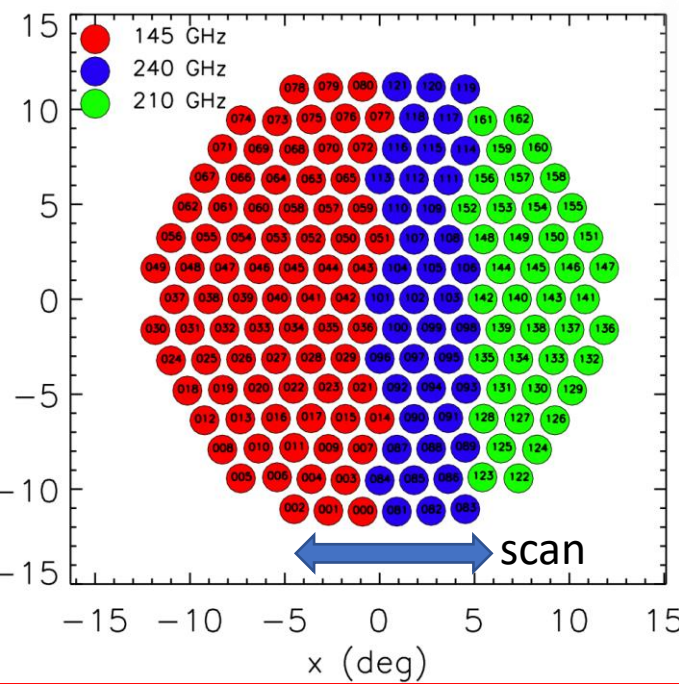
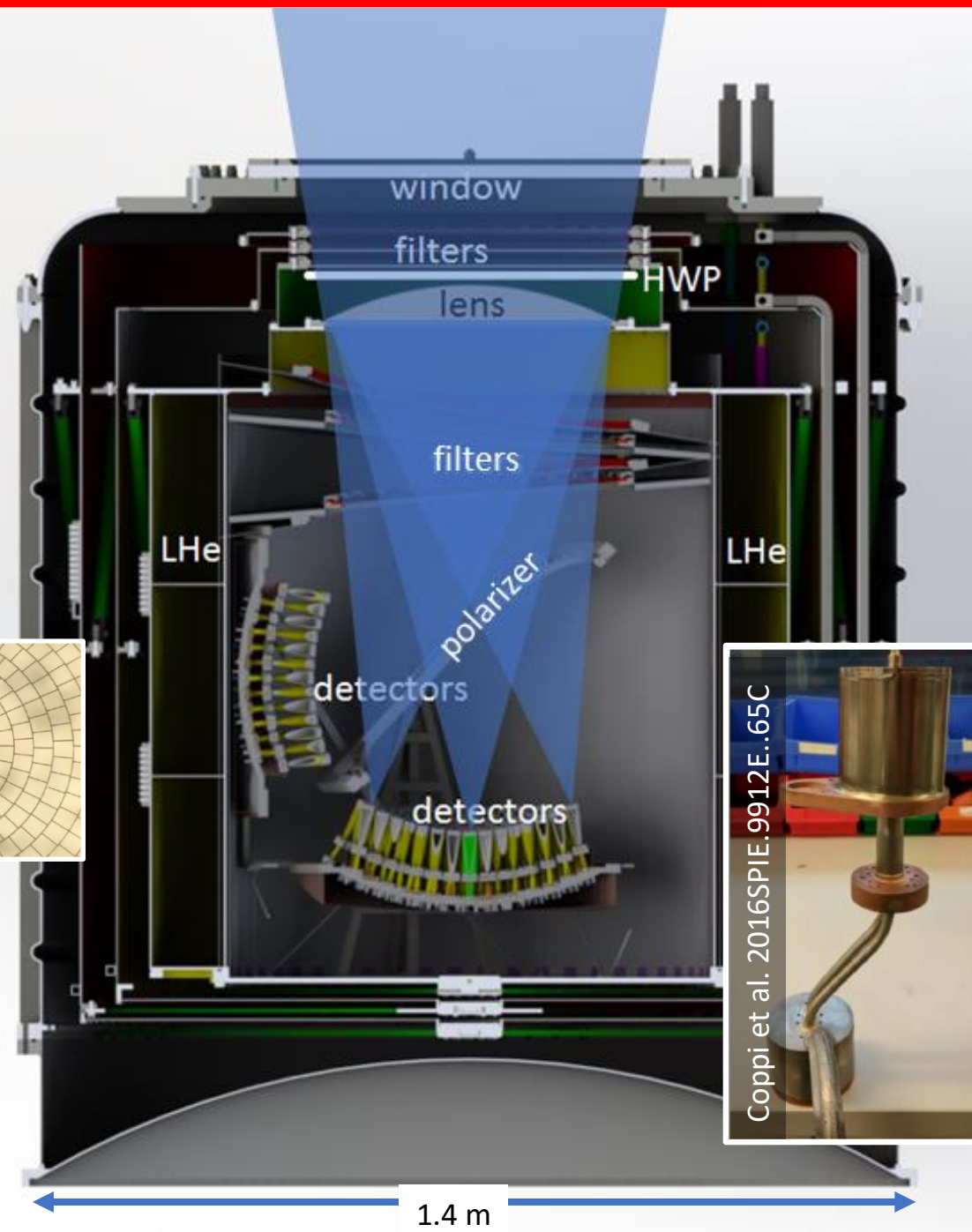
Rendering without ground/sun shields – a 1.6 tons payload



- The instrument is flown at 40 km altitude to mitigate the effects of earth's atmosphere.
- The instrument spins in azimuth to cover about 25% of the northern sky.

A Stokes polarimeter, with

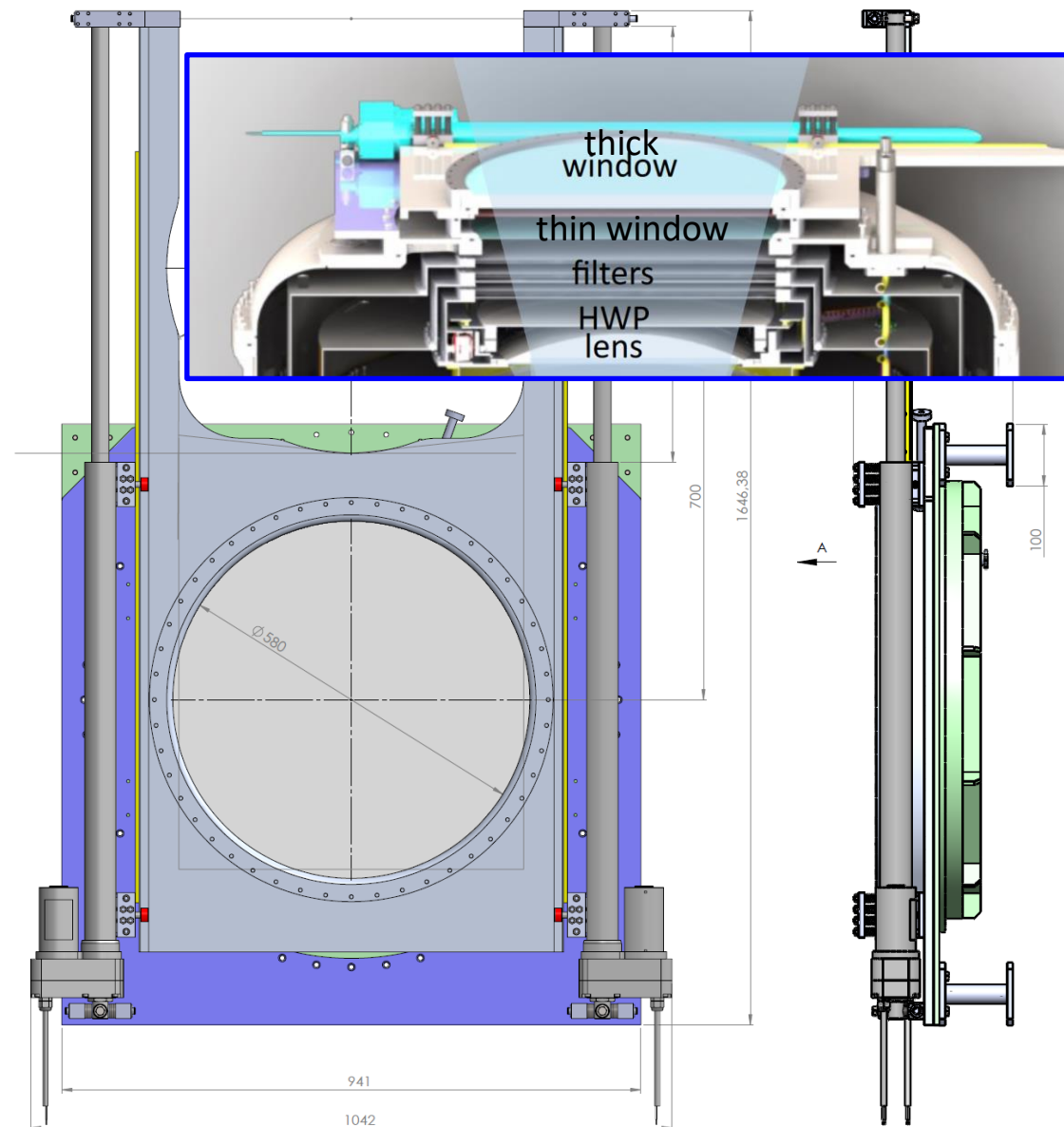
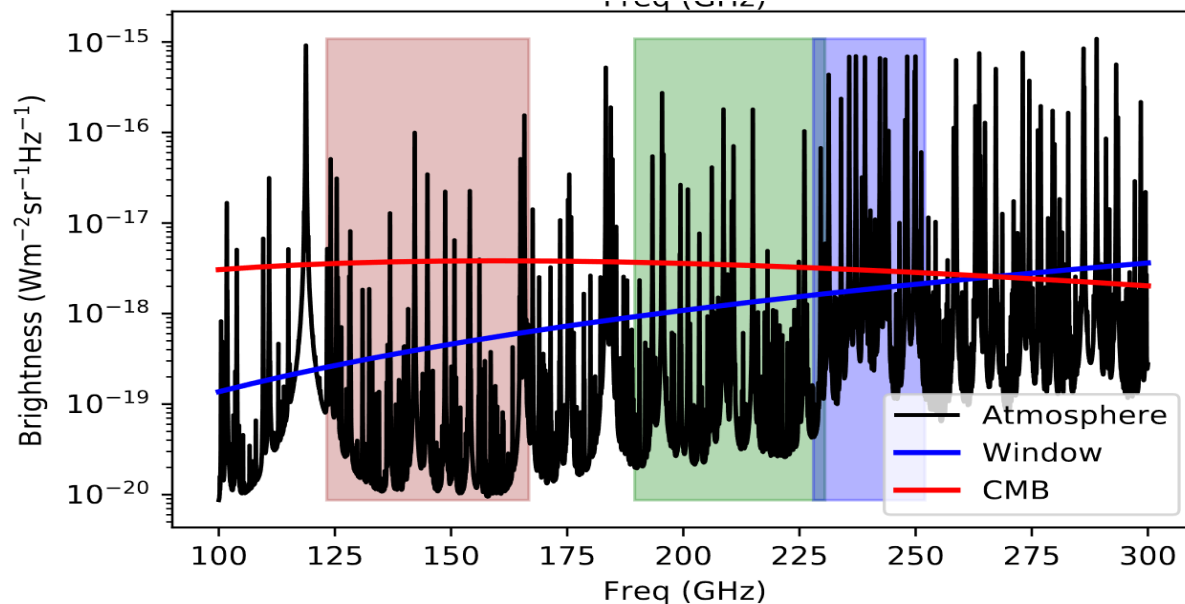
- A spinning HWP (10-15K)
- A single-lens telescope at 3K (490mm diameter with a 460 mm diam. cold stop)
- A 500mm diameter, 45° tilted wire grid at 2K, splitting the focused beams (f/1.75) in
- Two large focal planes accomodating 330 multimode feedhorns and bolometric detectors (8800 modes), covering a 20° diameter field of view, and cooled at 0.28 K.
- The main cryostat contains 250 liters of suprfuid L⁴He
- The sub-K cooler is a ³He refrigerator (filled with 24 liters STP).



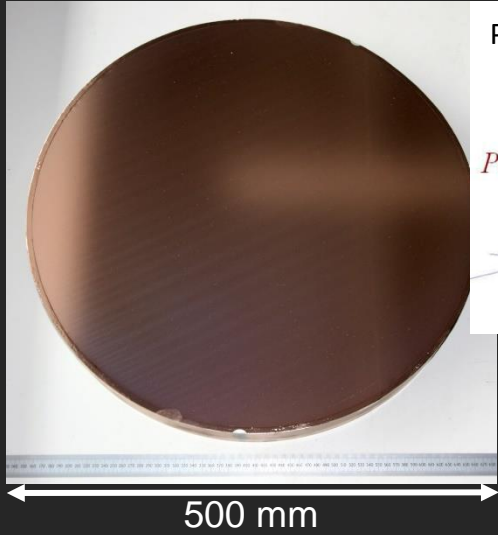
Coppi et al. 2016SPIE.9912E..65C

Reducing the background

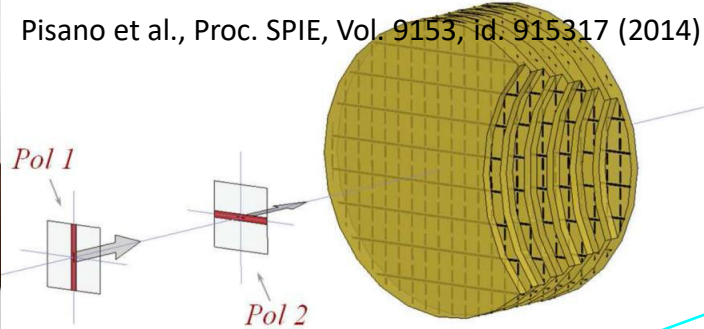
- For laboratory operations, LSPE uses a 60 cm diameter 1 cm thick HDPE window with integrated reflecting NDF.
- At float, the thick HDPE window is removed, leaving a very thin (1 mil) polypropylene window in place to separate the mild vacuum of the stratosphere from the high vacuum of the dewar interior.
- The mechanism is a larger version of the one used in the EBEX balloon flight (Zilic &, Rev. Sci. Inst. 88, 045112 (2017)).
- The emission of the thin window is less than the emission of the CMB in the bands of SWIPE.



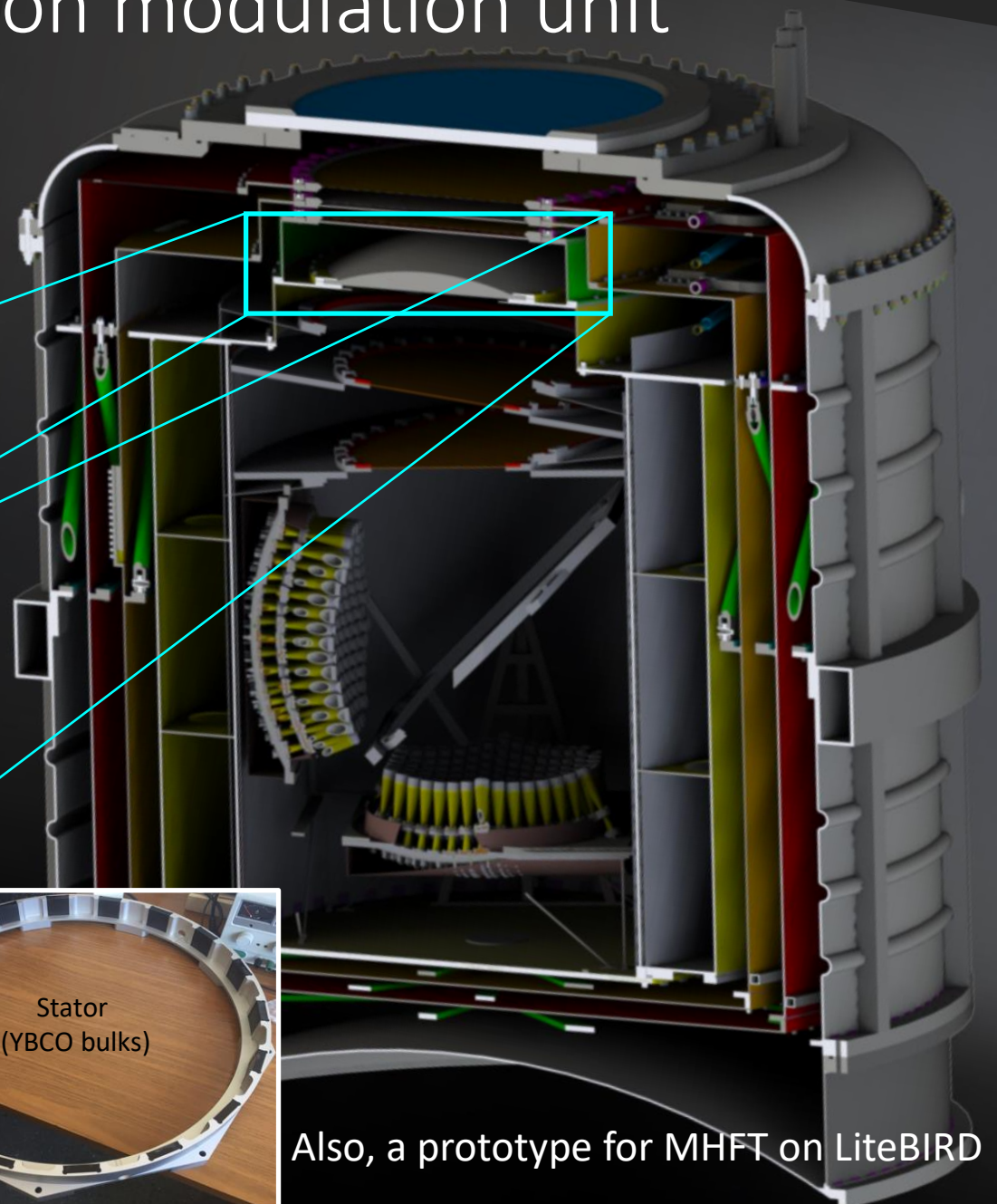
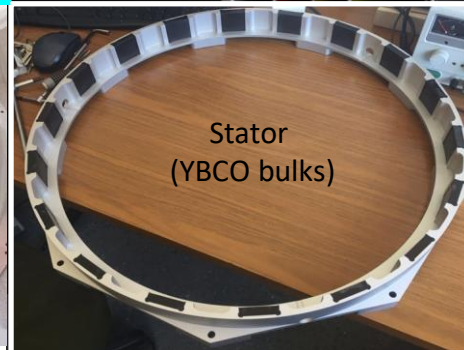
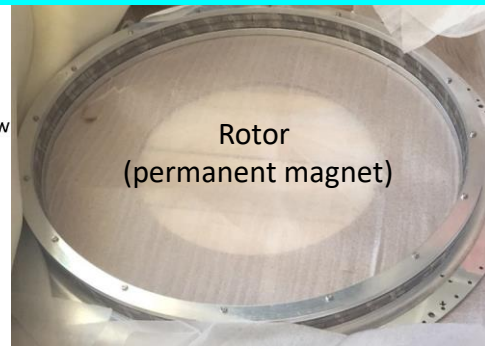
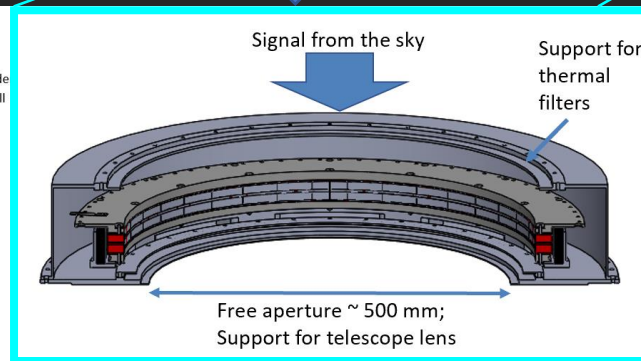
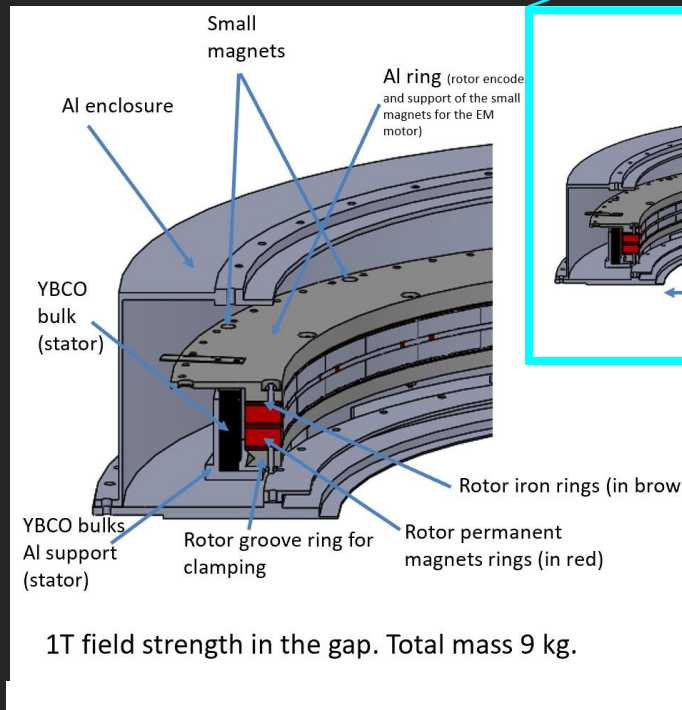
LSPE/SWIPE: Polarization modulation unit



Pisano et al., Proc. SPIE, Vol. 9153, id. 915317 (2014)



Metamaterials HWP
1 rps magnetically levitating
HWP rotator

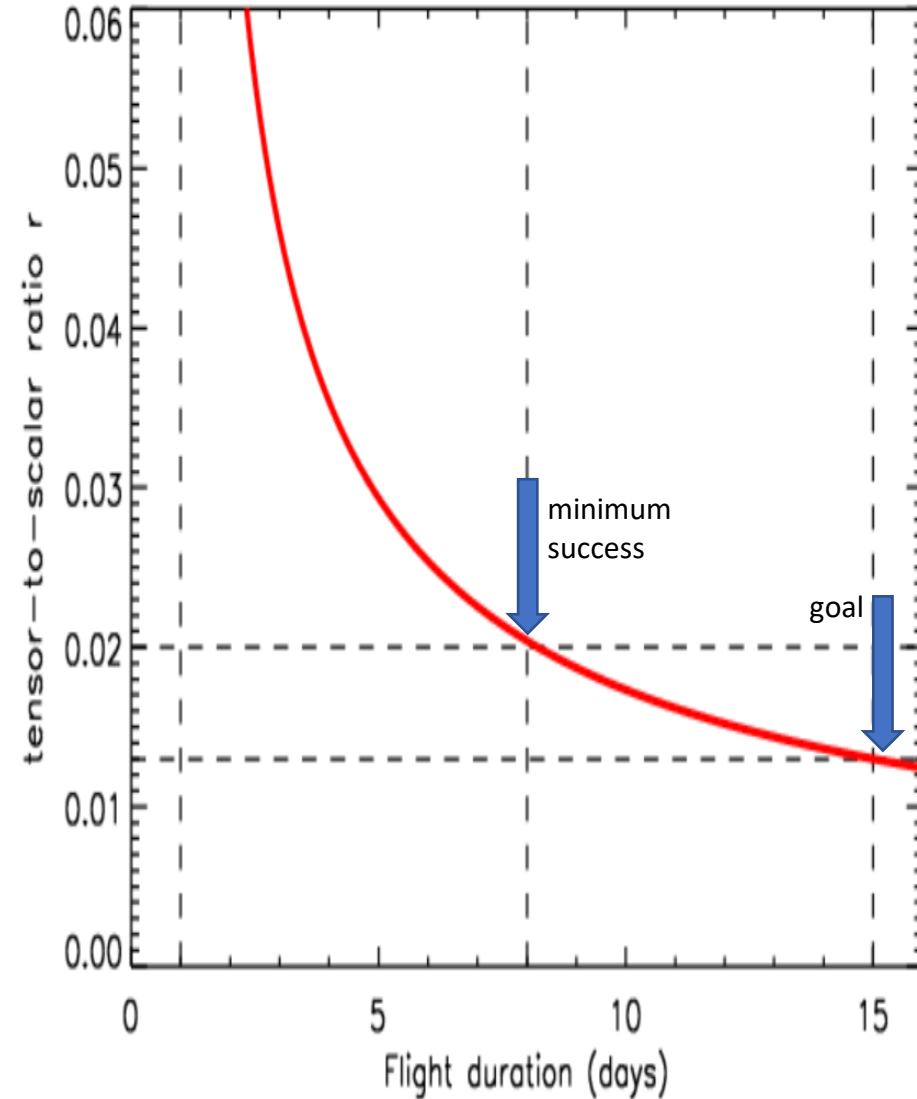
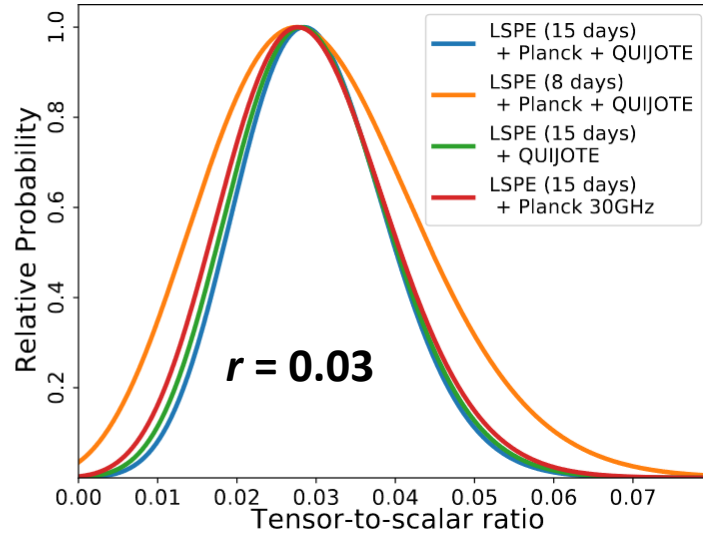
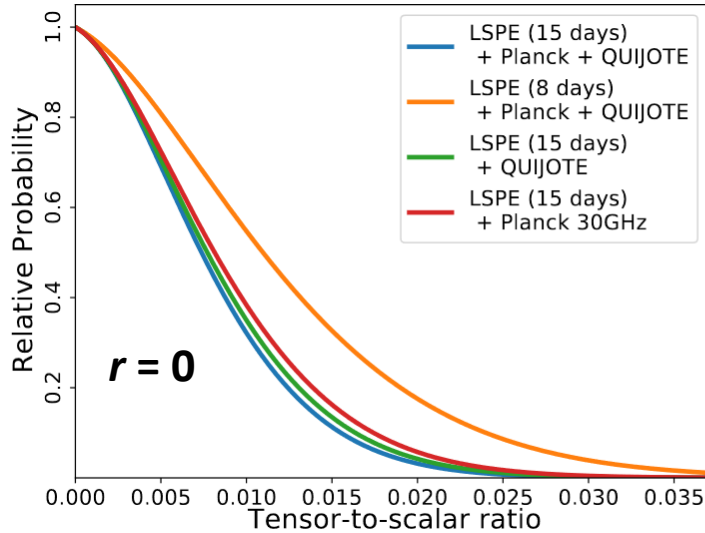


Also, a prototype for MHFT on LiteBIRD

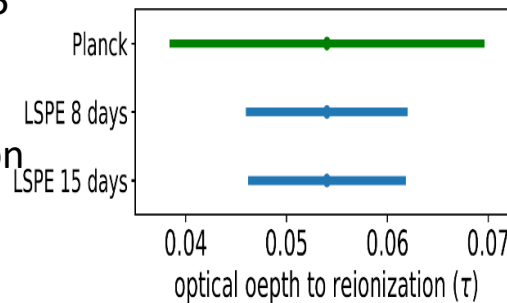
Expected performance of SWIPE-LSPE and requirements for the flight

<https://arxiv.org/abs/2008.11049>

<https://doi.org/10.1088/1475-7516/2021/08/008>



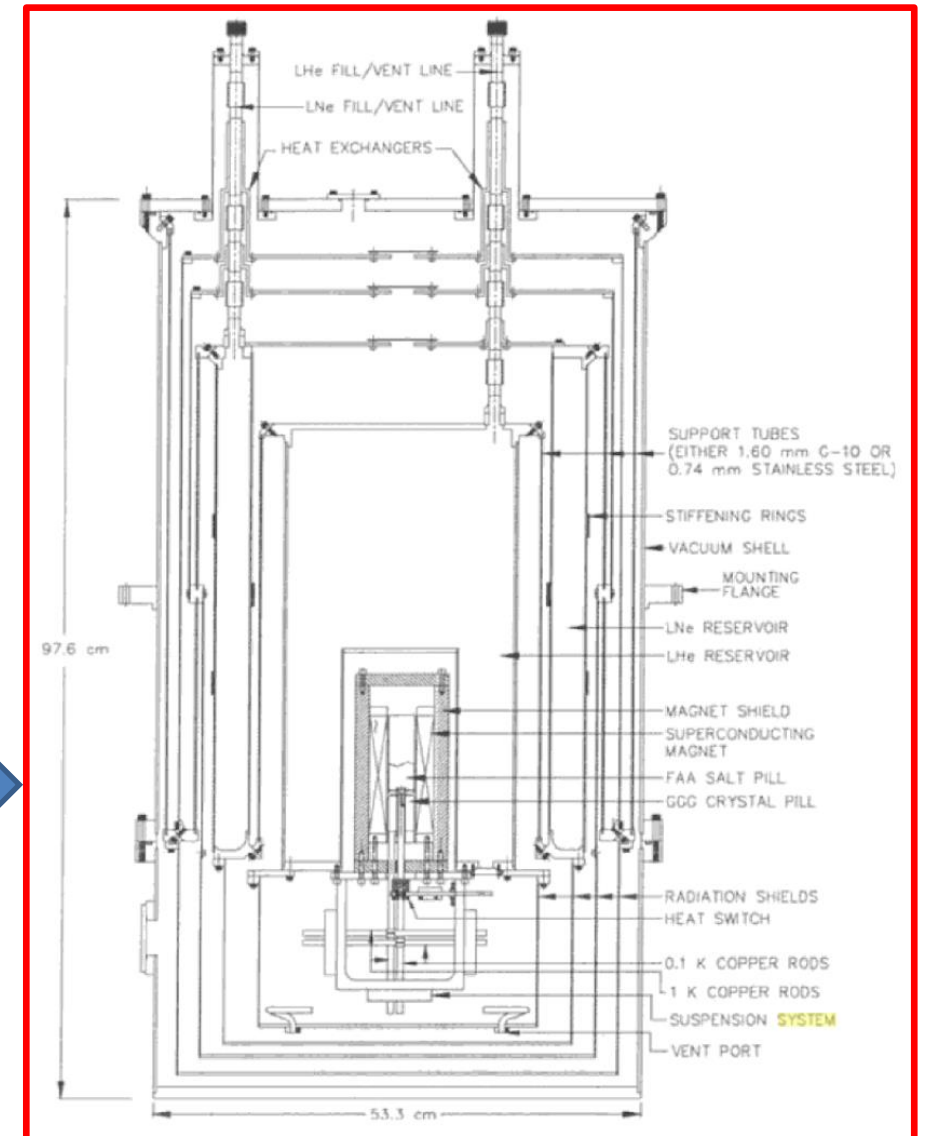
- If $r \ll 0.01$ LSPE-SWIPE provides a 95% CL U.L. $r < 0.015$
- If $r > 0.01$ LSPE-SWIPE provides a significant detection ($\sigma_r = 0.009$)
- The measurement of the optical depth to recombination is improved significantly wrt Planck:
- Long integration time (8 days minimum, 15 days goal)
- Night flight (to cover all azimuths with a telescope spinning in azimuth), Arctic circumpolar flight.
- Flight: end of 2023 if international situation allows



95% Confidence intervals for the optical depth

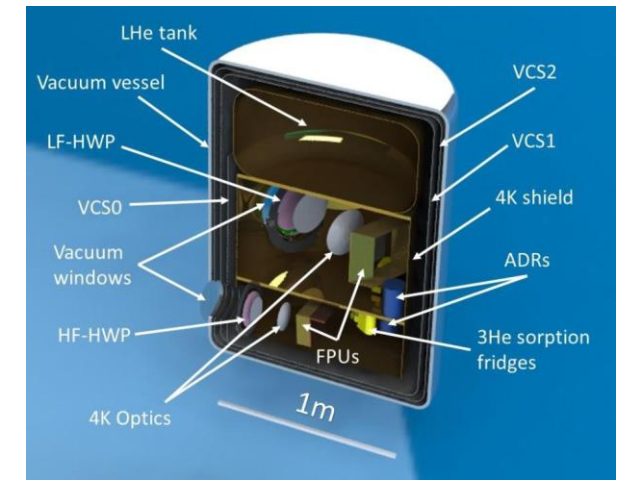
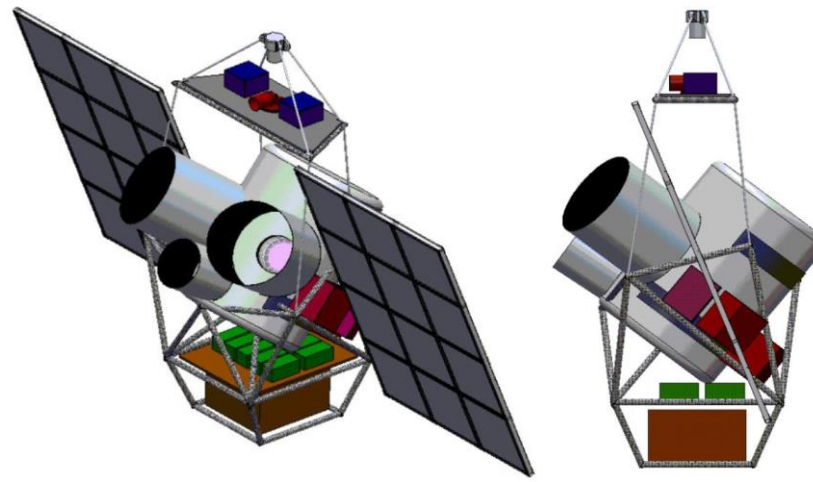
ULDB flights require new cryogenic systems

- Cryogenic systems for LDB, based on liquid cryogenics (LN₂, LHe) have a target hold time of 1 month and a mass at the launch of the order of 300 kg (see e.g. Masi et al. *Cryogenics*, 38, 319-324, 1998, Coppolecchia et al. *Cryogenics*, 110, 103129 2020)
- To exploit the longer flight duration (order of 100 days) of a ULDB and cope with the reduced payload mass compliance of sealed balloons, longer duration and lighter cryostats must be optimized.
- Solutions are possible either using cryogenic fluids:
 - A long lifetime balloon-borne cryostat and magnetic refrigerator J. O. Gundersen et al. 2013, *Advances in Cryogenic Engineering*, Quan-Sheng Shu et al. Eds. Springer
- or using **hybrid systems with mechanical coolers** for the intermediate temperature stage (as needed for large windows).

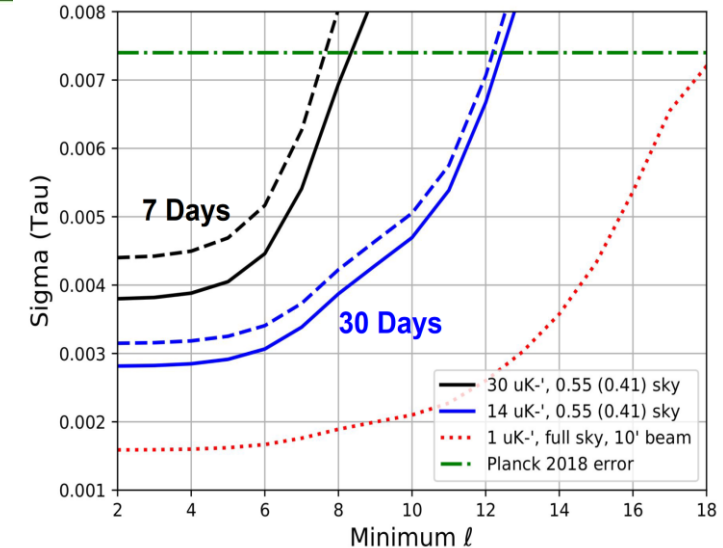
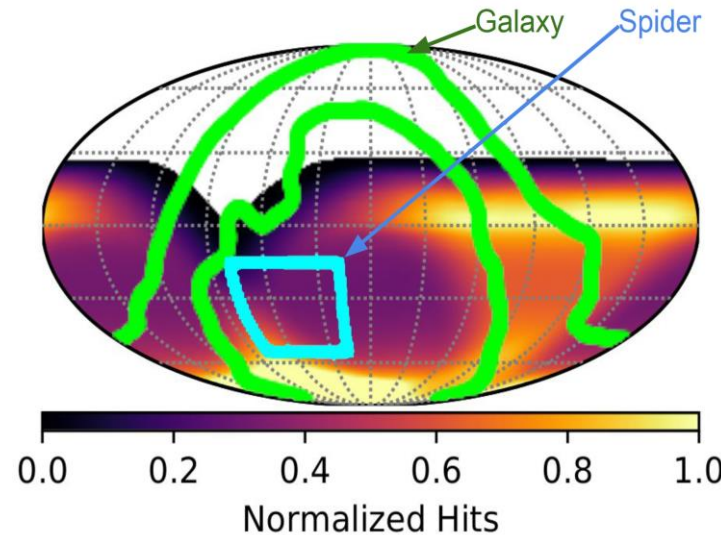


TAURUS (tau"R"us)

- Taurus will be deployed on a mid-latitude **super-pressure balloon** (>50 days, 2026), where it can observe approximately 70% of the sky.
- The instrument combines low temperature (100 mK) detectors with compact, cold optics and polarization modulators to provide a sensitive and robust view of the microwave sky in many frequency bands.
- Observing at high frequencies inaccessible from the ground enables the removal of polarized Galactic dust signals, which would otherwise obscure the cosmological information.
- The Taurus mission builds upon heritage from the SPIDER payload, and the science is highly complementary to the ground-based CMB-S4 experiment.
- Princeton (S. Benton, PI) + UIUC + NIST + WUSTL + Stockholm + Toronto + FNAL

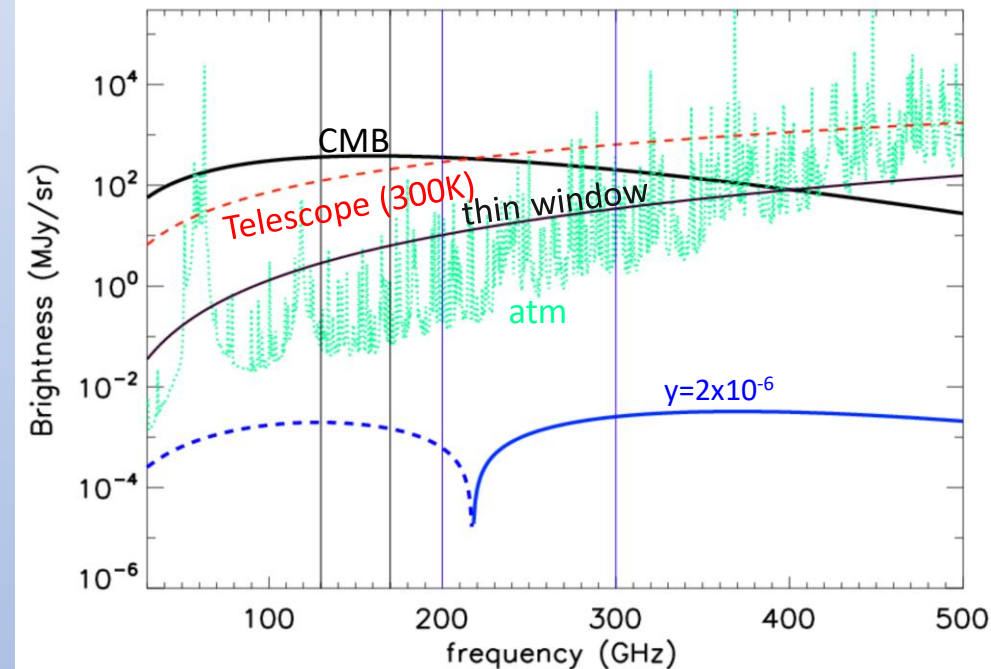
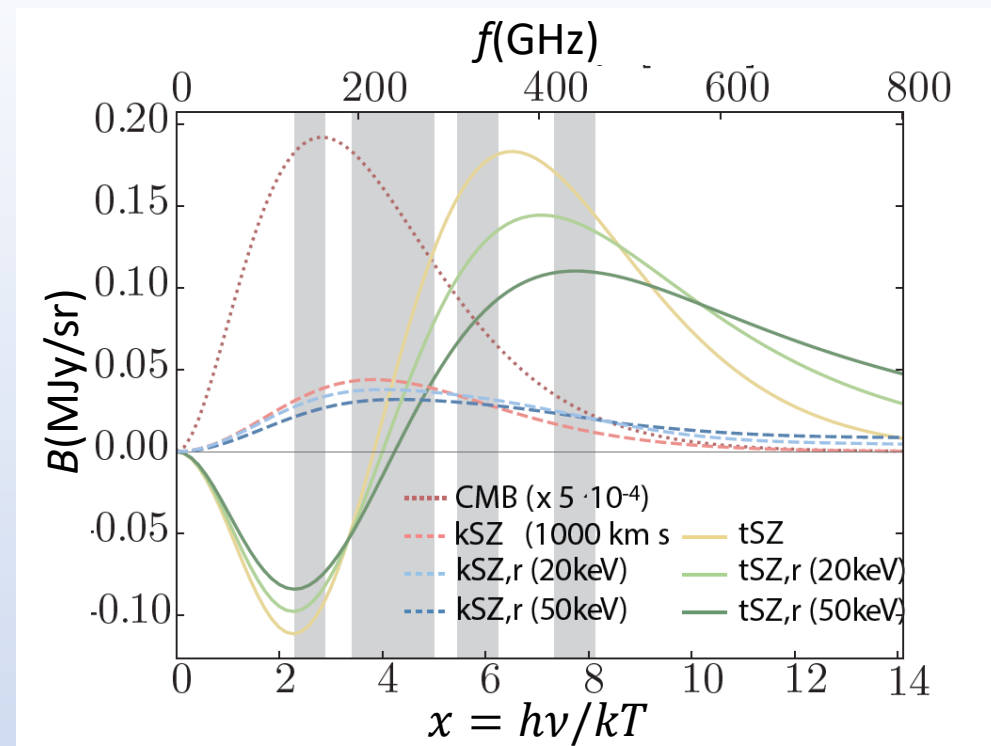


Band Center (GHz)	Bandwidth (GHz)	Beam FWHM (arcmin)	Number of Detectors	Absorbed Power (pW)	Detector Sensitivity ($\mu\text{K}_{\text{CMB}} \sqrt{\text{s}}$)	Instrument Sensitivity ($\mu\text{K}_{\text{CMB}} \sqrt{\text{s}}$)
150	40	60	3024	0.9	76	1.5
220	55	40	3024	1.1	123	2.4
280	70	60	2016	1.4	220	5.4
350	85	50	2016	1.6	550	13.4



Science Case 2 : Anisotropic spectral distortions

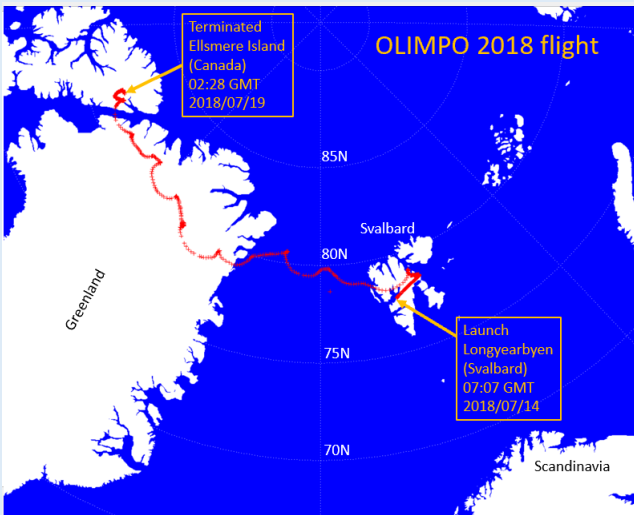
- Sunyaev-Zeldovich effect in clusters of galaxies and other ionized structures (thermal and kinetic):
 - Difficult to access from the ground at $f > 280$ GHz
 - Large (1° diameter) clusters and structures difficult to map from the ground even at 150 GHz, due to atmospheric fluctuations.
 - A 3m aperture telescope working at 450 GHz (balloon) matches the resolution of a 10m telescope working at 150 GHz (ground: SPT, ACT, ...).
 - Multiband photometry possible at depths and resolutions better than Planck, for a small clusters sample in a single LDB flight (longer integration on small sky patches, more detectors). This allows measurements of e.g. the ICM velocity structure, or mapping bridges between clusters / WHIM. tSZ + e-ROSITA provide mass-weighted temperatures.
 - Low resolution spectroscopy of the SZ possible, in mm/submm bands, to provide a number of spectral bins ($\Delta\nu \sim 1\text{-}5$ GHz) and allow for clean components separation.
- Line intensity mapping (LIM) of rotational CO lines (not properly CMB photons ...)
 - In the 400-600 GHz range can be measured from the stratosphere with a cryogenic telescope and spectrometer,
 - LIM data to be correlated to optical surveys to investigate star formation history.



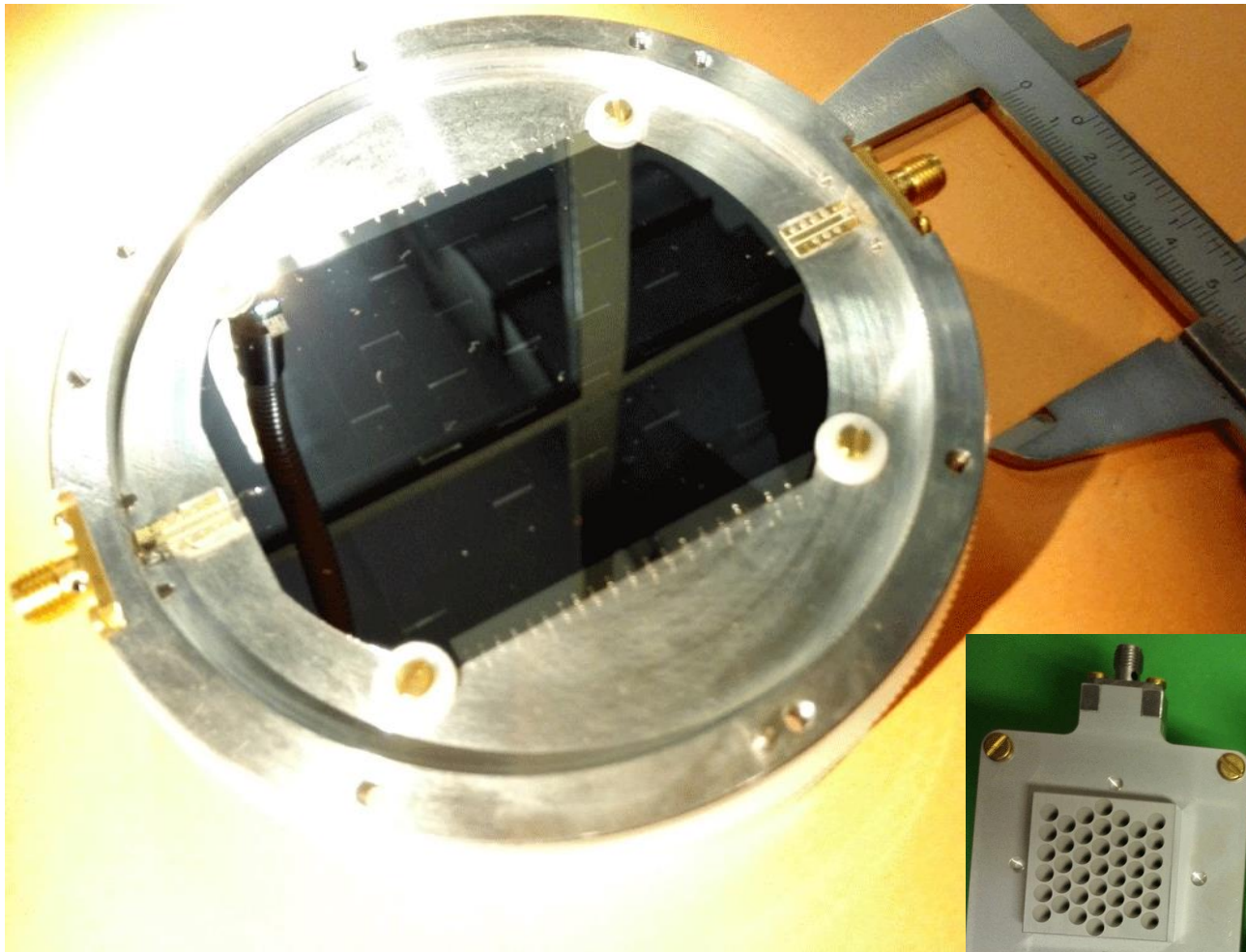
OLIMPO



- The OLIMPO experiment is a first attempt at spectroscopic measurements of the SZ.
- A large (2.6m aperture) balloon-borne telescope with a 4-bands photometric array and a plug-in room temperature **differential FTS** (150, 250, 350, 460 GHz).
- <http://olimpo.roma1.infn.it>



- OLIMPO launched at 07:09 GMT, 14/Jul/2018, from Longyearbyen (Svalbard)
- Great performance of Kinetic Inductance Detector Arrays, Telescope and Spectrometer.
- First Validation of KIDs in space conditions
- Satellite TM/TC failure - only LOS contact, first 20h – engineering flight

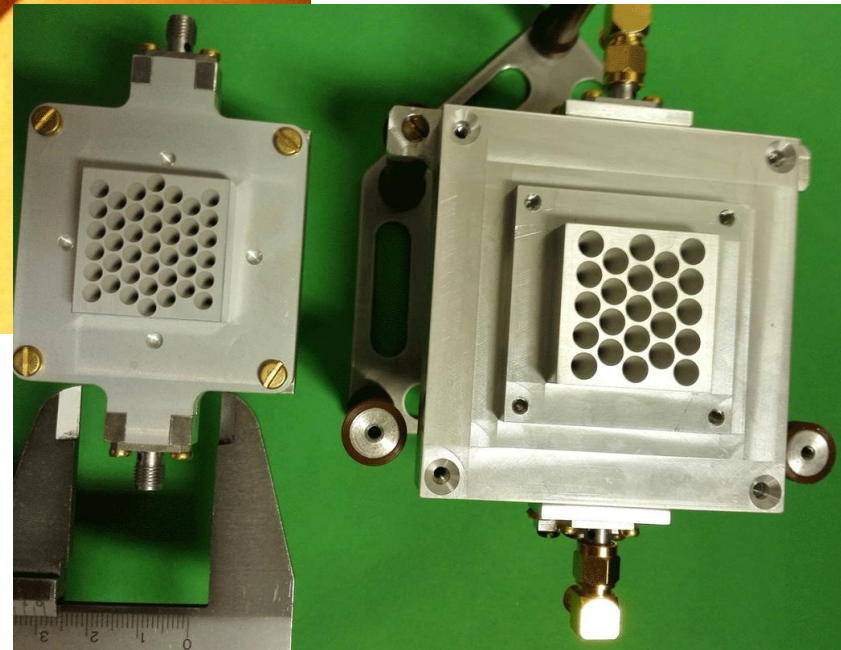


OLIMPO Kinetic Inductance Detectors

AL LEKIDs @
140, 200, 340, 480 GHz

100-600 MHz res.

CNR-IFN + Sapienza



- The instrument is based on a double Martin Puplett Interferometer configuration to avoid the loss of half of the signal.

- A wedge mirror splits the sky image in two halves I_a and I_b , used as input signals for both inputs of the two FTS's.

- In the FTSs the beam to be analyzed is split in two halves, and a variable optical path difference is introduced.

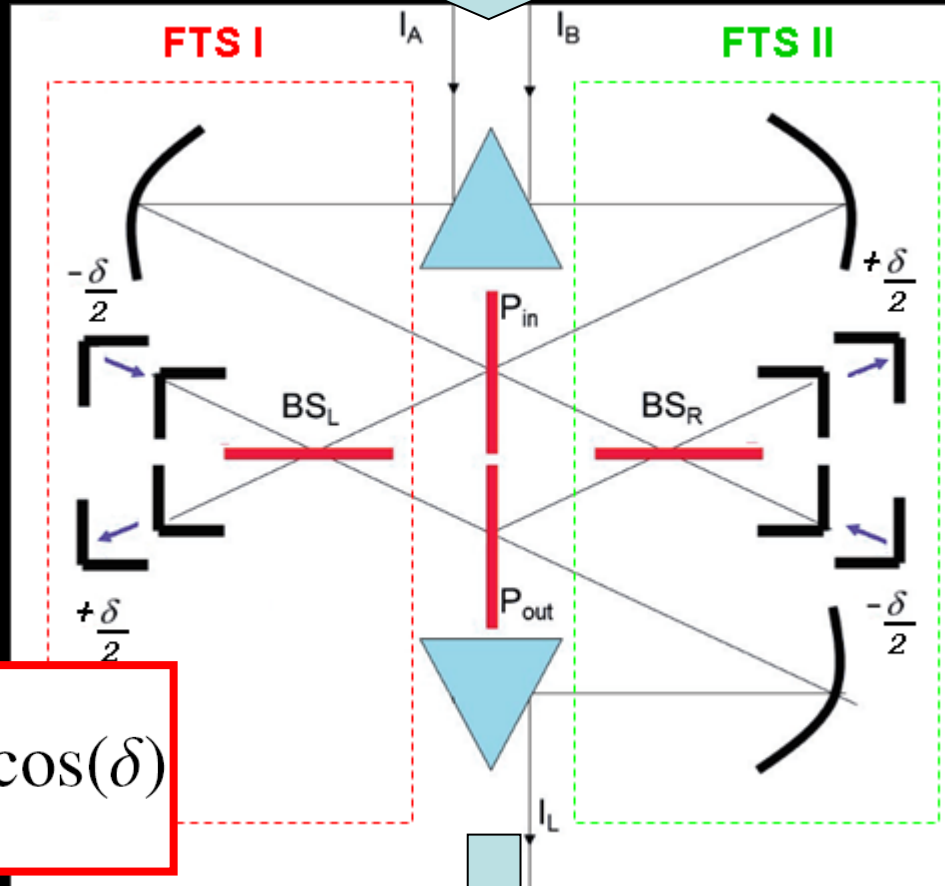
See Schillaci et al. A&A 565, A125, 2014 for a detailed description of the instrument. The output brightness is

$$I_L = \frac{1}{2}(I_a + I_b) + \frac{1}{2}(I_a - I_b) \cos(\delta)$$

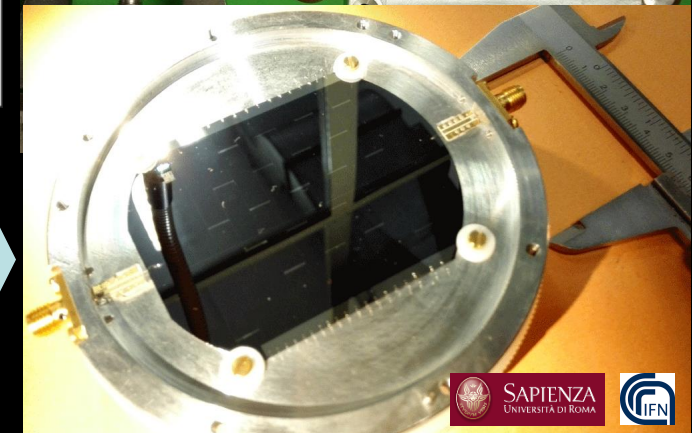
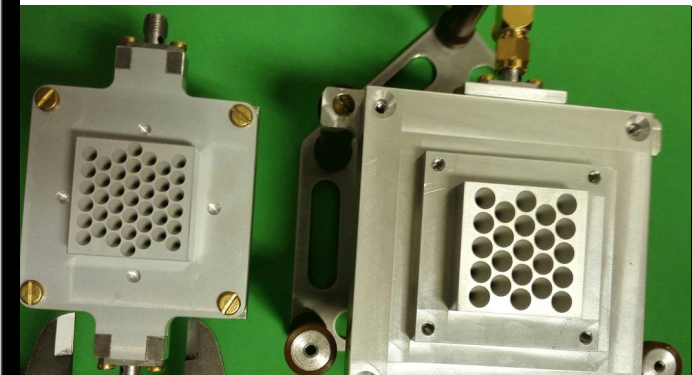
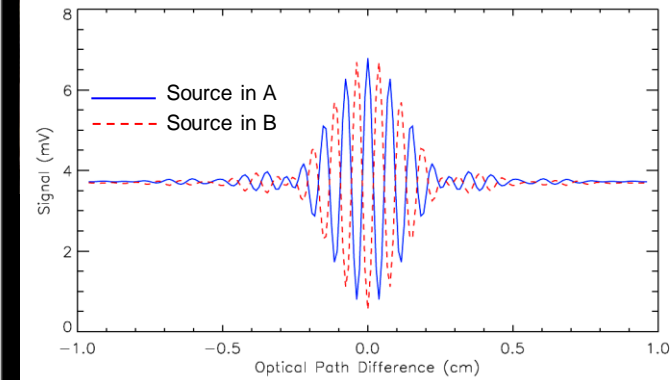
δ = variable phase shift, introduced by the variable optical path difference.

Only the *difference* between the two input brightnesses is modulated by the variable optical path difference. CMRR > 50 dB

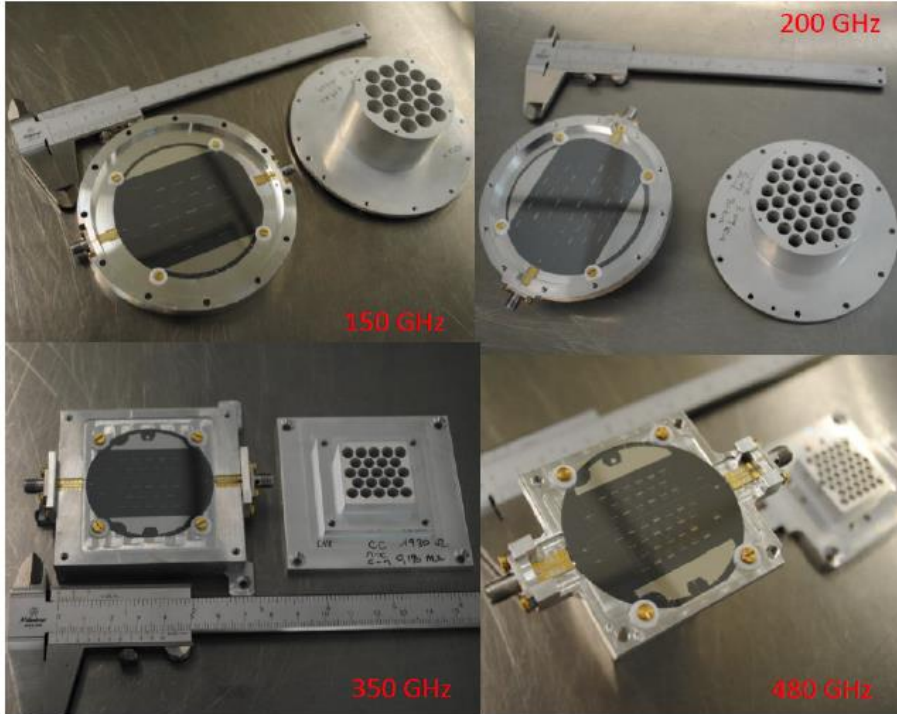
Olimpo Telescope



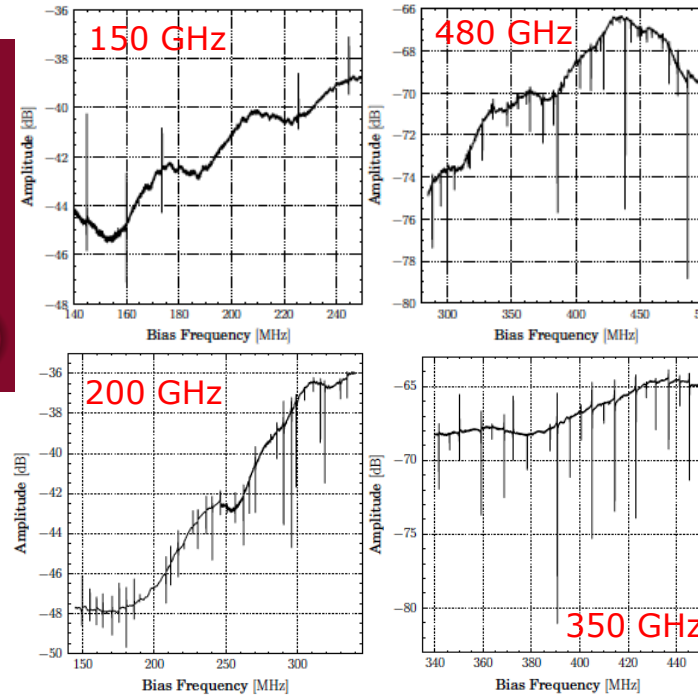
Olimpo
Cryostat
KID arrays



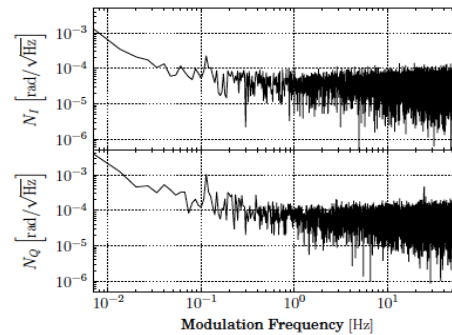
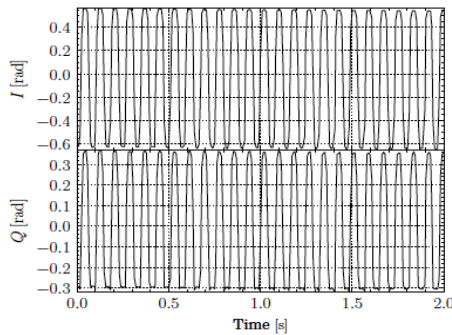
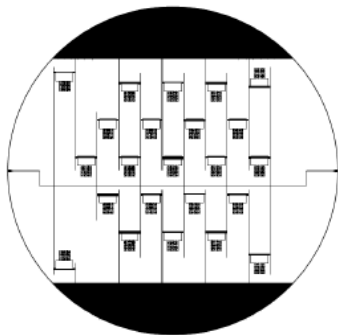
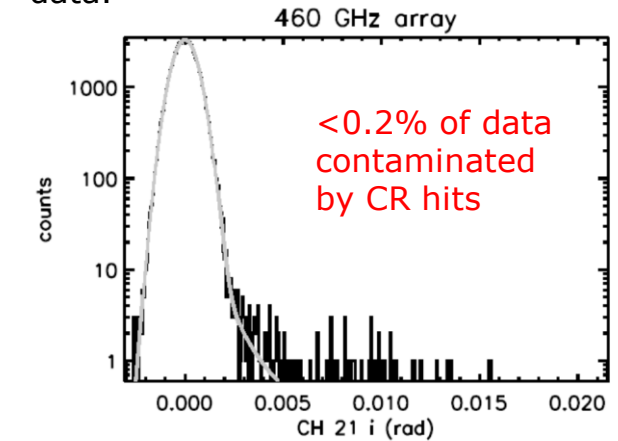
OLIMPO: Kinetic Inductance Detectors



CNRIEN Istituto di Fotonica e Nanotecnologie
SAPIENZA UNIVERSITÀ DI ROMA

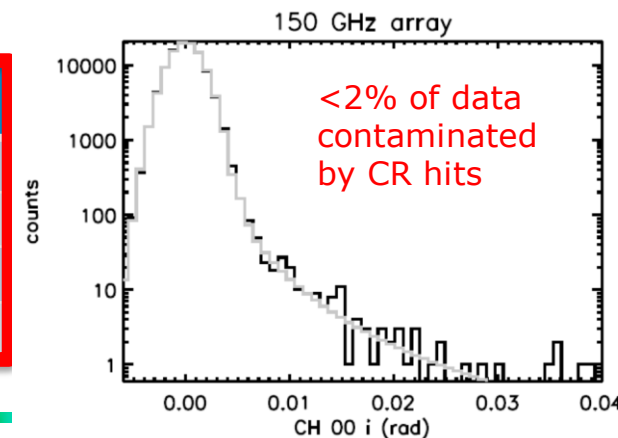


KIDs were tuned for the flight background and operated flawlessly at float. We measured photon noise limited performance, with Cosmic rays hits contaminating < 2% of the data.



Channel	$NET_{RJ} [mK/\sqrt{Hz}]$
150 GHz	0.180
200 GHz	0.145
350 GHz	0.288
480 GHz	0.433

typical NET



See Paiella et al. (2019) JCAP01(2019)039 - Masi et al. (2019) JCAP07(2019)003

Expected results from science flight

Photometric configuration

Instrument	Map Noise ($\mu\text{K}_{\text{CMB}}\text{-arcmin}$)				Notes
	150 GHz	250 GHz	350 GHz	480 GHz	
OLIMPO	1.4	0.7	9.1	26	5 clusters
OLIMPO-CIB	0.7	2.7	4.4	31	single- T_d fit residual
<i>Planck</i> [66]	33	47	150	3700	full sky
CCAT-P [67]	N/A	15	107	407	wide survey (20k deg ²)
CCAT-P [67]	N/A	3	21	81	deep survey (100 deg ²)
CMB-S4 [68]	1.5	4.8	59	N/A	LAT config "2" (17k deg ²)

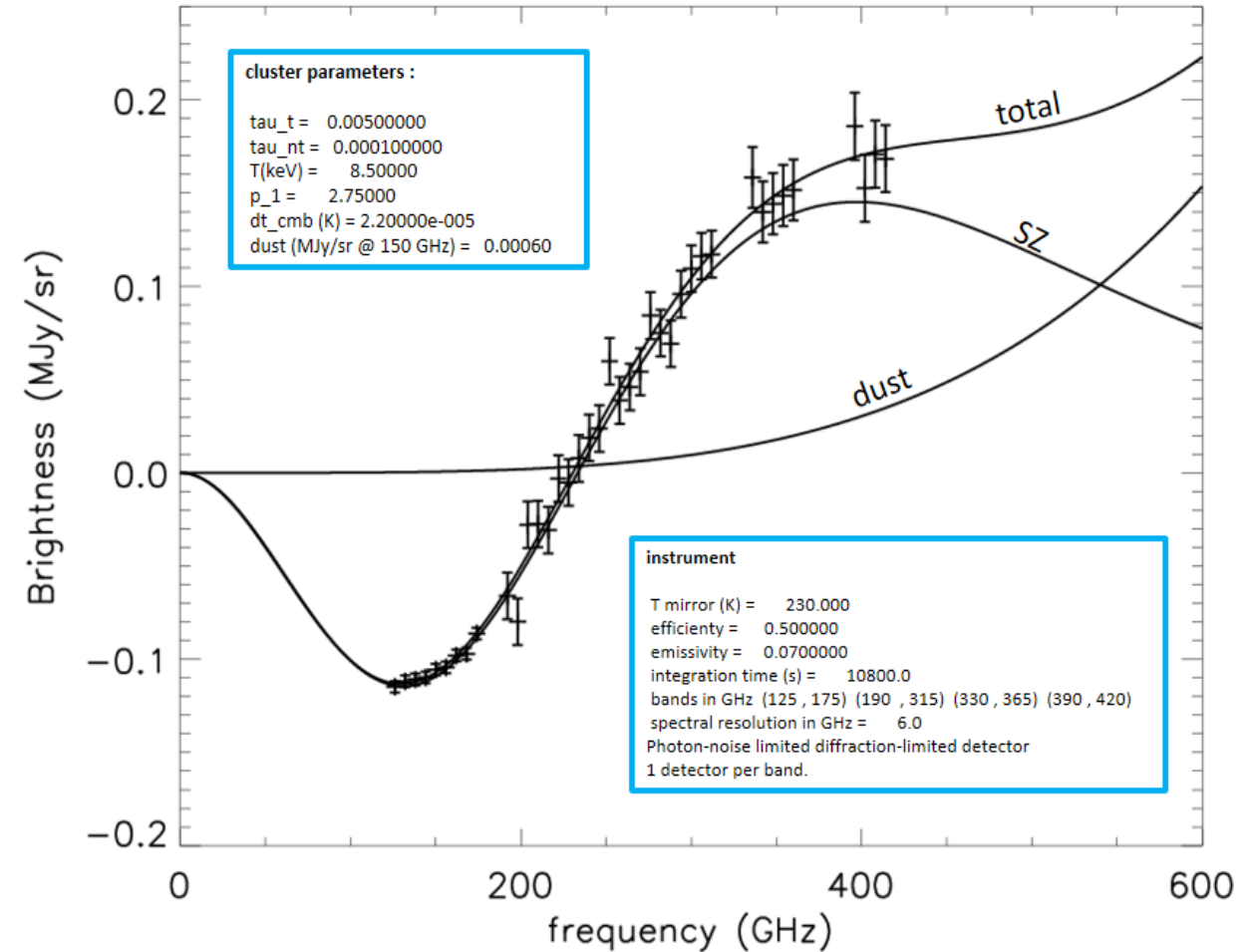
After the engineering flight, OLIMPO is currently looking for a scientific flight opportunity (Antarctic LDB).

Targets:

- A selection of a few a highly relaxed cool-core systems
- A morphologically regular object lacking a cool core
- A major merger with an ICM shock and significant radio emission
- A pre-merger pair connected by an emission bridge potentially associated with a filament.

This diversity will help mitigate selection-related systematics in our ensemble results.

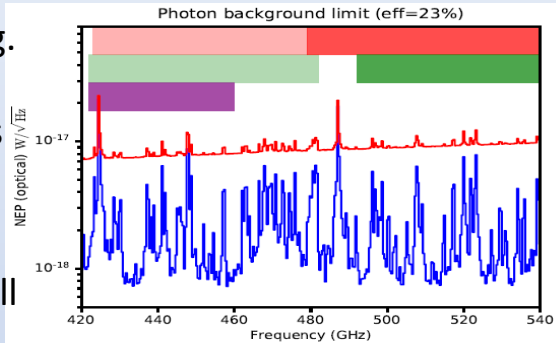
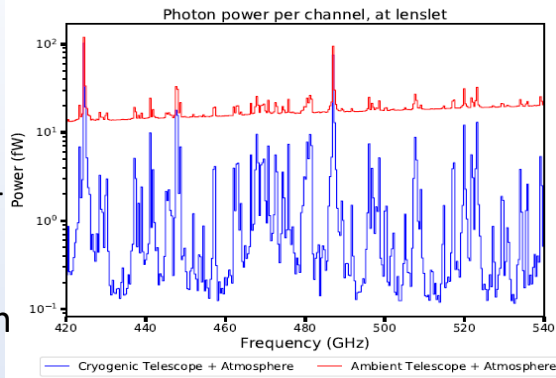
Spectroscopic configuration



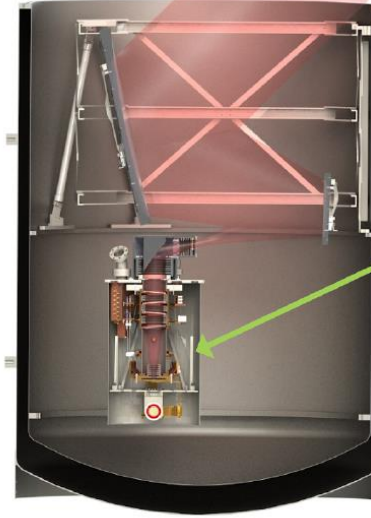
EXCLAIM

Cataldo+, arXiv:2101.11734

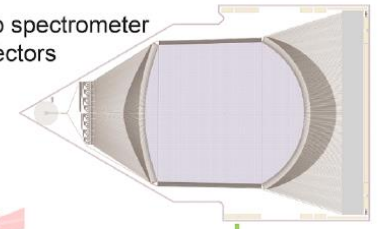
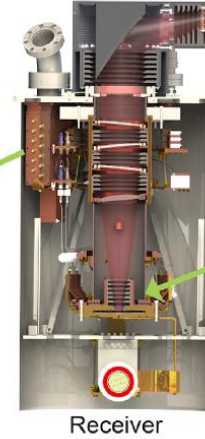
- The EXperiment for Cryogenic Large-Aperture Intensity Mapping (EXCLAIM) is a balloon-borne far-infrared telescope that will survey star formation history over cosmological time
- EXCLAIM will map the emission of redshifted carbon monoxide and singly-ionized carbon lines in windows over a redshift range $0 < z < 3.5$, following an innovative approach known as intensity mapping.
- Intensity mapping measures the statistics of brightness fluctuations of cumulative line emissions instead of detecting individual galaxies, thus enabling a blind, complete census of the emitting gas.
- To detect this emission unambiguously, EXCLAIM will cross-correlate with a spectroscopic galaxy catalog.
- The EXCLAIM mission uses a cryogenic design to cool the telescope optics to approximately 1.7 K. The telescope features a 90-cm primary mirror to probe spatial scales on the sky from the linear regime up to shot noise-dominated scales.
- The telescope optical elements couple to six μ -Spec spectrometer modules, operating over a 420-540 GHz frequency band with a spectral resolution of 512 and featuring microwave kinetic inductance detectors.
- the expected 2σ sensitivity to the surface brightness-bias product for $0 < z < 0.2$ (SDSS MAIN) for CO $J = 4-3$, $J = 5-4$, $0.2 < z < 0.4$ for $J = 5-4$, $J = 6-5$ (BOSS LOWZ), $0.4 < z < 0.7$ for $J = 6-5$ (CMASS), and $2.5 < z < 3.5$ for [CII] (QSO) are [0.15; 0.28; 0.30; 0.37; 0.45; 13] kJy/sr, respectively.



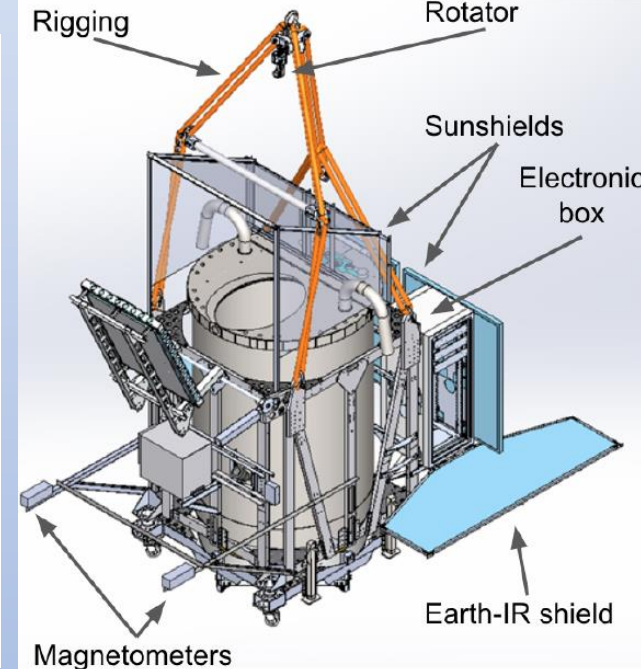
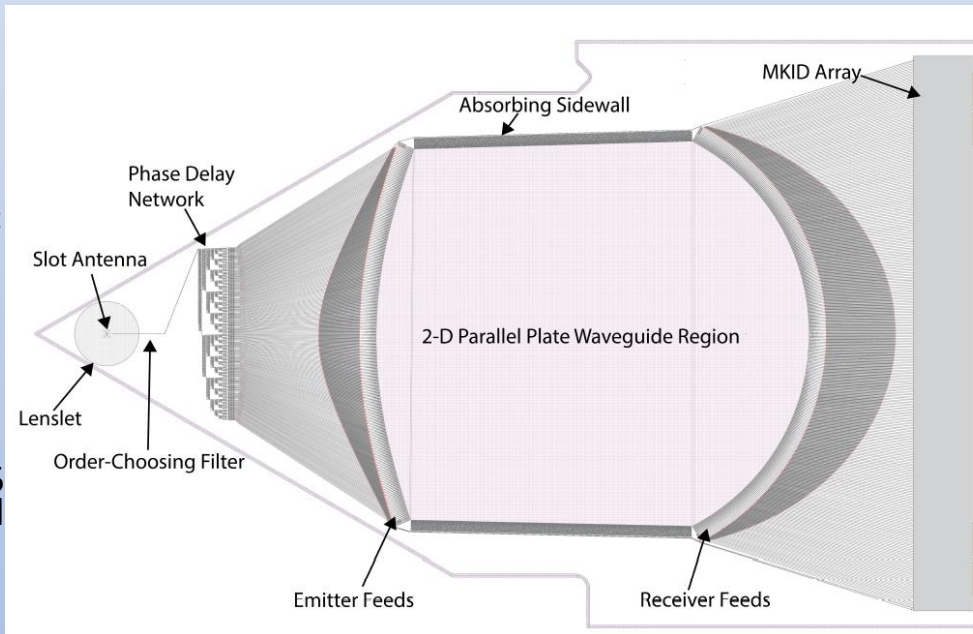
Balloon-borne cryogenic telescope



μ -Spec on-chip spectrometer with MKID detectors

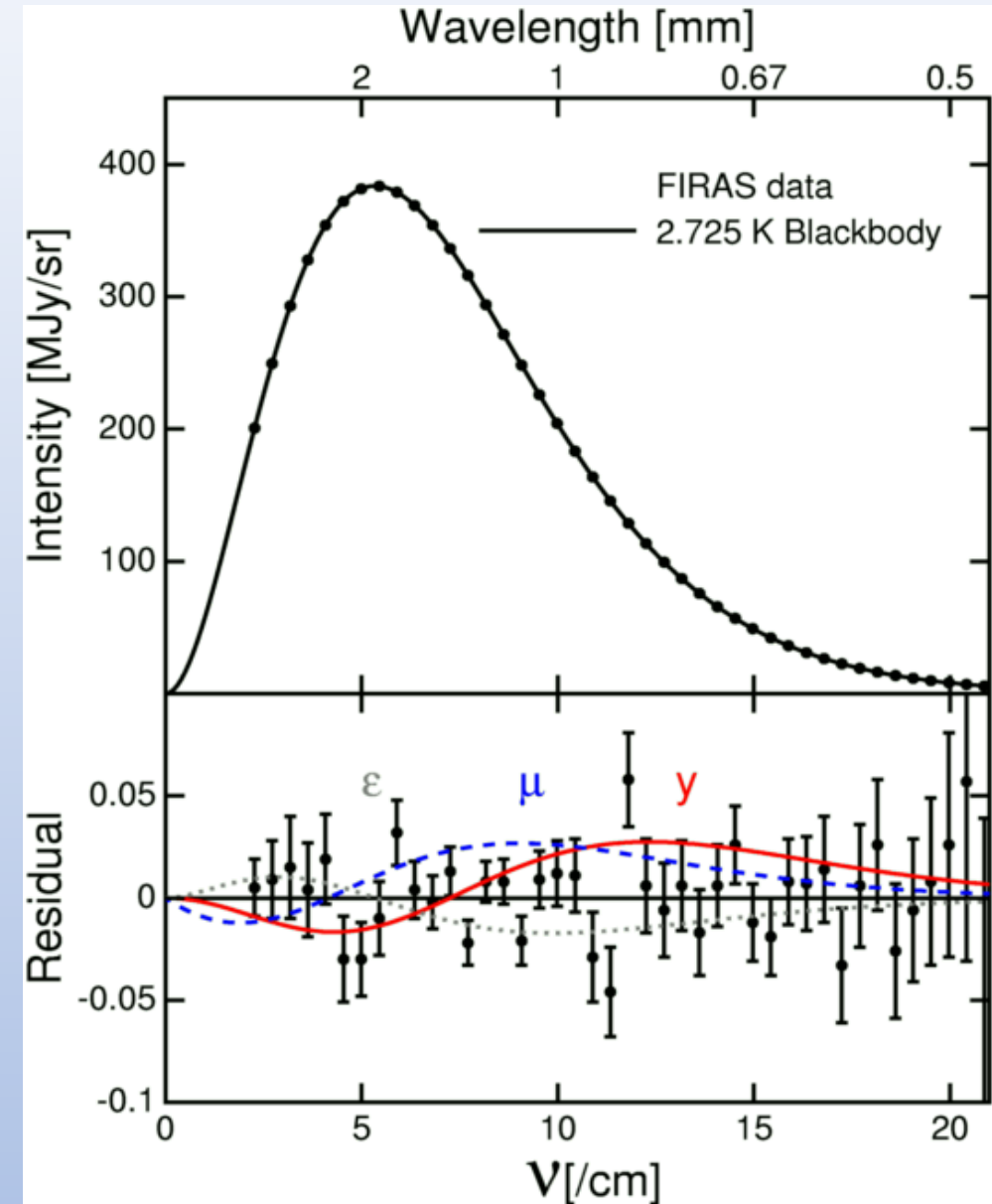


Focal plane assembly with 6 spectrometers at 100 mK



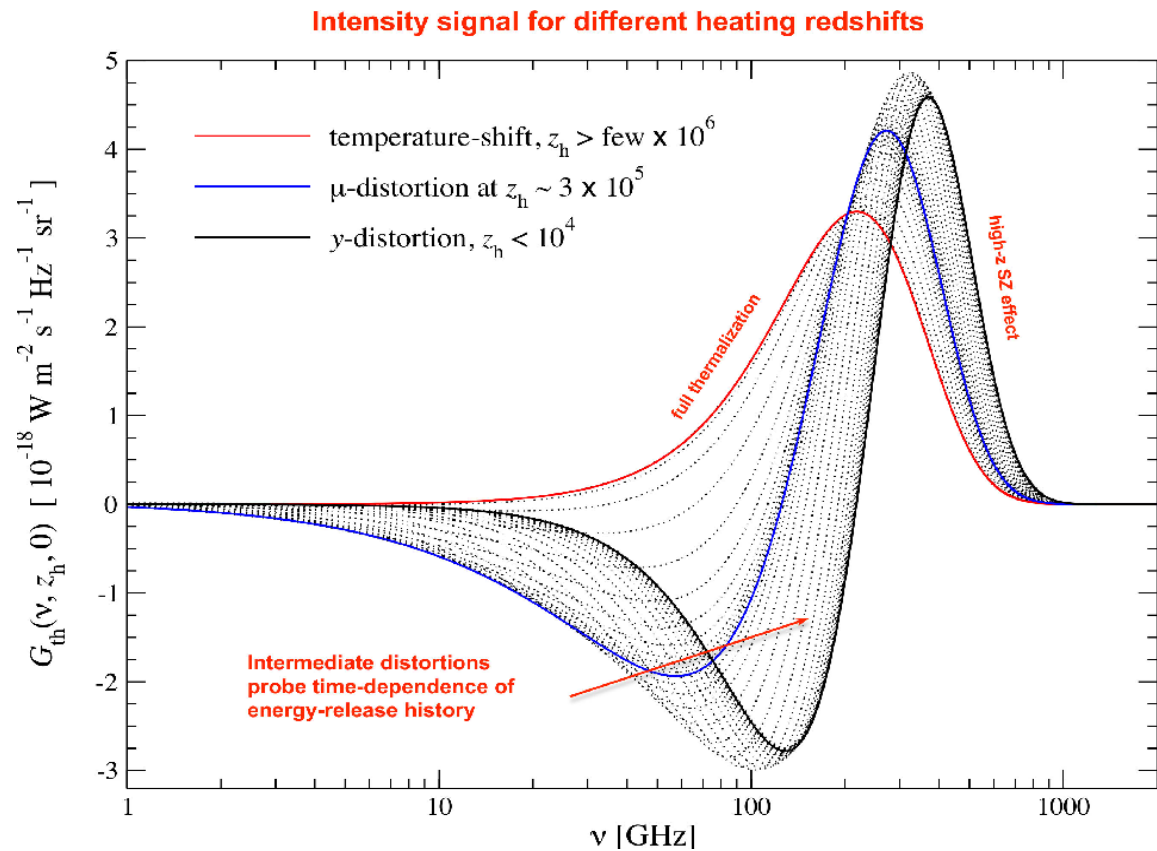
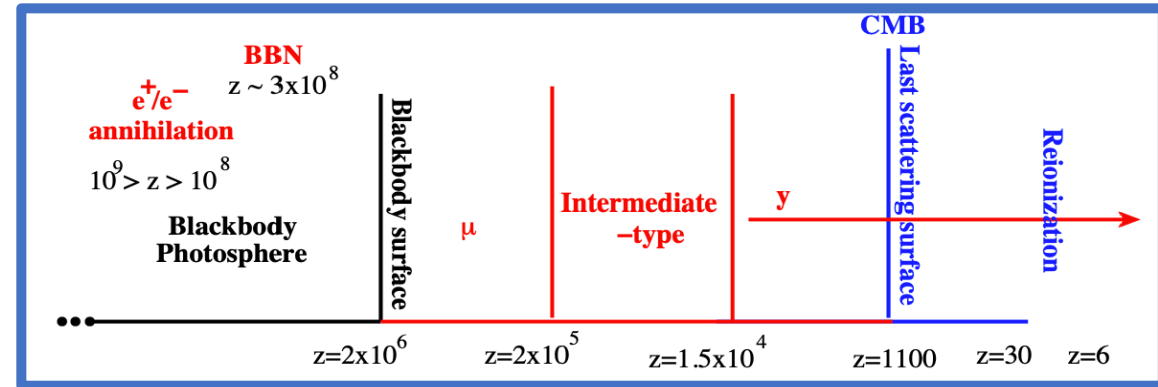
Science Case 3 : Isotropic spectral distortions

- In the primeval fireball, CMB photons are frequently scattered by free electrons, and efficiently thermalized, thus acquiring their blackbody spectrum.
- After recombination, CMB photons do not interact with matter anymore, and the blackbody spectrum is maintained, with its temperature scaling as the inverse of the scale factor.
- This has been measured by COBE-FIRAS: **a perfect blackbody spectrum**, within deviations, if any, < 100 ppm of its maximum brightness.
- If there was any deviation from thermal equilibrium, the result would be a *spectral distortion*, a deviation from a pure Planck spectrum.
- **Spectral deviations are expected, at a level of 20 ppm or lower.** See e.g. J. Chluba, R. A. Sunyaev MNRAS (2012) 419 1294
- The obvious choice for this measurement is to use an absolute spectrometer on a satellite (see e.g the PIXIE proposal).
- Can we attempt a measurement from a stratospheric balloon ?



Isotropic spectral distortions

- Two classes of phenomena lead to distortions:
 - Energy injection (due to matter – photons interactions)
 - Production of energetic photons or particles (i.e. entropy variations)
- Depending on when these phenomena happened, the generated distortion is, or is partially, or is not reabsorbed by thermalization processes.
- Very early departures ($z > 2 \times 10^6$) are thermalized (to a higher temperature).
- Later releases produce isotropic distortions with different amplitudes and spectral shapes: intermediate energy releases produce a Bose-Einstein (μ) distortion; late energy releases produce a Compton (y) distortion.
- The distortion signature from different energy-release scenarios is not just given by a superposition of pure μ - and pure y -distortion. The small residual beyond μ - and y -distortion contains information about the exact time-dependence of the energy-release history.
- A rich information content to be exploited, if isotropic distortions are detected.**



Wide theoretical literature

- Early works

- Zeldovich & Sunyaev, 1969, Ap&SS, 4, 301
- Sunyaev & Zeldovich, 1970, Ap&SS, 7, 20
- Illarionov & Sunyaev, 1975, Sov. Astr., 18, 413

- Additional important milestones

- Danese & de Zotti, 1982, A&A, 107, 39
- Burigana, Danese & de Zotti, 1991, ApJ, 379, 1
- Hu & Silk, 1993, Phys. Rev. D, 48, 485
- Hu, 1995, PhD thesis

- More recent overviews

- Sunyaev & Chluba, 2009, AN, 330, 657
- Chluba & Sunyaev, 2012, MNRAS, 419, 1294
- Chluba, 2013, MNRAS, 436, 2232 & ArXiv:1405.6938

- Many physical phenomena involved; some are unavoidable:

- **Cooling by adiabatically expanding ordinary matter** (Chluba, 2005; Chluba & Sunyaev 2011; Khatri, Sunyaev & JC, 2011)
- **Heating by decaying or annihilating relic particles** (Kawasaki et al., 1987; Hu & Silk, 1993; McDonald et al., 2001; JC, 2005; JC & Sunyaev, 2011; JC, 2013; JC & Jeong, 2013)
- **Evaporation of primordial black holes & superconducting strings** (Carr et al. 2010; Ostriker & Thompson, 1987; Tashiro et al. 2012; Pani & Loeb, 2013)
- **Dissipation of primordial acoustic modes & magnetic fields** (Sunyaev & Zeldovich, 1970; Daly 1991; Hu et al. 1994; JC & Sunyaev, 2011; Chluba et al. 2012 - Jedamzik et al. 2000; Kunze & Komatsu, 2013)
- **Cosmological recombination radiation** (Zeldovich et al., 1968; Peebles, 1968; Dubrovich, 1977; Rubino-Martin et al., 2006; JC & Sunyaev, 2006; Sunyaev & JC, 2009)
- **Signatures due to first supernovae and their remnants** (Oh, Cooray & Kamionkowski, 2003)
- **Shock waves arising due to large-scale structure formation** (Sunyaev & Zeldovich, 1972; Cen & Ostriker, 1999)
- **SZ-effect from clusters; effects of reionization** (Refregier et al., 2003; Zhang et al. 2004; Trac et al. 2008)
- **Additional exotic/new physics processes** (Lochan et al. 2012; Bull & Kamionkowski, 2013; Brax et al., 2013; Tashiro et al. 2013)

Examples:

Constraining primordial density fluctuations and inflation

Experimental Astronomy (2021) 51:1515–1554

1521

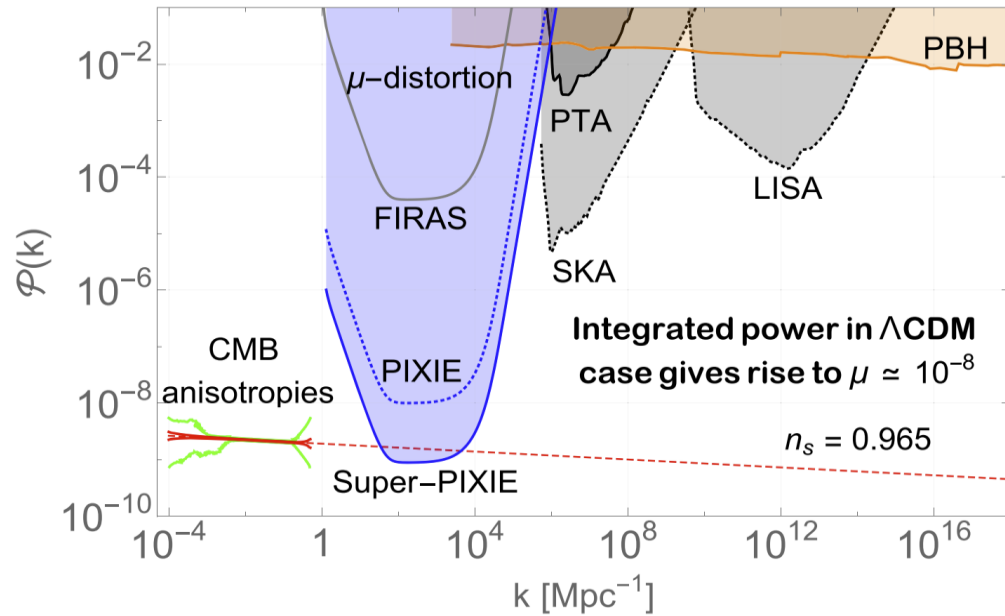


Fig. 2 Forecast constraints (95 % c.l.) on the primordial power spectrum for features with a k^4 profile that cuts off sharply at some larger wavenumber k_p (see [81], for more details). μ -distortions constrain perturbations at scales and levels inaccessible to other probes. Early-Universe models with enhanced small-scale power at $k \simeq 10 - 10^4 \text{ Mpc}^{-1}$ will be immediately ruled out if no distortion with $\mu > 2 \times 10^{-8}$ is detected. The figure is adapted from [82]

Constraining decaying particles yield and lifetime

1526

Experimental Astronomy (2021) 51:1515–1554

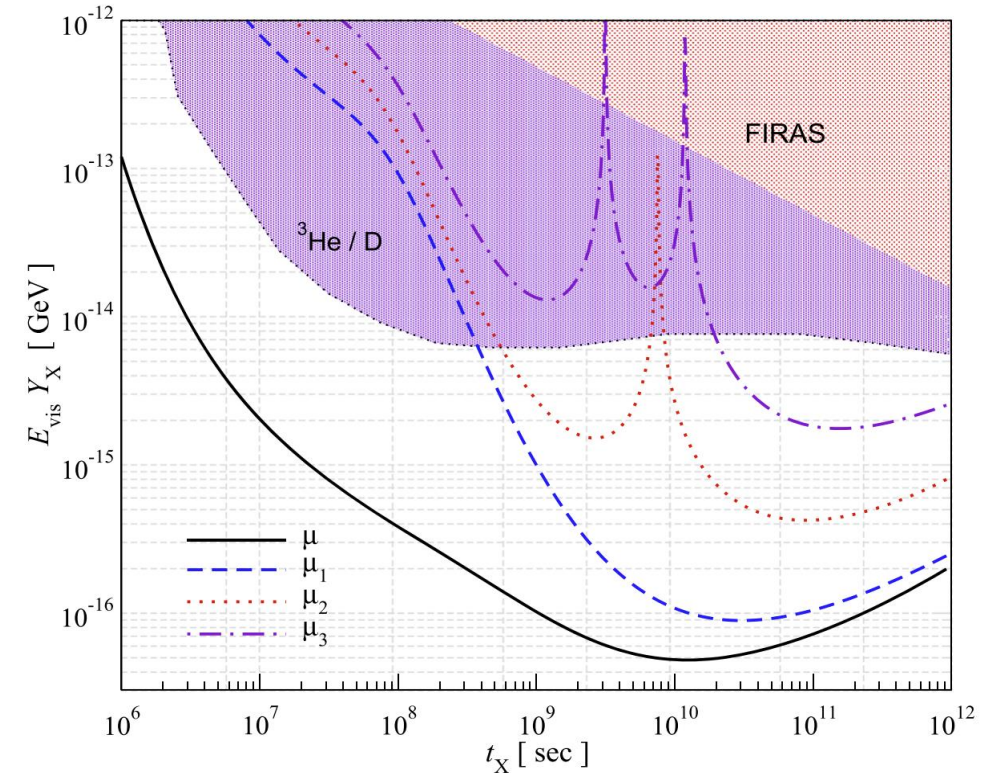
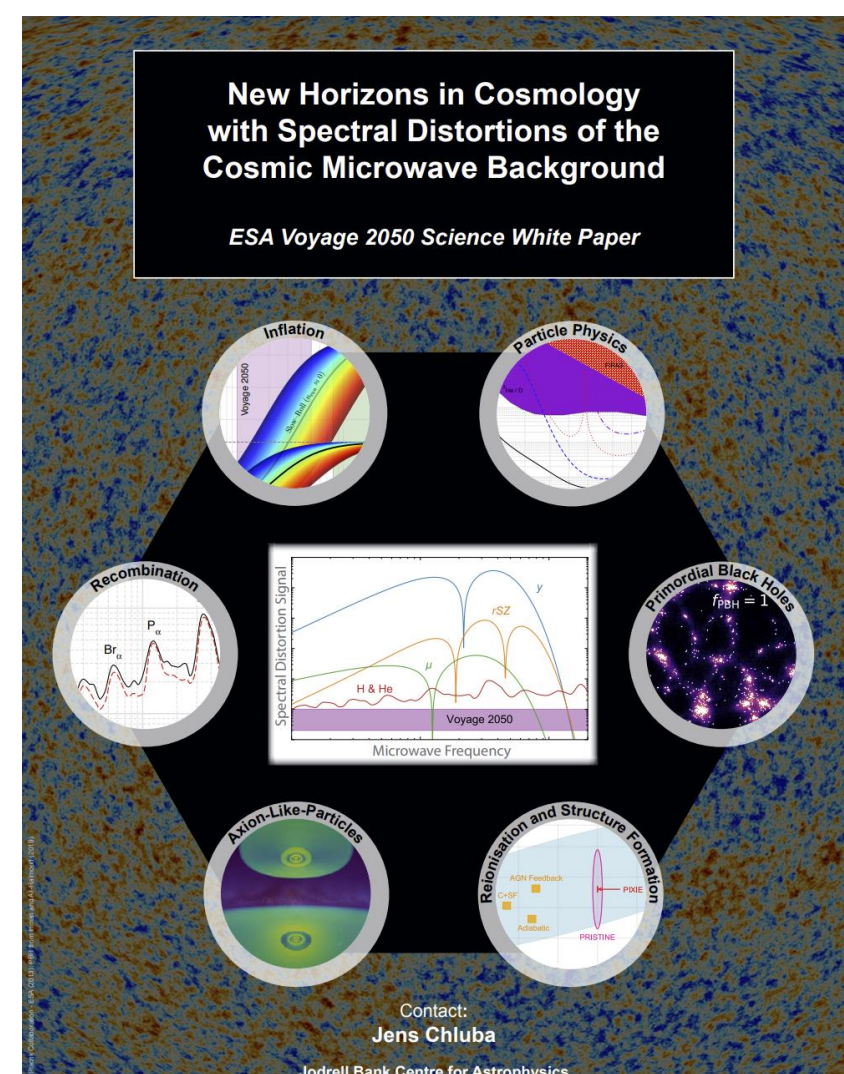


Fig. 5 Constraints on the yield variable, $E_{\text{vis}} Y_X$ (e.g., see [151], for details), from electromagnetic particle decay for varying lifetime, t_X . For the distortion forecast a spectral sensitivity of $\sigma(\mu) \simeq 10^{-8}$ (aka *SuperPIXIE*) was assumed. The parameters μ_i describe extra time-dependent information available from the r -type distortion (see [17], for details). For comparison we quote the constraints from [151, 152] for decays into e^+e^- derived from the ${}^3\text{He}/\text{D}$ abundance ratio. Future spectral distortion measurements could improve the constraint on decaying particles with lifetimes $t_X \simeq 10^7 - 10^{12}$ by orders of magnitude. Using the r -type distortion we could furthermore break the degeneracy between particle yield and lifetime, should a significant distortion signal be detected [13, 17]. Figure adapted from [17]

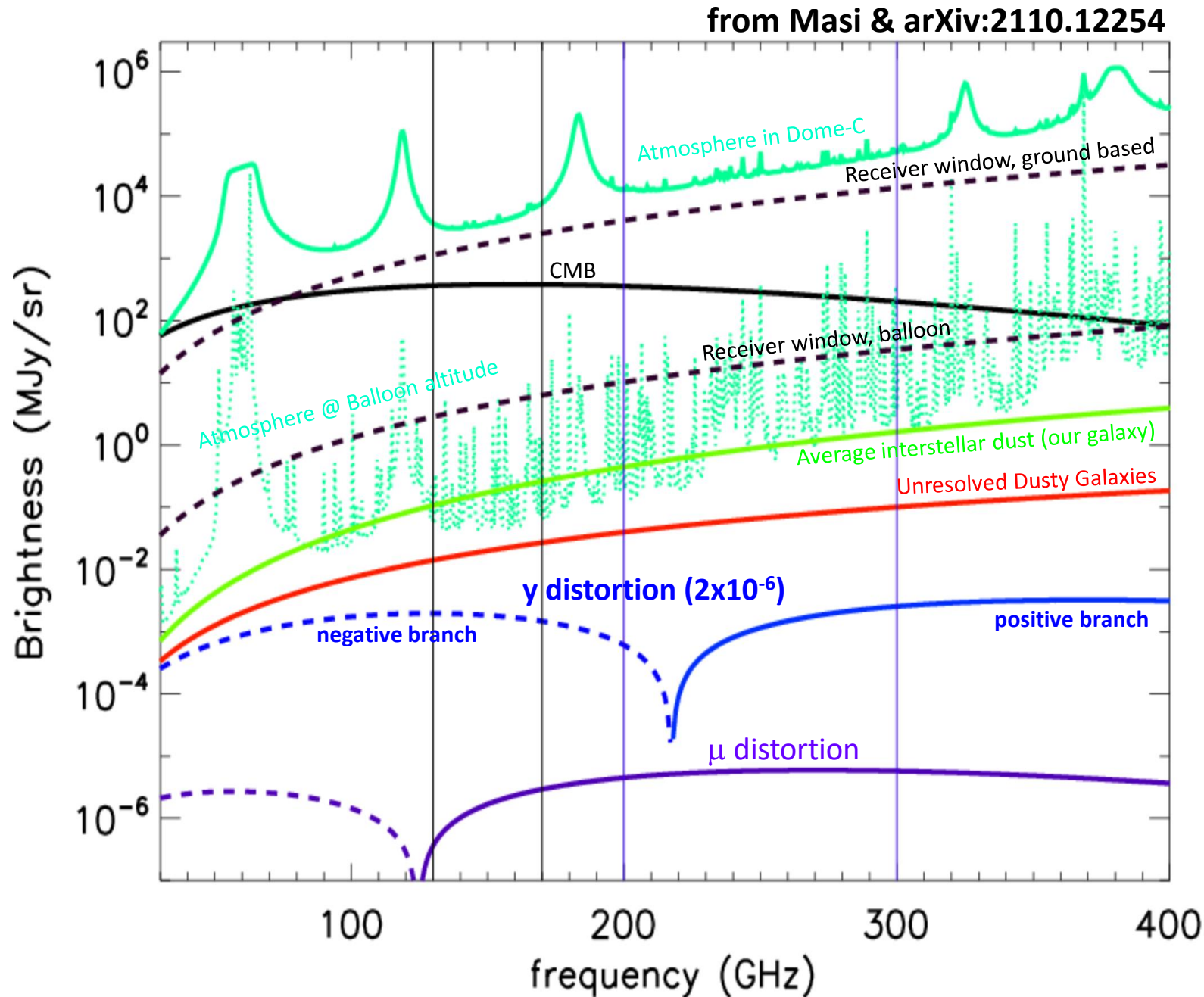
Wide theoretical literature

- **Take home messages from theoretical literature:**
- Isotropic spectral distortions add a new dimension to CMB science since they probe the thermal history at different stages of the Universe.
- Several guaranteed signals are expected
 - y -distortion from post recombination ionized matter
 - Silk damping signal & recombination radiation
- Complementary and independent information:
 - cosmological parameters from the recombination radiation
 - New/additional test of large-scale anomalies
- Test various inflation models
 - damping of the small-scale power spectrum
- Discovery potential
 - decaying particles, including dark matter generation
 - other exotic sources of distortions
- **Additional take home message: isotropic spectral distortions are small, but for several of them we do have a reliable expectation value for the amplitude.**
- For example, the Comptonization due to post recombination ionized matter along the line of sight produces $y=1.8 \times 10^{-6}$



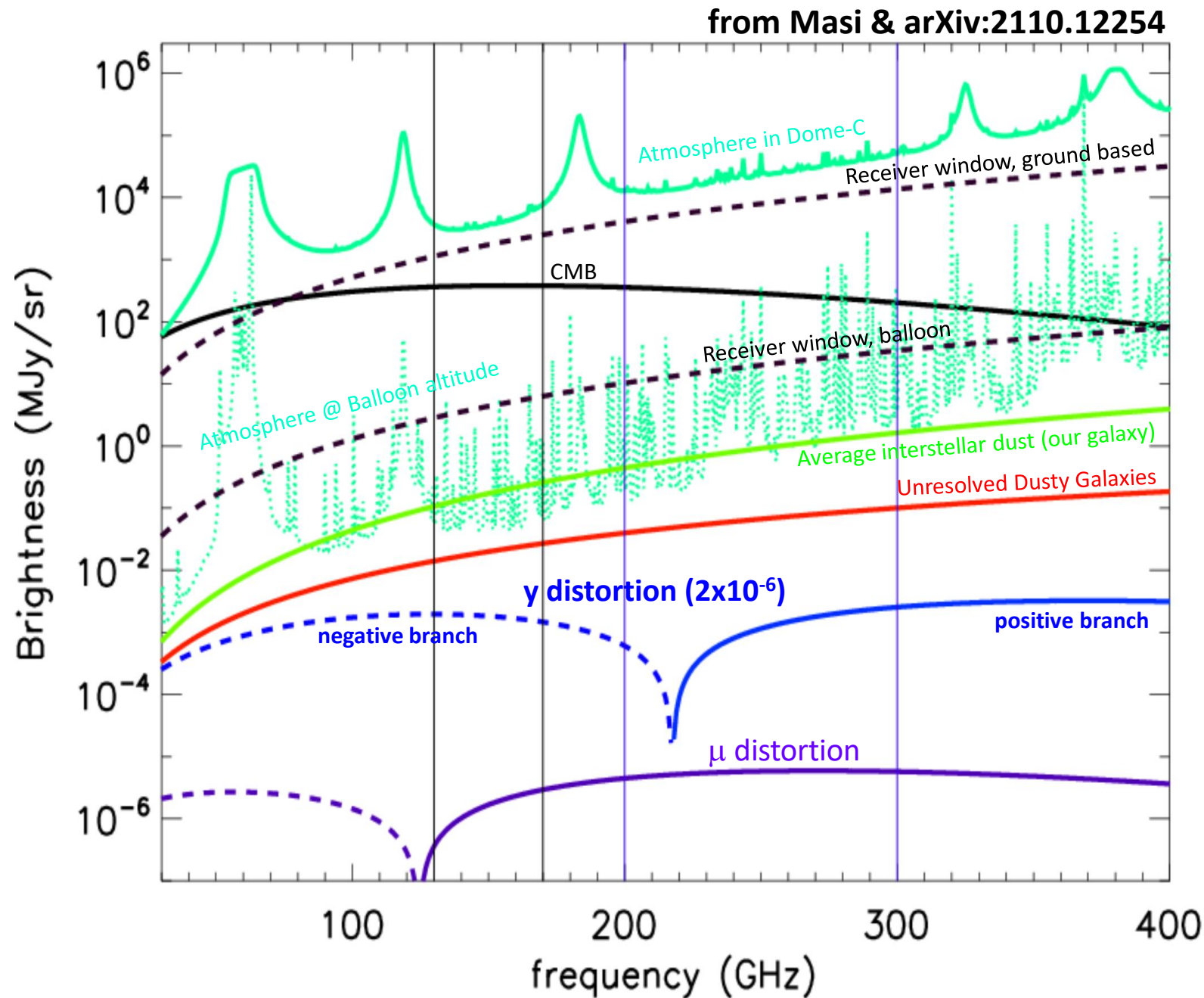
Reality check

- The isotropic distortion signals are embedded in much stronger isotropic local and astrophysical foregrounds.
- To avoid local foregrounds (atmosphere, instrument), the final measurement requires a space mission.
- Ground-based and balloon-borne measurements are necessary to validate instrument solutions, measurement strategies, and astrophysical foregrounds.
- In the best *ground-based environment*, the largest distortion signal is ~ 6 orders of magnitude smaller than the emission of the atmosphere: a very difficult situation.



A way forward

- In the best *balloon-borne environment*, the largest distortion signal is ~ 3 orders of magnitude smaller than the residual emission of the atmosphere, which is smaller than the CMB and comparable to other isotropic astrophysical foregrounds.
- The undistorted isotropic CMB can be rejected by a nulling instrument (like a Martin-Puplett FTS), where the sky brightness is compared to an internal blackbody at 2.725K.
- The residual emission from the receiver window can be monitored and subtracted by introducing controlled temperature changes.
- This tells us that a **pathfinder balloon-borne instrument can measure the largest γ distortion and the astrophysical foregrounds.** Efficient separation is expected due to the very different spectral shapes.



A staged approach

1) Pathfinder *ground-based* implementation: COSMO, on-going (PRIN, PNRA), see also ASPERA at low frequencies. COSMO will be used to validate the differential spectrometer measurement approach, well beyond FIRAS, using:

- A cryogenic Fourier Transform Spectrometer with ultra-high CMRR
- Tunable cryogenic reference blackbody for nulling
- Window temperature modulation method
- Fast KIDs detectors with fast atmospheric modulation to monitor and remove atmospheric fluctuations

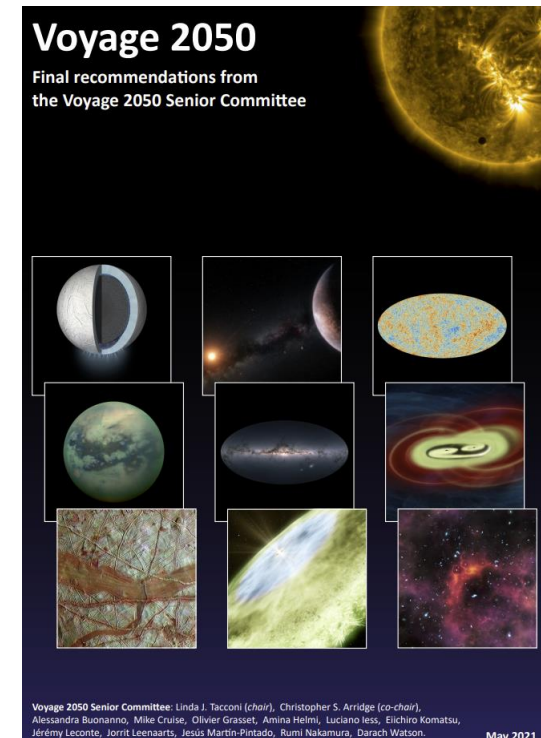
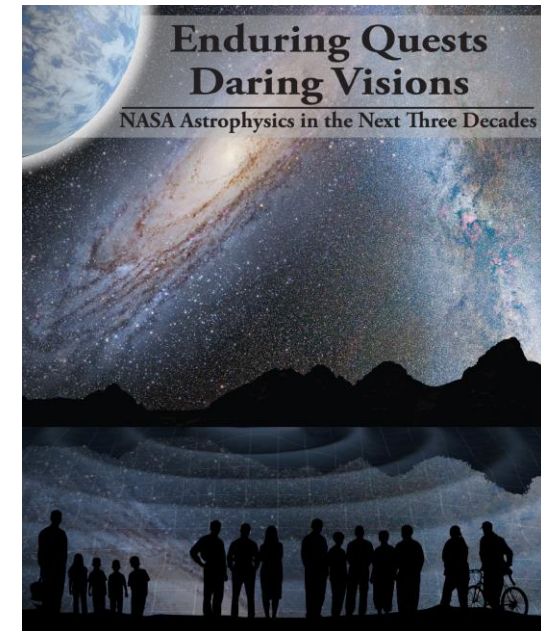
2) Same/similar hardware on a *stratospheric balloon* (in a LHe cryostat): COSMO-Balloon (ASI-Cosmos study), or BISOU (CNES study)

- To measure the largest γ distortion, the astrophysical foregrounds, and demonstrate the efficiency of the separation methods

3) A dedicated *satellite mission*. (PIXIE, CORE, PRISTINE, FOSSIL, V2050 proposals)

- Note that the importance of this science has been officially recognized by
- NASA: 30 years study 2014: <https://arxiv.org/abs/1401.3741>
- ESA: Voyage 2050: <https://www.cosmos.esa.int/documents/1866264/1866292/Voyage2050-Senior-Committee-report-public.pdf>
- However, none of the proposals above has been approved, yet.

- The staged approach depicted here will certainly help the community to produce a convincing proposal, not only from the point of view of science, but also from the instrumental, methodological and programmatic points of view.

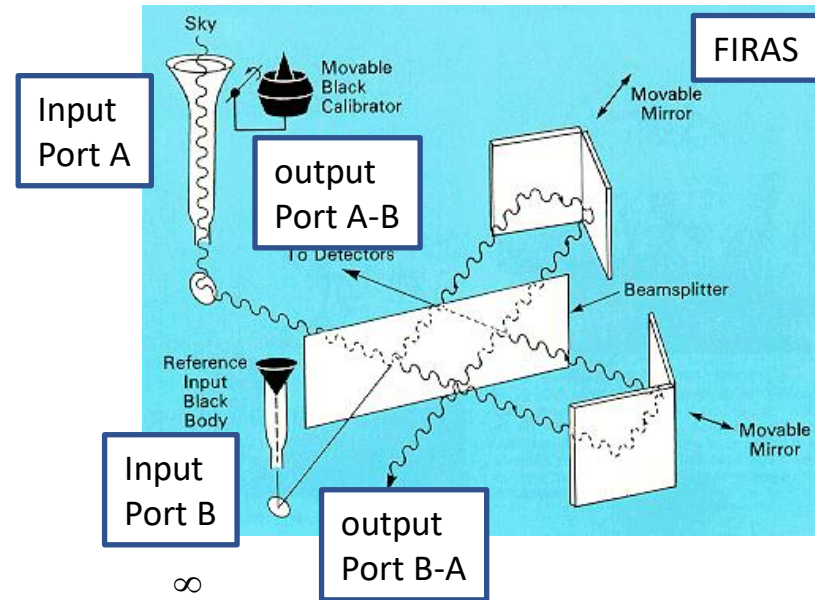


The observable is small,
compared to ... everything.

- Great scientific importance of measuring spectral distortions in the CMB – Cosmology and Fundamental Physics.
- Distortion signals are *guaranteed to exist*, but are *very small* compared to
 - detector noise,
 - instrument emission,
 - atmospheric emission and fluctuations,
 - foregrounds,
 - the CMB itself.
- Intelligent measurement methods required. Experimentalists way behind theorists.
- Here focus on a pathfinder experiment, balloon-borne, which does not target at the smallest distortions, but tries to exploit at best existing, relatively cheap opportunities.

Absolute measurement approach

- The Martin-Pupplett Fourier Transform Spectrometer used in FIRAS and PIXIE has two input ports.
- The instrument is intrinsically differential (DFTS), measuring the spectrum of the difference in brightness at the two input ports. Normally one port looks at the sky, the other one at an internal reference blackbody



Sky
measurement

$$I_{SKY}(x) = C \int_0^{\infty} [S_{SKY}(\sigma) - S_{REF}(\sigma)] rt(\sigma) \{1 + \cos[4\pi\sigma x]\} d\sigma$$

Calibration
measurement

$$I_{CAL}(x) = C \int_0^{\infty} [S_{CAL}(\sigma) - S_{REF}(\sigma)] rt(\sigma) \{1 + \cos[4\pi\sigma x]\} d\sigma$$

COSMO

(COSmic Monopole Observer)

- **COSMO** is a pathfinder spectral distortions experiment, ground-based (Dome-C) in its first implementation.
- A second balloon-borne implementation is under study.
- The instrument is a cryogenic **Differential Fourier Transform Spectrometer**, comparing the sky brightness to an accurate internal blackbody.



SAPIENZA
UNIVERSITÀ DI ROMA

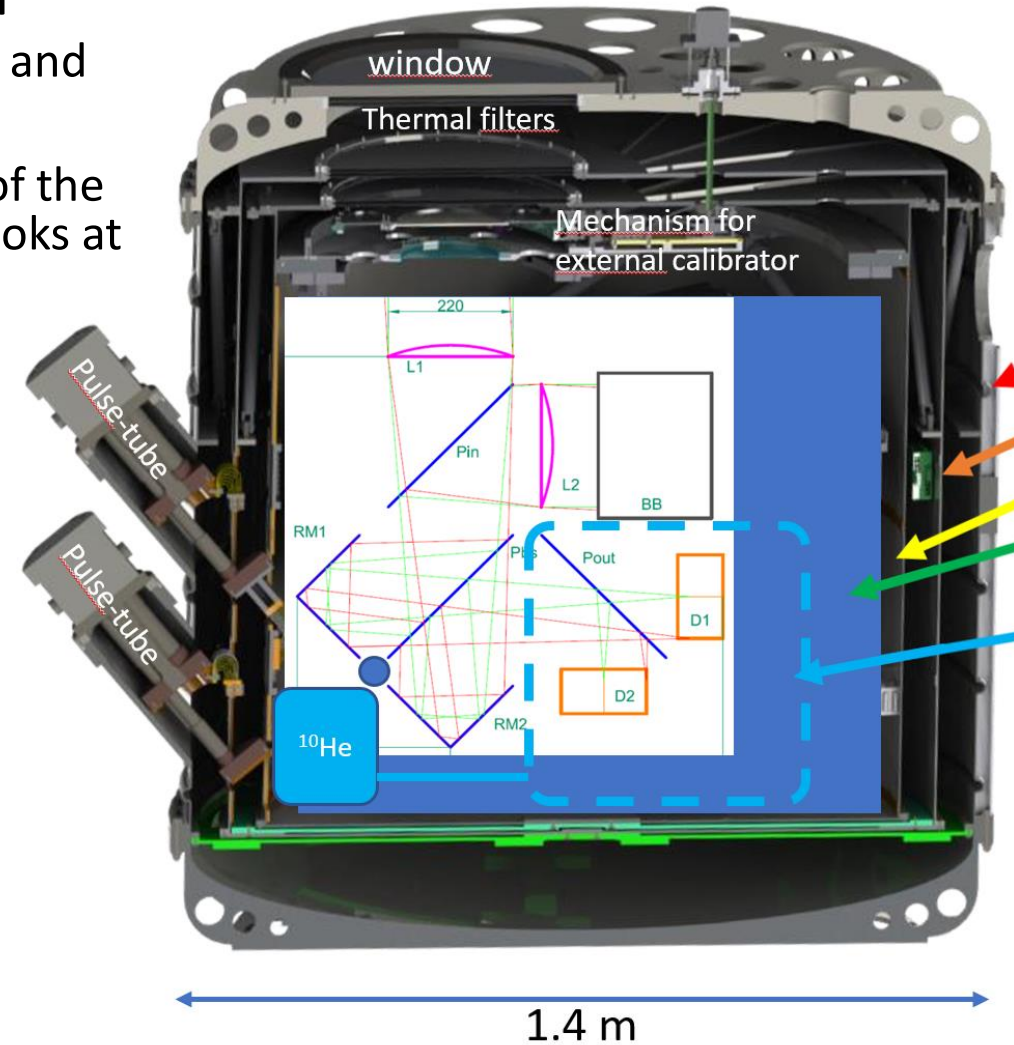
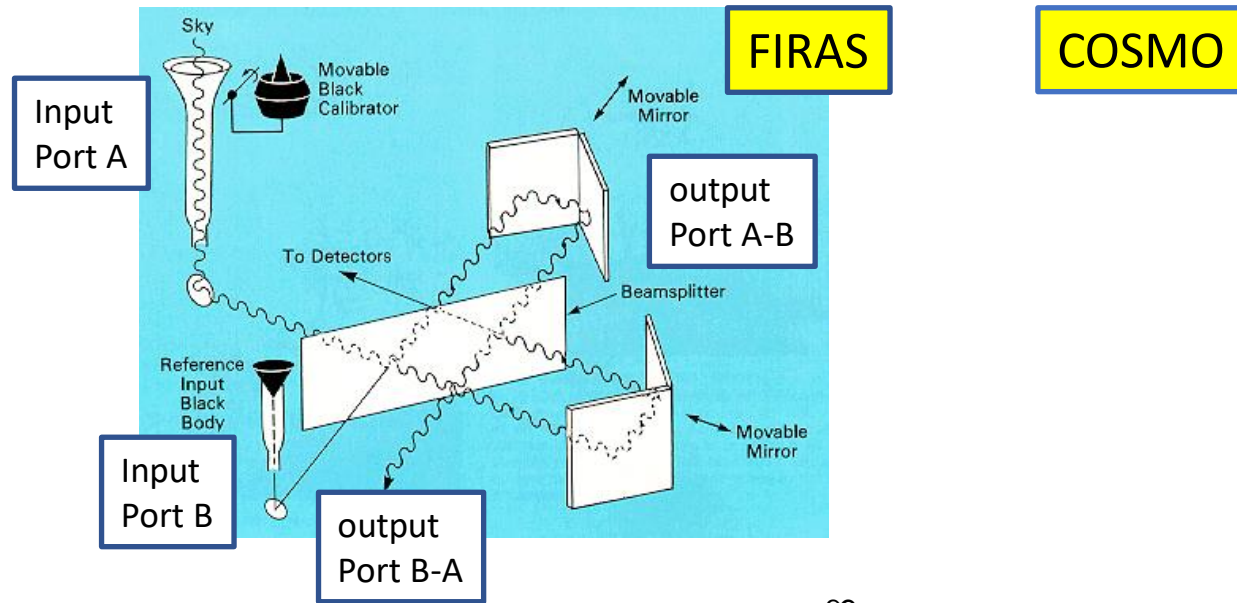


*E. Battistelli, P. de Bernardis, S. Cibella, F. Columbro, A. Coppolecchia, M. Bersanelli, G. D'Alessandro, M. De Petris, C. Franceschet, M. Gervasi, A. Limonta, L. Lamagna, E. Manzan, E. Marchitelli, S. Masi, L. Mele, A. Mennella, A. Paiella, G. Pettinari, F. Piacentini, L. Piccirillo, G. Pisano, S. Realini, C. Tucker, M. Zannoni



Absolute measurement approach

- The Martin-Pupplett Fourier Transform Spectrometer used in FIRAS and PIXIE has two input ports.
- The instrument is intrinsically differential, measuring the spectrum of the difference in brightness at the two input ports. Normally one port looks at the sky, the other one at an internal reference blackbody.
- For calibration, a movable blackbody fills the sky port.

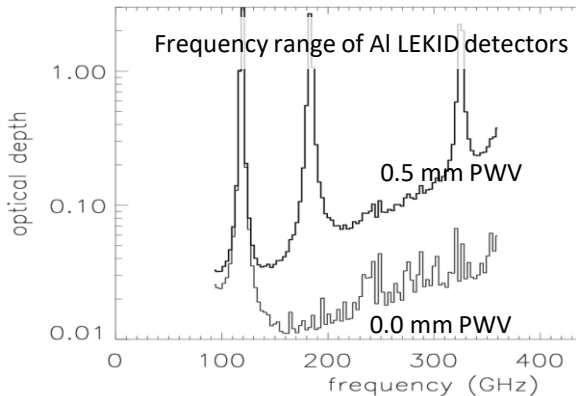


Sky measurement

$$I_{SKY}(x) = C \int_0^{\infty} [S_{SKY}(\sigma) - S_{REF}(\sigma)] rt(\sigma) \{1 + \cos[4\pi\sigma x]\} d\sigma$$

Calibration measurement

$$I_{CAL}(x) = C \int_0^{\infty} [S_{CAL}(\sigma) - S_{REF}(\sigma)] rt(\sigma) \{1 + \cos[4\pi\sigma x]\} d\sigma$$



Coping with atmospheric emission

COSMO will operate from the Concordia French-Italian base in Dome-C (Antarctica) ... the best site on Earth, extremely cold and dry ! But still has to cope with some atmospheric emission.

COSMO uses fast detectors (KIDs) and fast elevation scans to separate atmospheric emission and its long-term fluctuations from the monopole of the sky brightness.

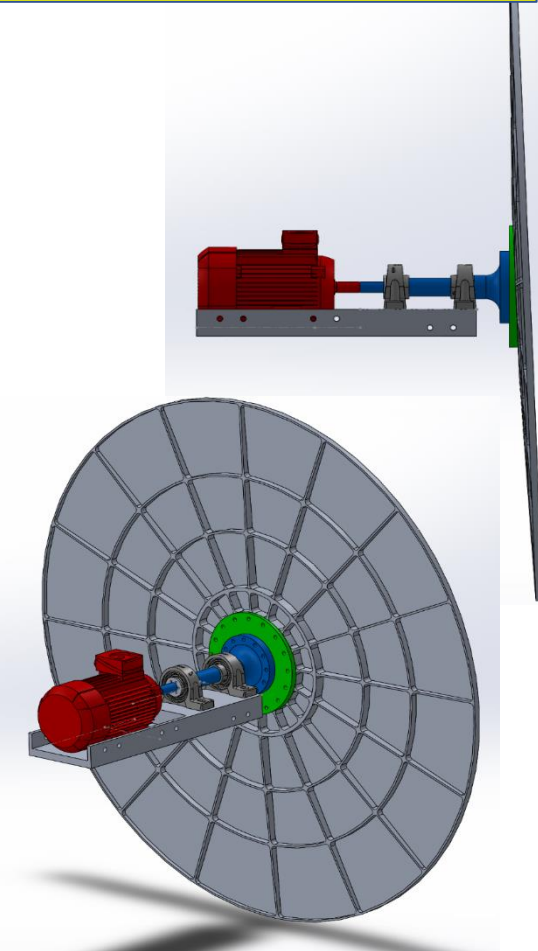
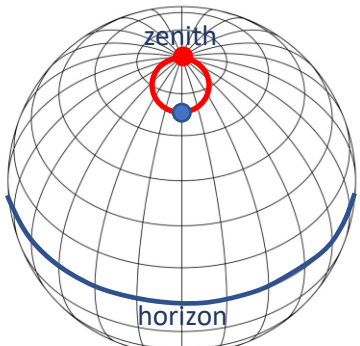
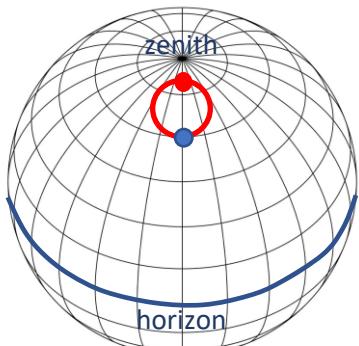
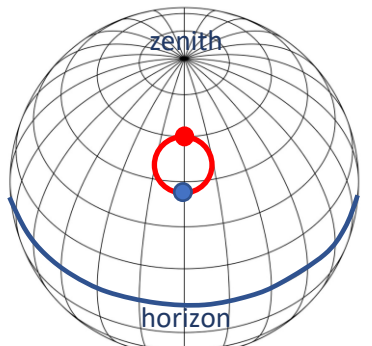
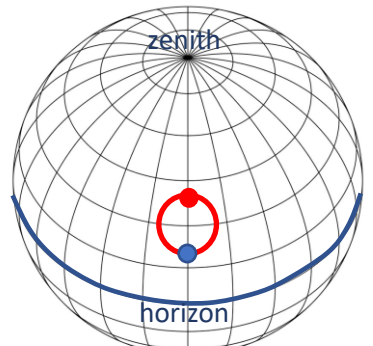
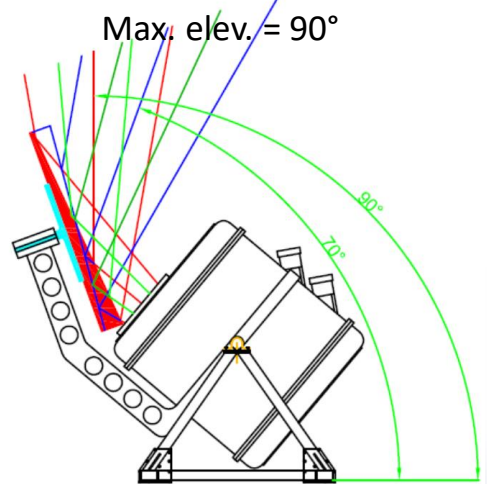
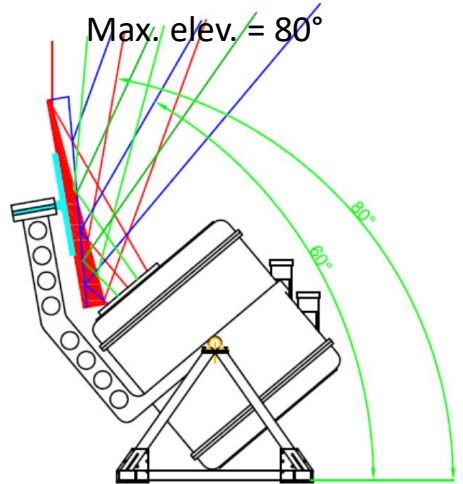
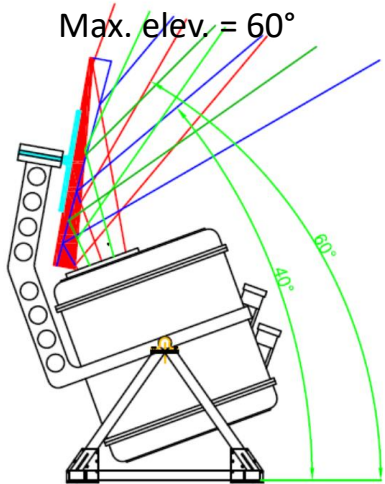
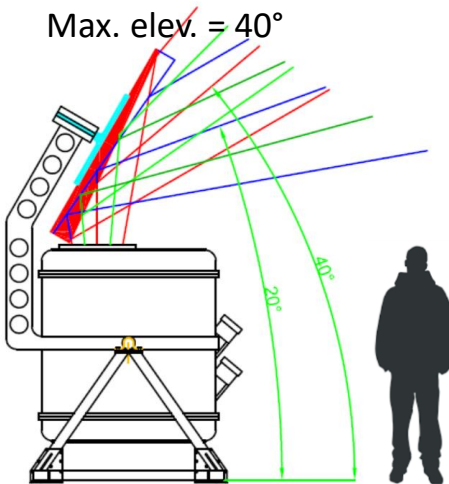
A fast spinning wedge mirror (>1000 rpm!) steers the boresight direction on a circle, 20° in diameter, scanning a range of elevations (and corresponding atmospheric optical depths) while the cryogenic interferometer scans the optical path difference.

Cryostat tilt = 0°
 PT tilt = 40°
 Min. elev. = 20°
 Max. elev. = 40°

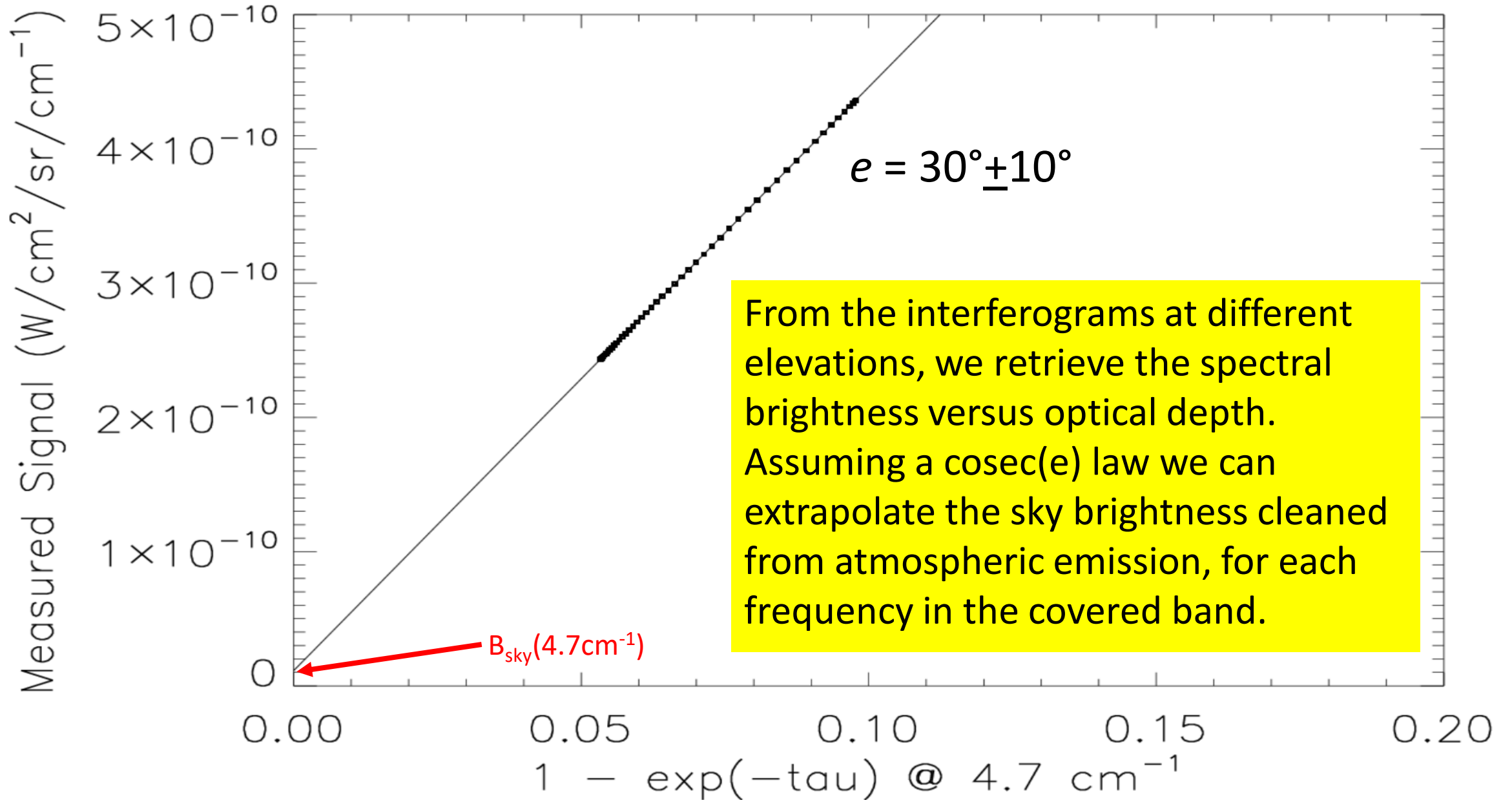
Cryostat tilt = 20°
 PT tilt = 20°
 Min. elev. = 40°
 Max. elev. = 60°

Cryostat tilt = 40°
 PT tilt = 0°
 Min. elev. = 60°
 Max. elev. = 80°

Cryostat tilt = 50°
 PT tilt = -10°
 Min. elev. = 70°
 Max. elev. = 90°

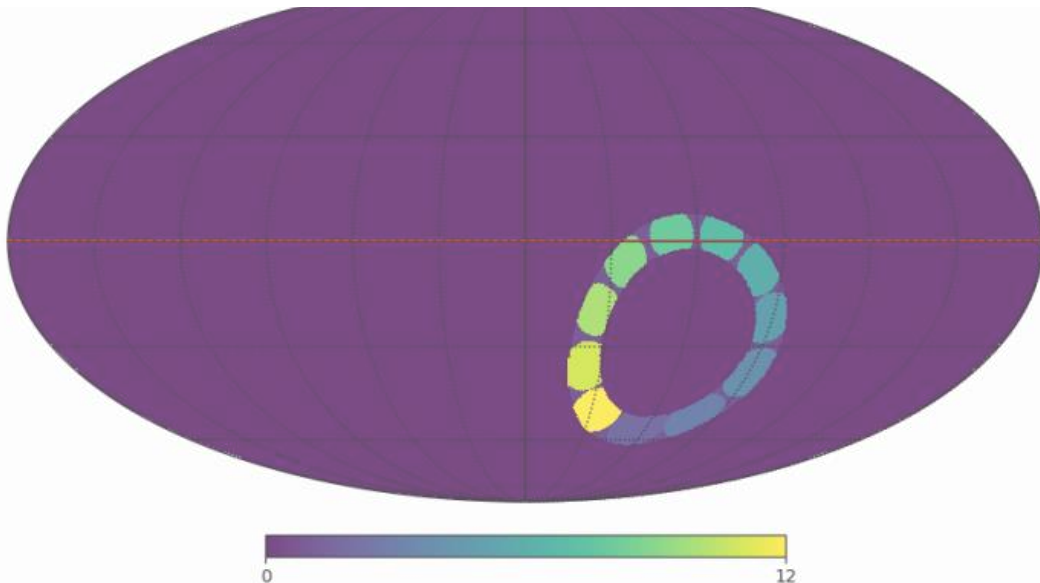
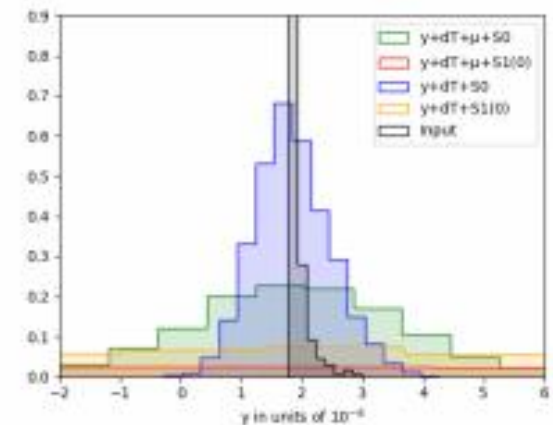
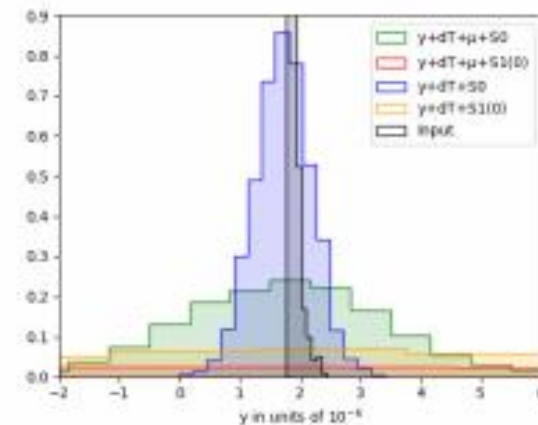
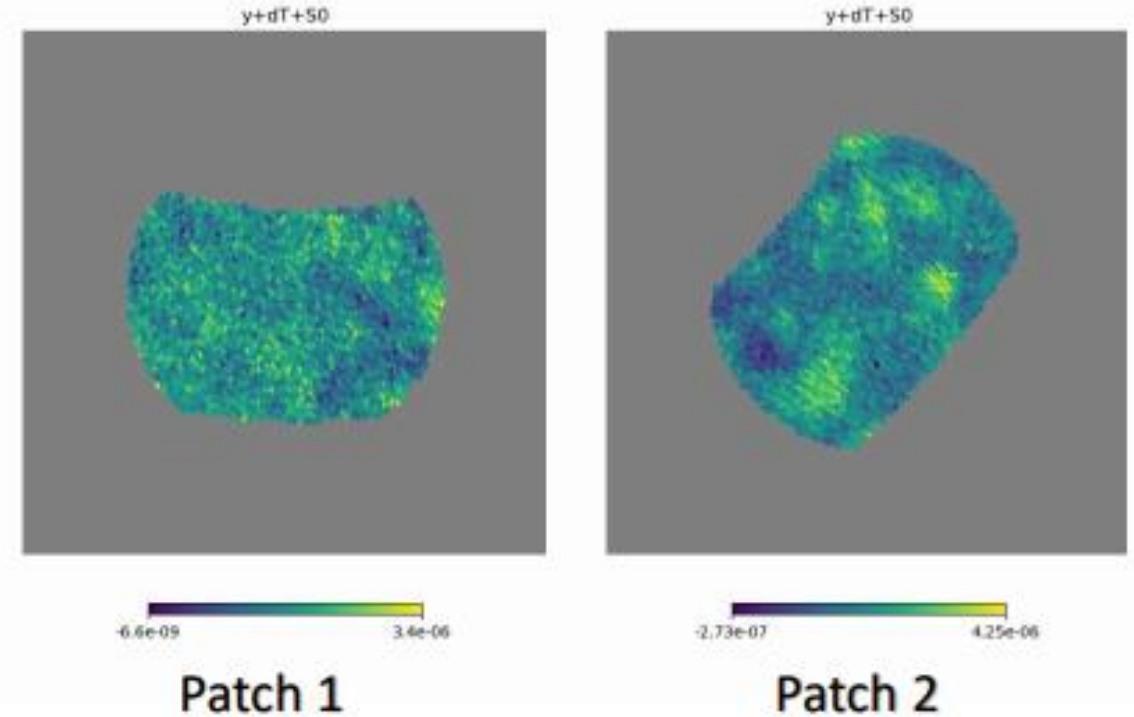


Coping with atmospheric emission



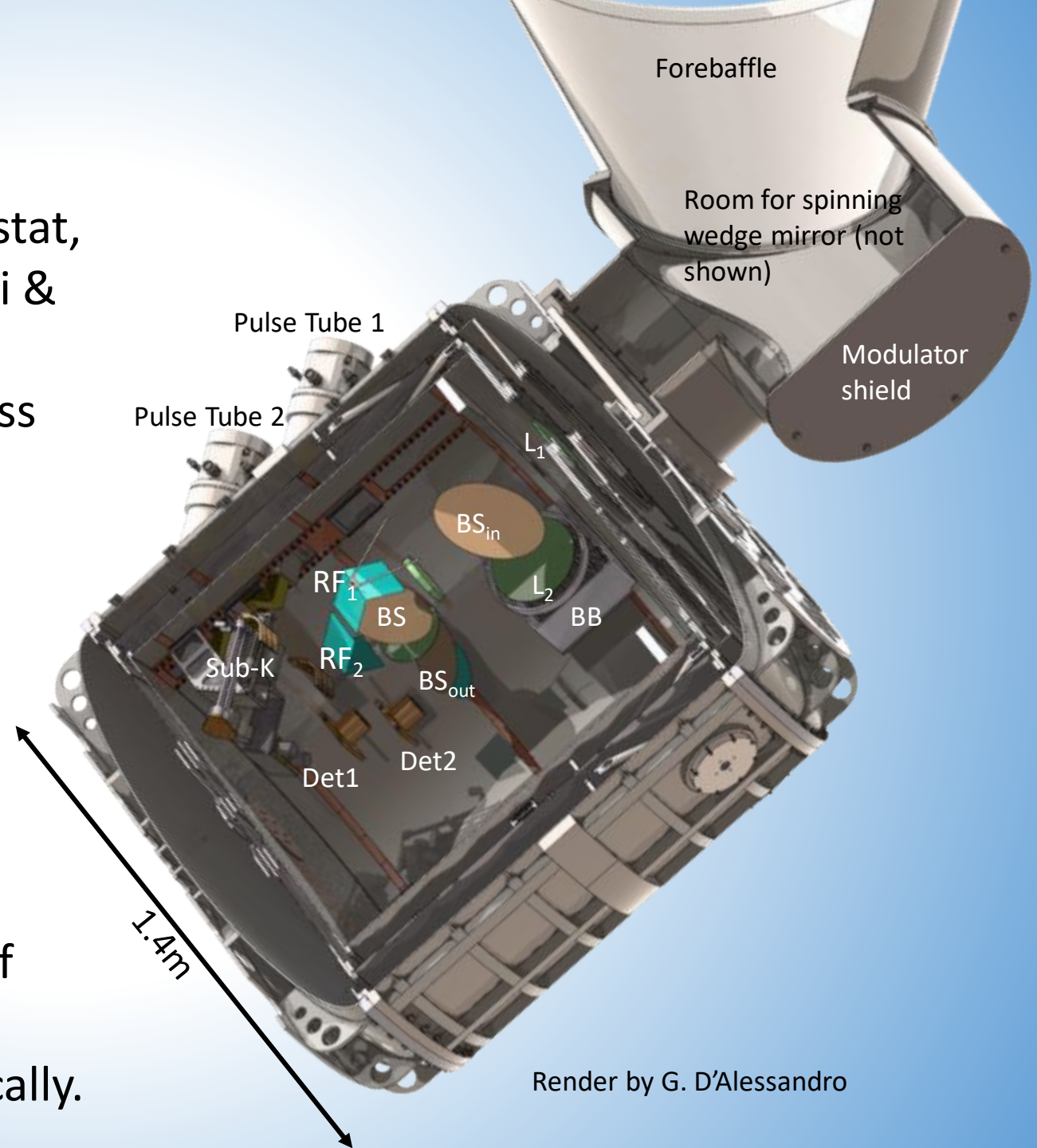
Performance Forecast

- Assuming photon noise limited performance, dominated by the atmospheric emission (AM model) and cryostat window (with $\varepsilon = 1\%$)
- Observing site: Dome-C. Daily coverage of 11 sky patches at high elevation, 1 year of integration.
- ILC-based simulations: COSMO can extract the isotropic Comptonization parameter (assumed to be $y = 1.77 \cdot 10^{-6}$) as $y = (1.76 \pm 0.26) \cdot 10^{-6}$ in the presence of the main Galactic foreground (thermal dust) and of CMB anisotropy, and assuming perfect atmospheric emission removal (L. Mele)

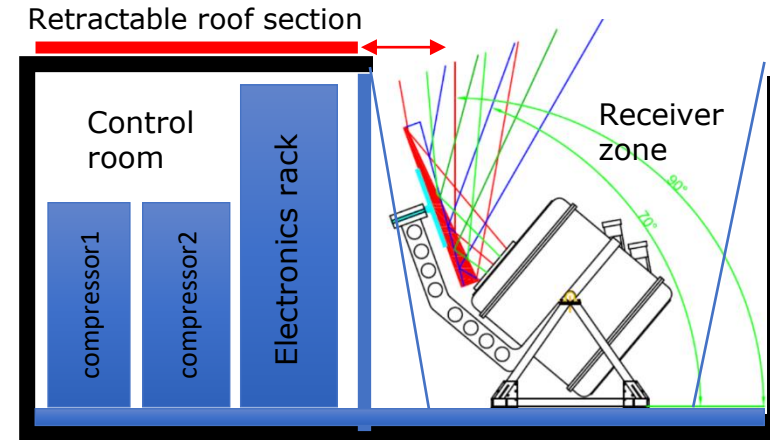
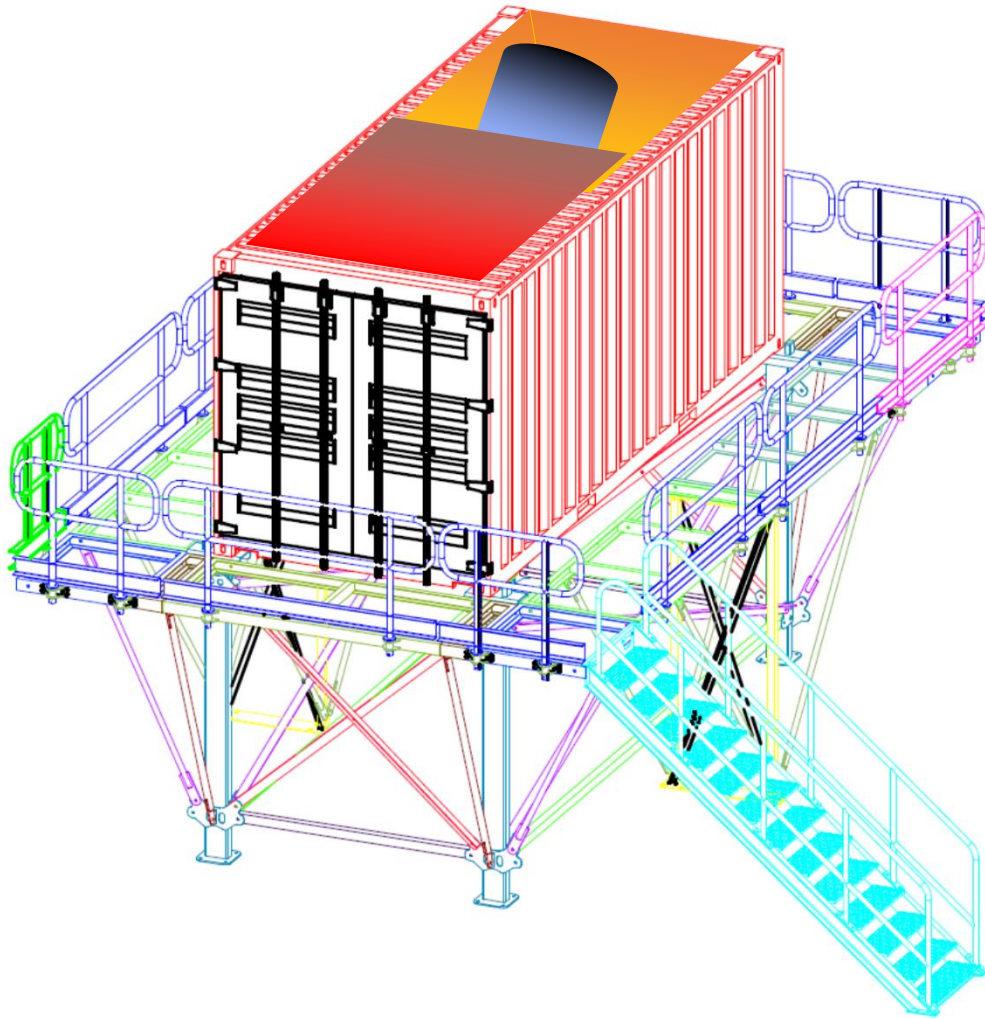


Instrument Implementation

- Instrument inside a pulse-tube based cryostat, twin of the one developed for QUBIC (Masi & JCAP 2021)
- Cryostat height 1.54m, diameter 1.4m, mass 350kg.
- The spinning wedge mirror for sky scans is mounted on top of the vacuum window.
- A large, absorbing forebaffle protects the spinning wedge from straylight.
- The interferometer operates at cryogenic temperature (close to 2.7K)
- The optical path difference modulation is obtained by translating one of the two roof mirrors by means of a frictionless cryomechanism, actuated electromagnetically.



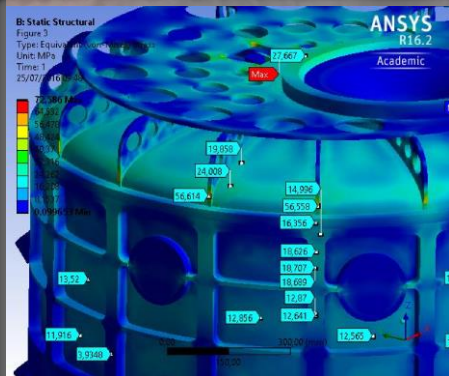
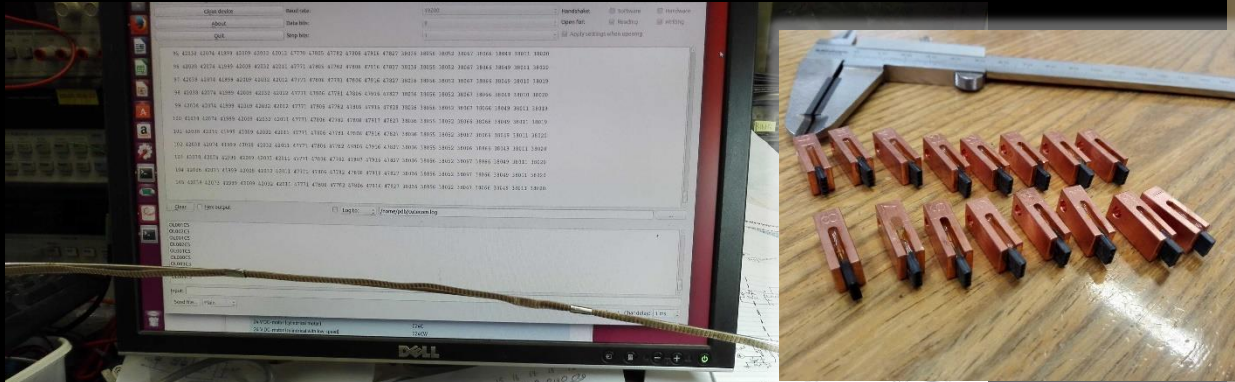
On-site Implementation



- Experiment in a thermally insulated container
- Warm section with electronics and compressors.
- Cold section with receiver. No window. Shields.
- The same container used for tests and shipment
- Palafitte as usual in Dome-C (e.g. superDARN)
- Installation site: near astronomy lab
- Energy needed: 20 kW for 100 days (feedback from program is necessary)
- **SCHEDULED FOR STARTING OBSERVATIONS IN 2024/25**

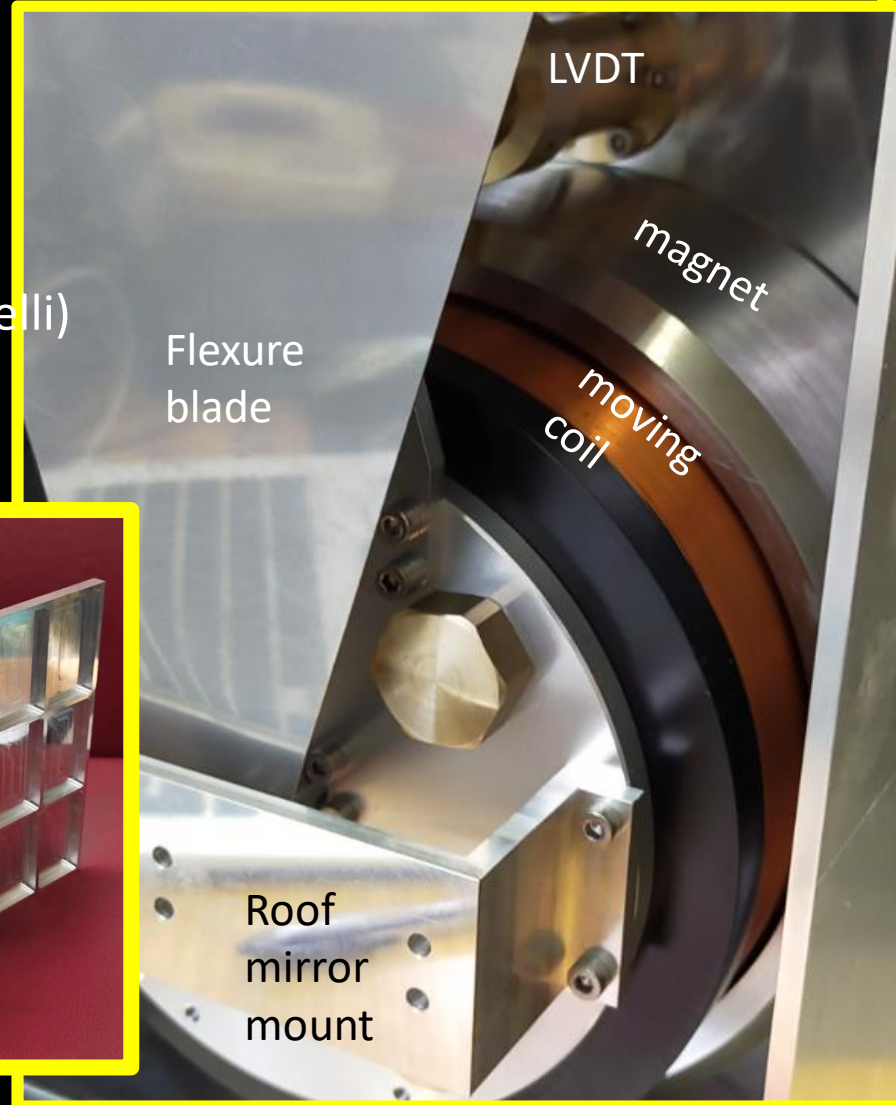
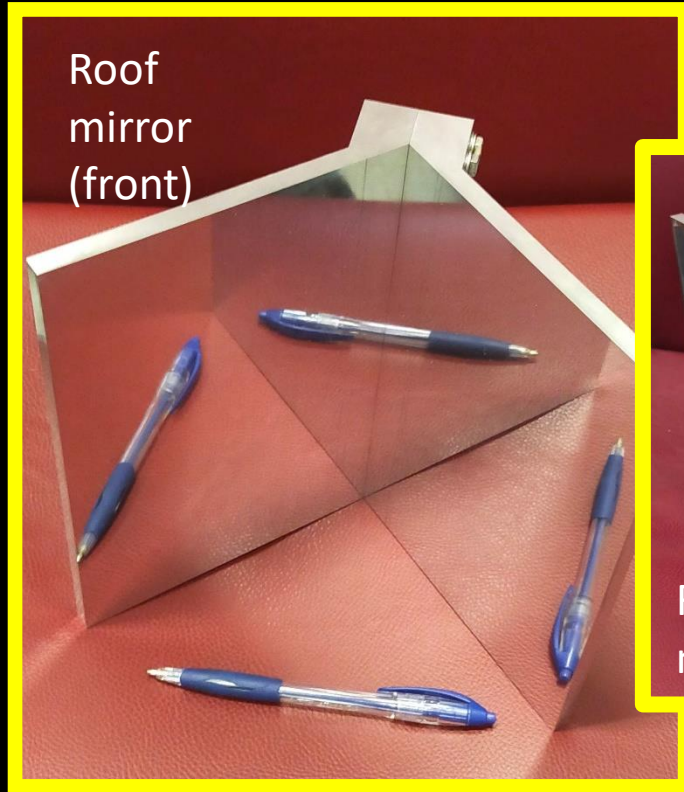
Thanks to Gianluca Bianchi-Fasani for palafitte dwg.

COSMO hardware



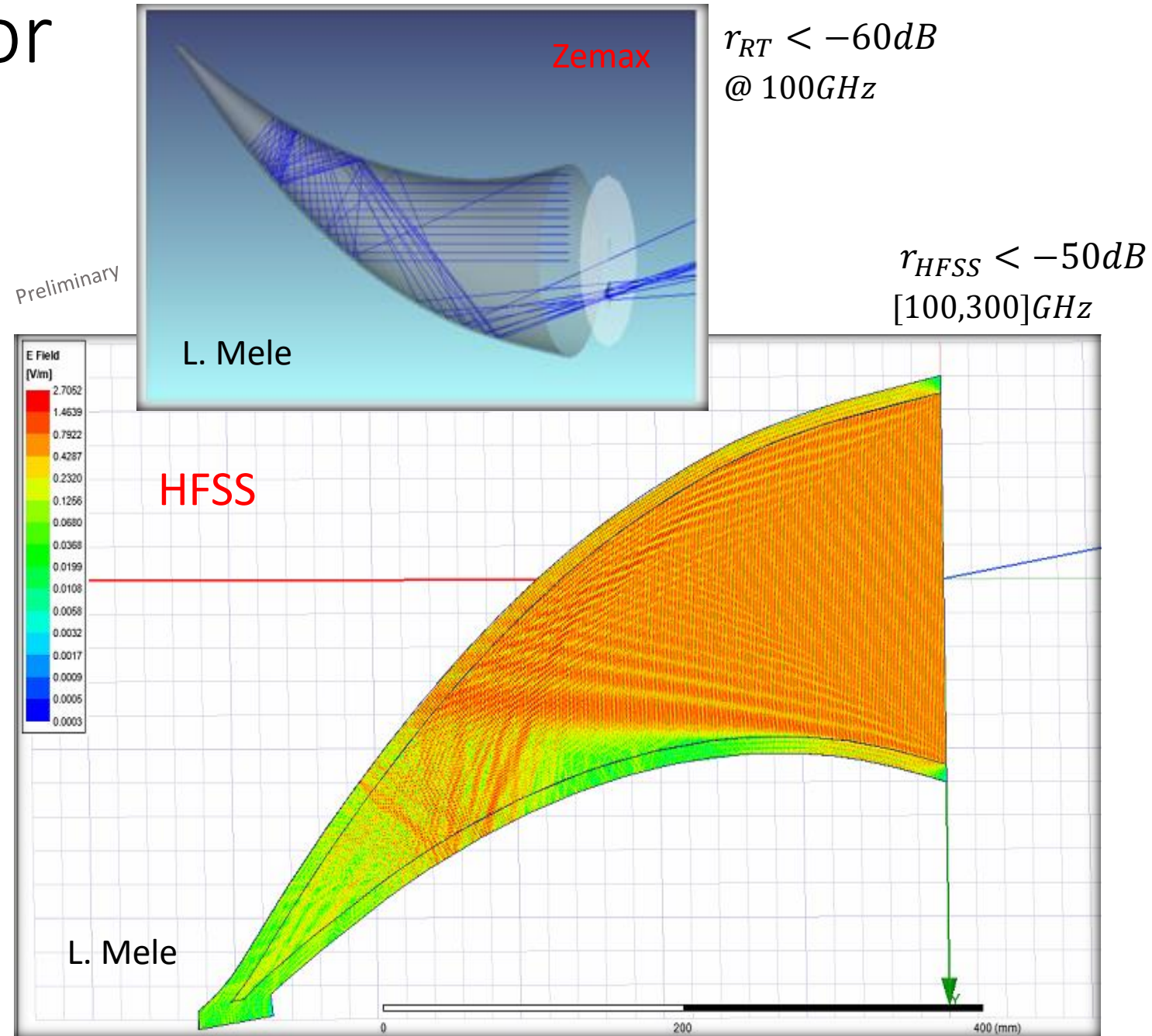
Variable Delay Line for the FTS

- Cryogenic operation – frictionless design to minimize heat load
- Based on a powerful voice coil with steel flexure blades support, to move one roof mirror. up to 0.2 cm/s.
- Voice coil delivered, assembly built.
- Eddy currents in moving coil support minimized by means of a dielectric coil support.
- Electronics being developed (E. Marchitelli)



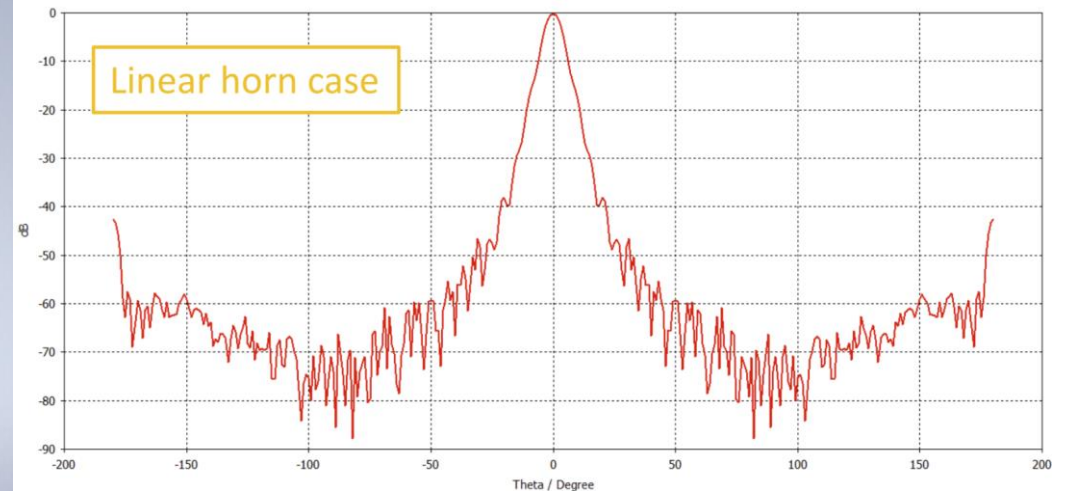
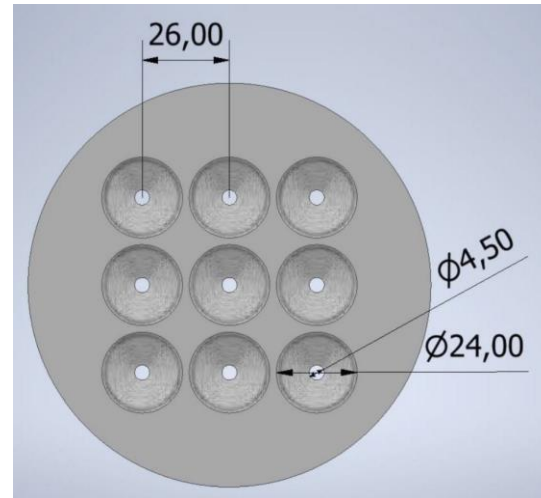
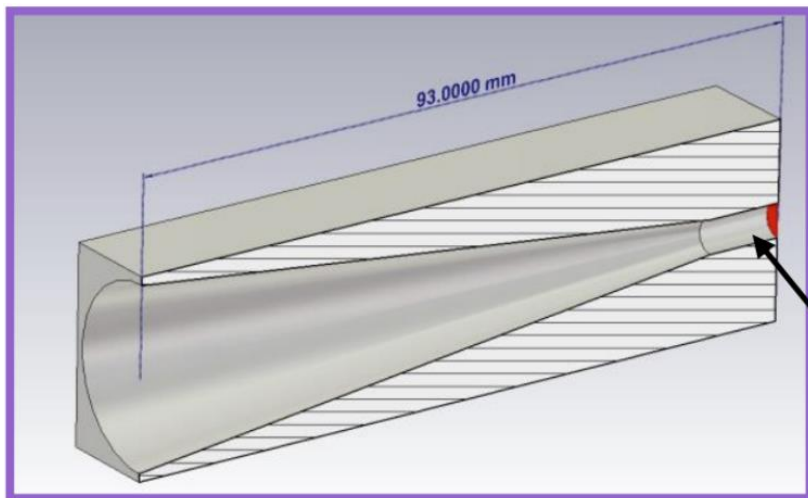
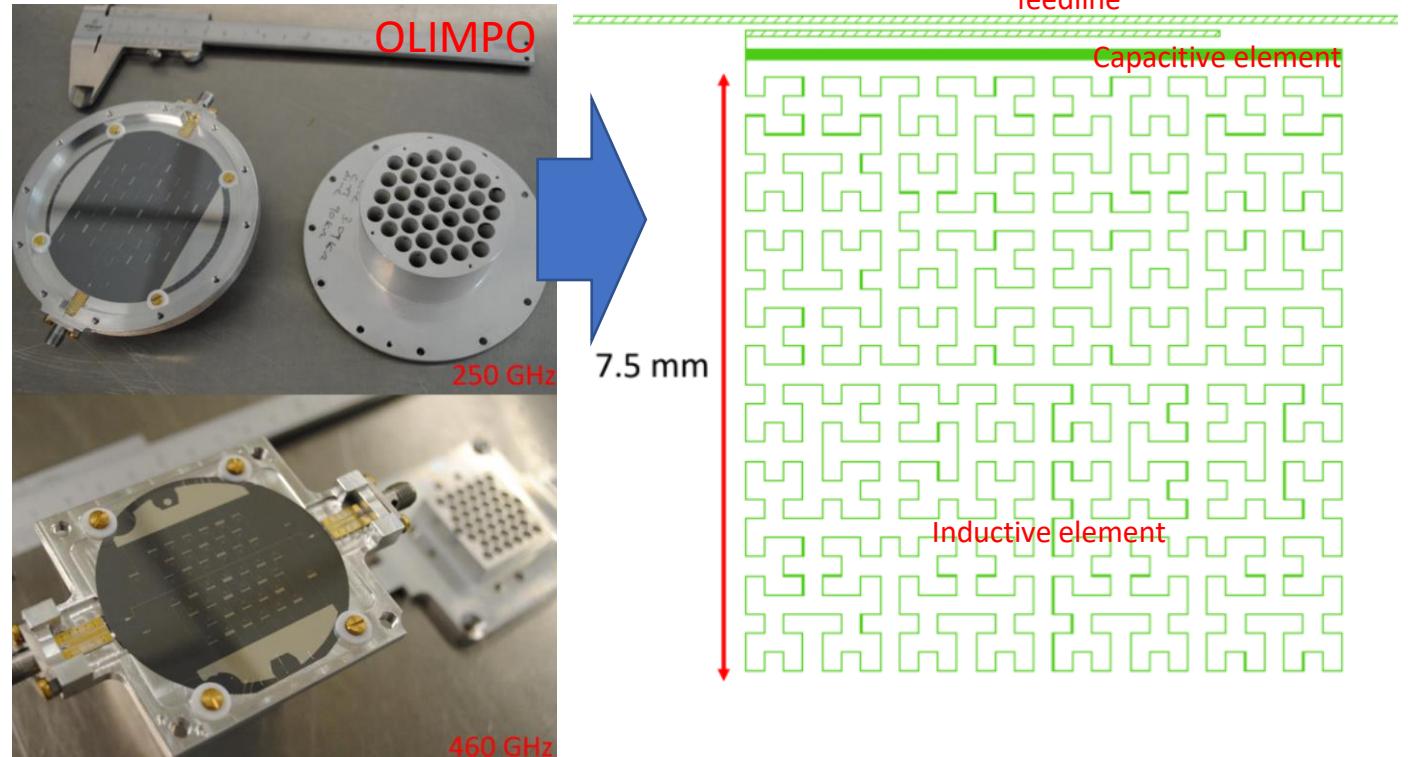
Blackbody calibrator

- Emissivity $\rightarrow 1$
- Low thermal gradients (single compact element)
- Ray Tracing approach (RT): Maximization of the # of reflections with the absorbing coating (cr-110, Emerson & Cuming)
- EM approach with HFSS modelling.
- Reflectivity lower than 1 ppm, to be better evaluated experimentally.
- Fabrication of Cu support for validation prototype started recently.



Detectors & Feedhorns

- COSMO uses two small arrays of multi-moded Al Kinetic Inductance Detectors, fabricated with the same process developed for the OLIMPO ones (Paiella et al. 2019, Masi et al. 2019).
- The two arrays cover the 130-160 GHz and the 200-300 GHz bands.
- Optimization in progress (A. Paiella).
- The KIDs are coupled to Al multi-mode feedhorns. Optimization in progress (E. Manzan).



Detectors Readout

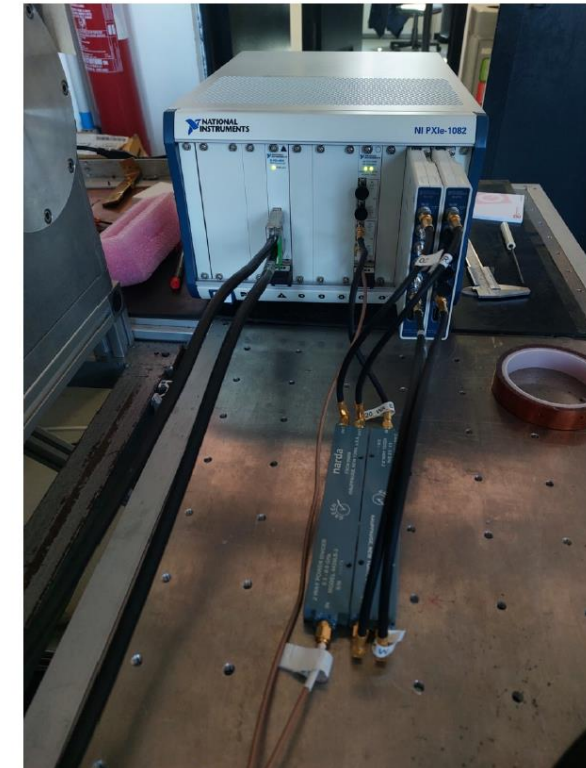
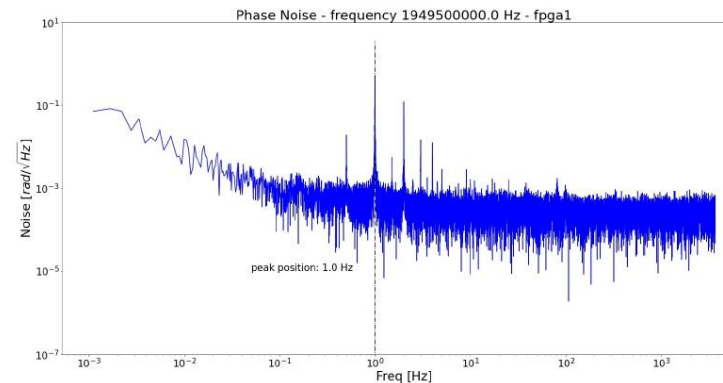
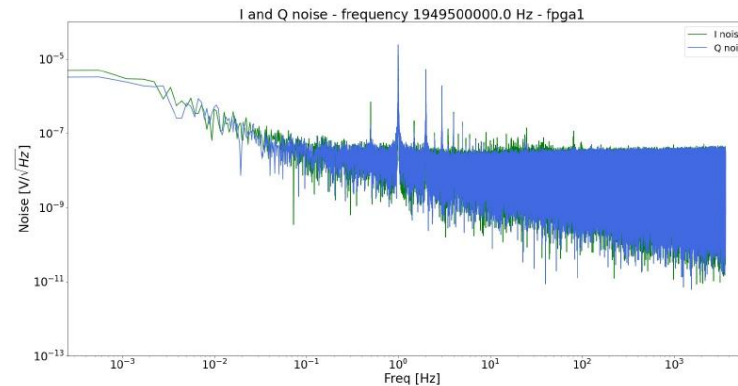
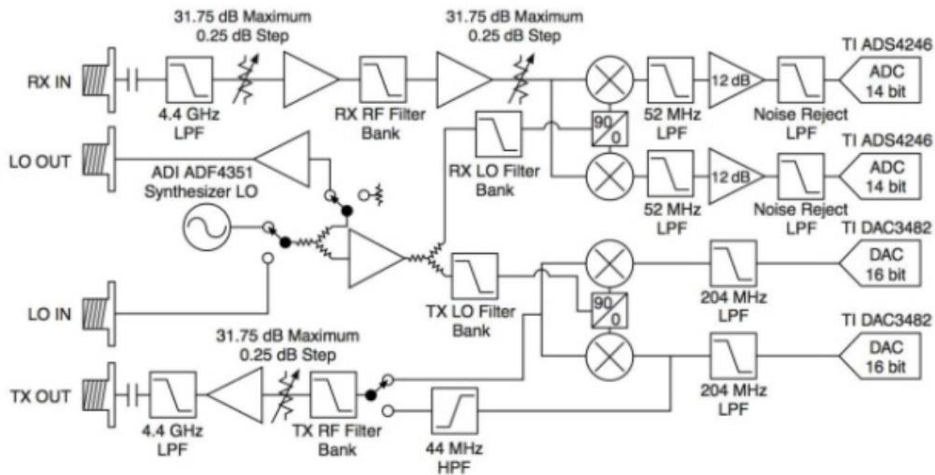
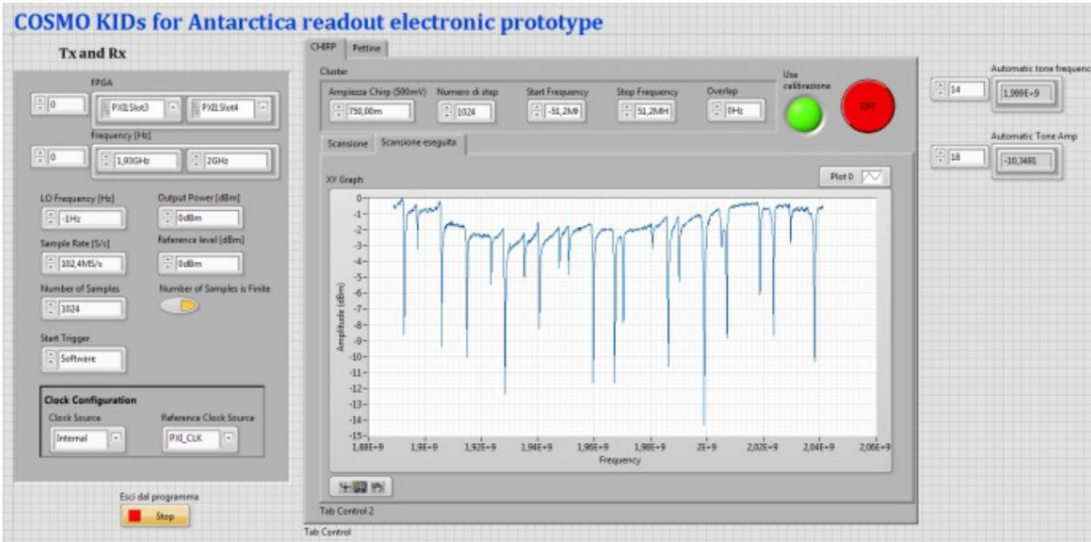


Warm Readout Electronics

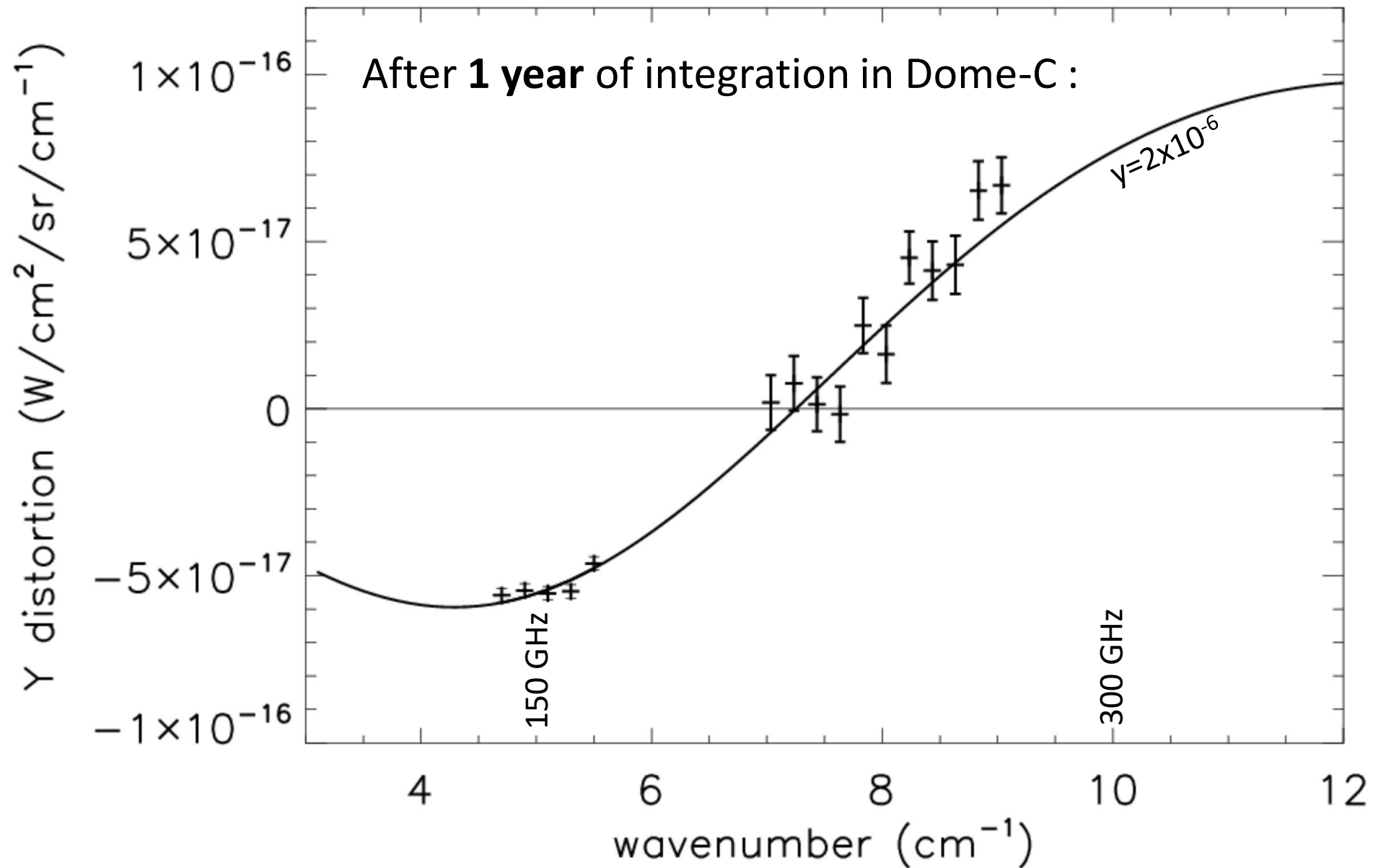
SW developed by Andrea Limonta

Data Analysis and Test by Giulia Conenna and Andrea Limonta

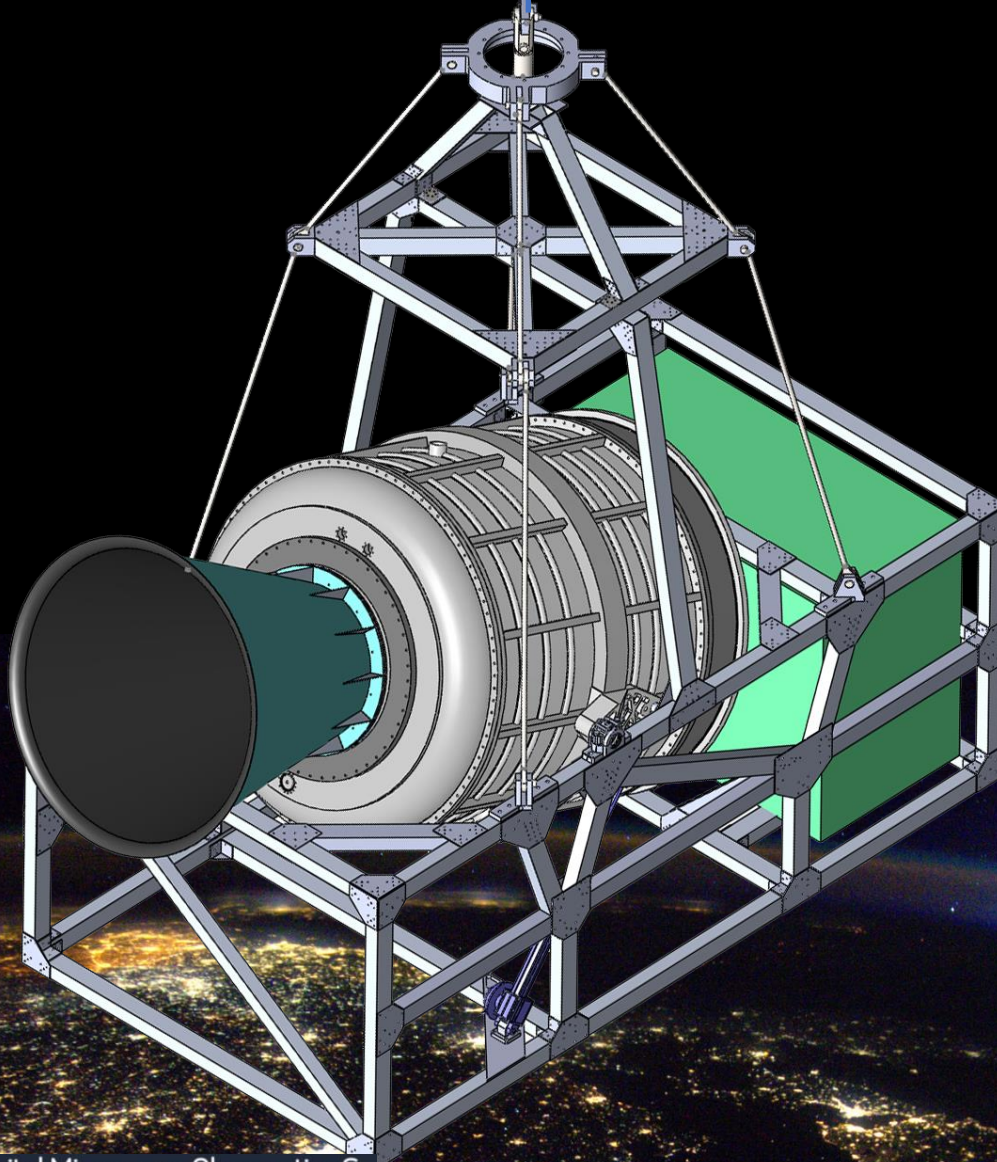
- First read-out mKID electronics based on commercial devices (NI)
- High acquisition rate (currently 15 kHz, target 60 kHz for 18 KIDs)
- Performances comparable with ROACH boards



Simplistic Forecast

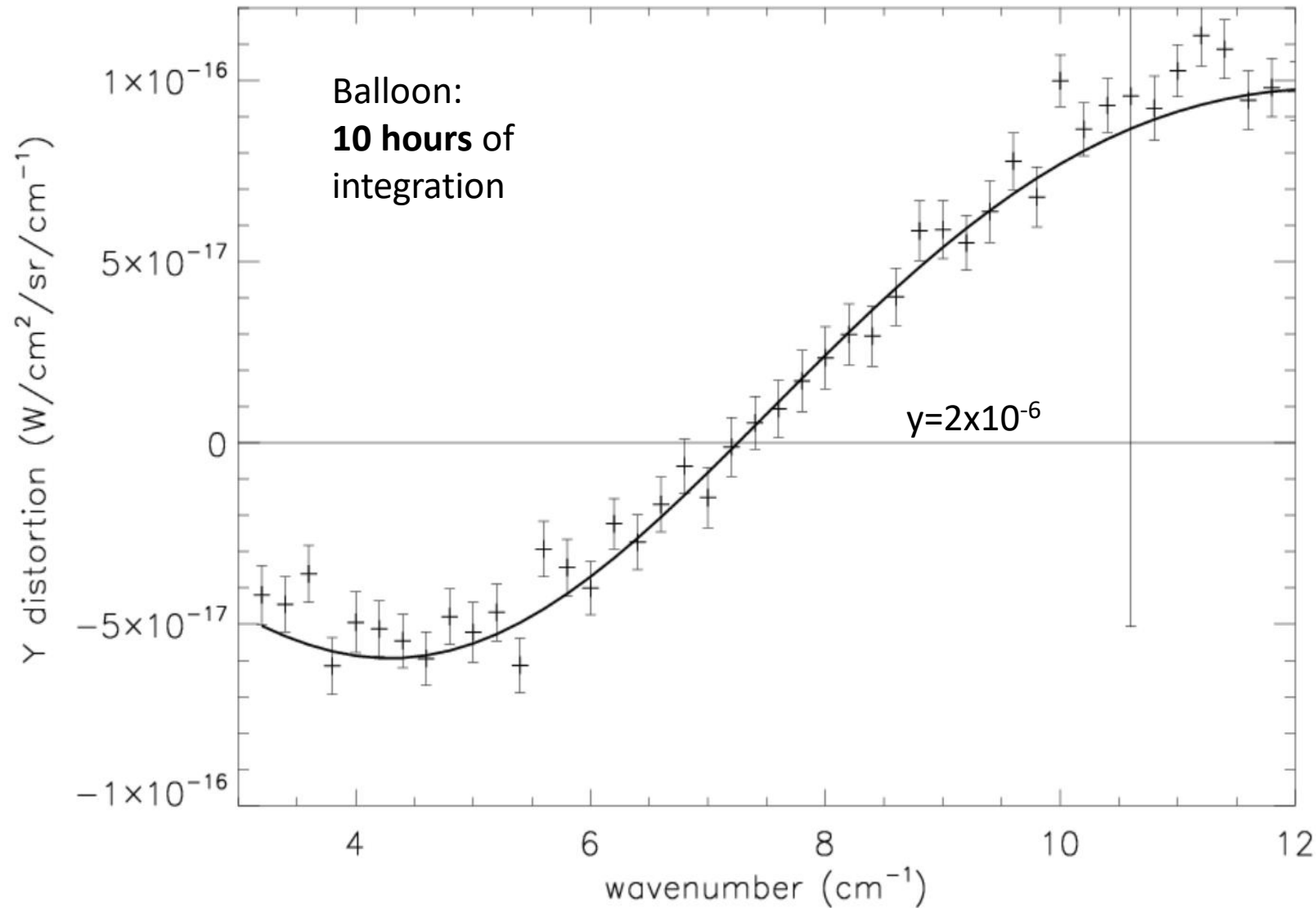


The future of COSMO: a balloon-borne instrument



- **Reuse of most of the LSPE** LDB gondola
<http://lspe.roma1.infn.it>
- Suitable LHe cryogenic system
- Possible to add (slower) sky modulator
- Might gain a factor 10 wrt COSMO on the ground.
- We have the capacity to provide - in house:
 - Detectors (KIDs from OLIMPO)
 - Readout electronics (OLIMPO)
 - Cryogenic system (LSPE)
 - Cryogenic FTS (OLIMPO/COSMO)
 - Modulator (COSMO)
 - Gondola / ACS (LSPE)
 - Data processing / analysis
- French/UK/US collaborators interested to join and provide needed hardware.
- Might merge with French proposal BISOU (CNES study, modulator configuration TBD)
- **Long duration balloon** (14 days at float, NASA summer circumantarctic flight OK, polar night better)
- Might be ready to launch in **2027/28**.

The future of COSMO: a balloon-borne instrument



Feasibility study carried out with ASI – COSMOS project.
Synergic effort in France (BISOU)



Component Separation

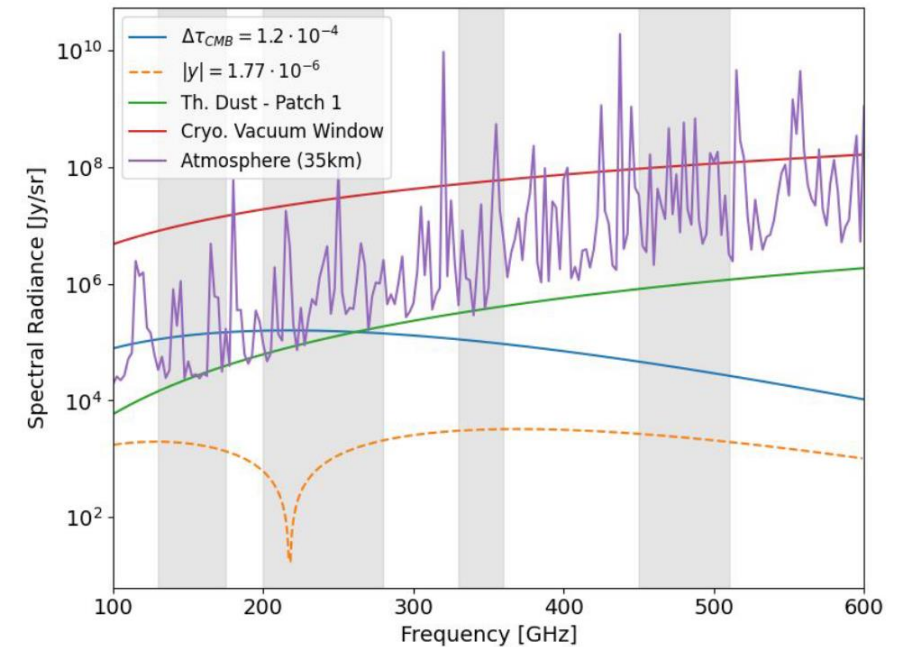
Lorenzo Mele - Sapienza

Monte Carlo Markov Chain (MCMC)

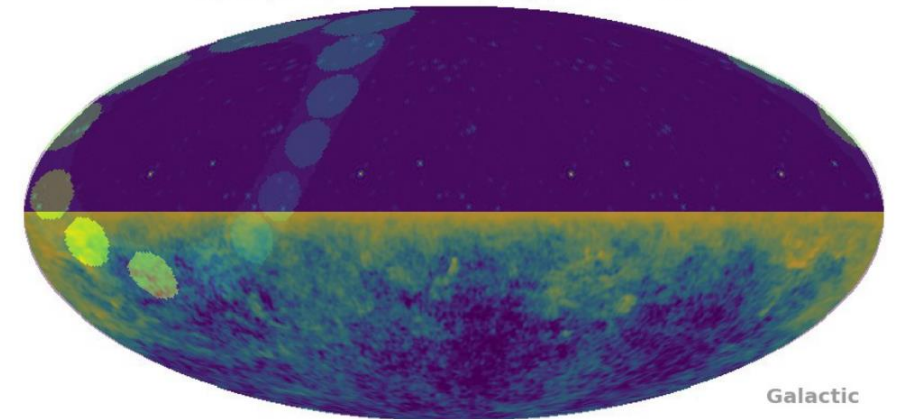
- Use multi-frequency data in a single sky patch
- No spatial information of the spectral components
- Parameter Optimization by Maximizing the likelihood

Input Maps (nside=64, FWHM=1°, v=150GHz+250GHz+350GHz+480GHz bands, $\Delta v=5\text{GHz}$)

- PySM model of Thermal Dust emission (*d2*)
- PySM model of CMB anisotropies (*c1*) + deviation from the currently known CMB monopole $\Delta\tau = \frac{T_{cmb}-T_0}{T_0} = 1.2 \cdot 10^{-4}$
- Isotropic Compton y-map with $\langle y \rangle = 1.77 \cdot 10^{-6}$ +SZ-signal from galaxy clusters (*Sehgal et al. (2010)* available at LAMBDA-simulations)
- Isotropic signal from the cryostat vacuum window (as a gray-body with flat emissivity <0.1% over the bands and temperature T=240K)
- Different sky patches where the MCMC is applied
- Photon noise limited performance (cryostat thin Mylar window, atmospheric emission, CMB monopole)

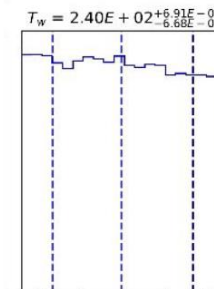
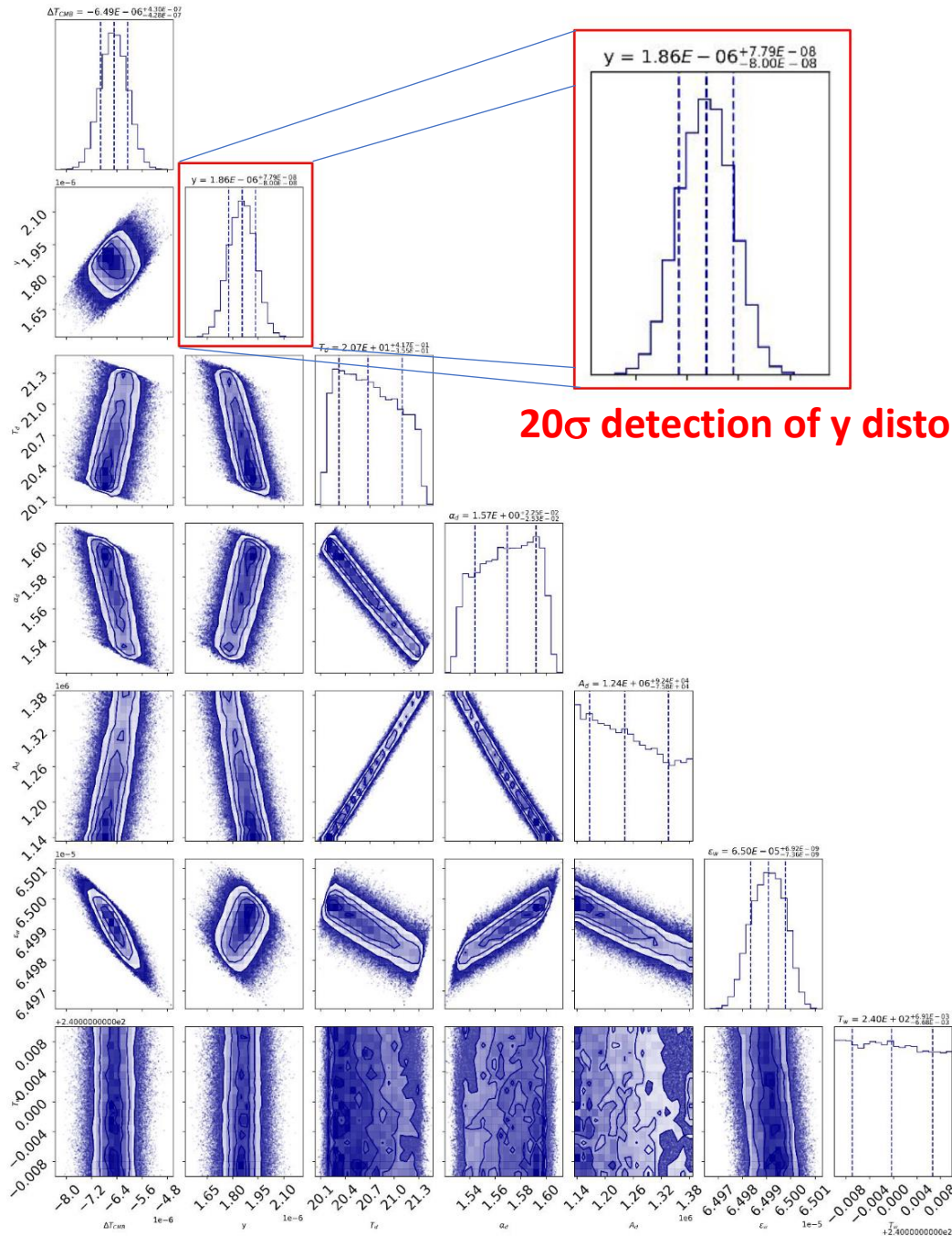


Input y Map: SZ+isotropic $|y| = 1.77 \cdot 10^{-6}$



275GHz PySM
thermal dust map

- MCMC applied to the single sky patch, taking the average signal of the pixels in the patch
- Priors on Thermal Dust parameters 10%
- Priors on vacuum window: emissivity 10%, temperature **0.01K** (*Lakeshore Cryogenics*)
- Gaussian posteriors on the distortion parameters, non-Gaussian for foreground parameters, hitting the prior limit





BISOU a Balloon Project for Spectral Observations of the Early Universe



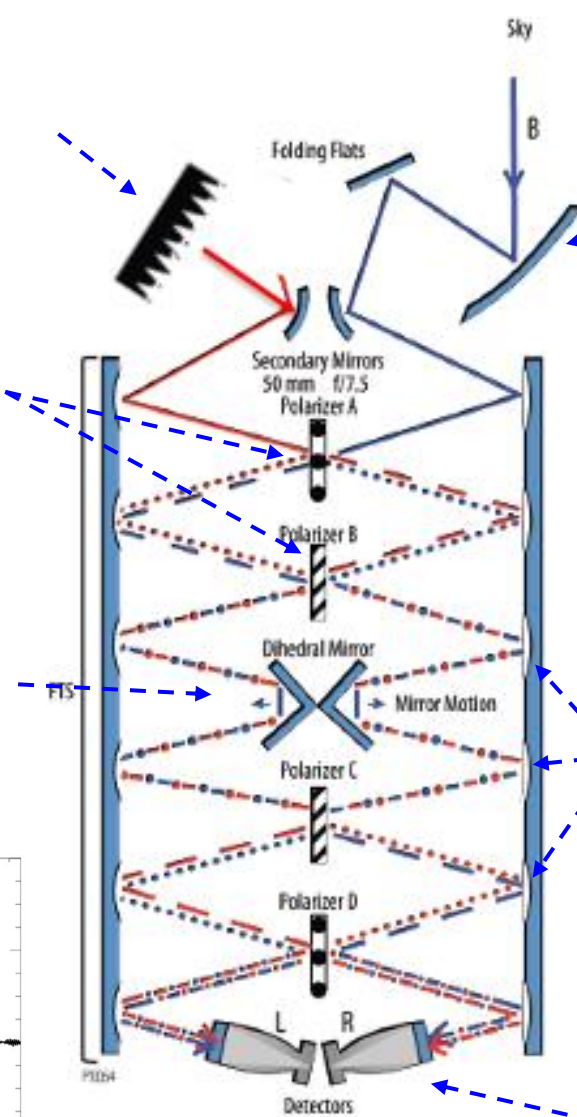
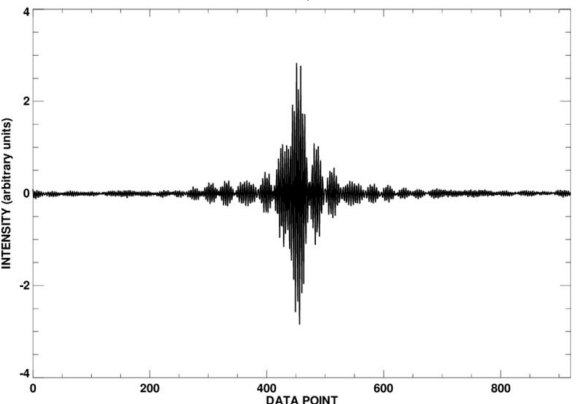
B. Maffei
for the BISOU collaboration

Instrument: measurement principle

Calibrator at 2.7K
(reference for differential measurement)

FTS beam dividers
(polarisers at different angles) - Also act as beam combiners

FTS scanning mirror for interferogram



Beam coming from the sky

Telescope primary setting the spatial resolution (in conj. with feed/detector)

Electric field from the sky input: $E_{x,sky}$; $E_{y,sky}$ linearly polarised along x and y directions

Electric field from calibrator $E_{x,cal}$; $E_{y,cal}$ - Both equal if unpolarised

FTS mirrors

Detectors at each output of the FTS

A. Kogut et al, 2011

$$P_{Lx} = \frac{1}{2} \int (E_{x,sky}^2 + E_{y,cal}^2) + (E_{x,sky}^2 - E_{y,cal}^2) \cos(4z\omega/c) d\omega$$

$$P_{Ly} = \frac{1}{2} \int (E_{x,cal}^2 + E_{y,sky}^2) - (E_{x,cal}^2 - E_{y,sky}^2) \cos(4z\omega/c) d\omega$$

$$P_{Rx} = \frac{1}{2} \int (E_{x,cal}^2 + E_{y,sky}^2) + (E_{x,cal}^2 - E_{y,sky}^2) \cos(4z\omega/c) d\omega$$

$$P_{Ry} = \frac{1}{2} \int (E_{x,sky}^2 + E_{y,cal}^2) - (E_{x,sky}^2 - E_{y,cal}^2) \cos(4z\omega/c) d\omega$$

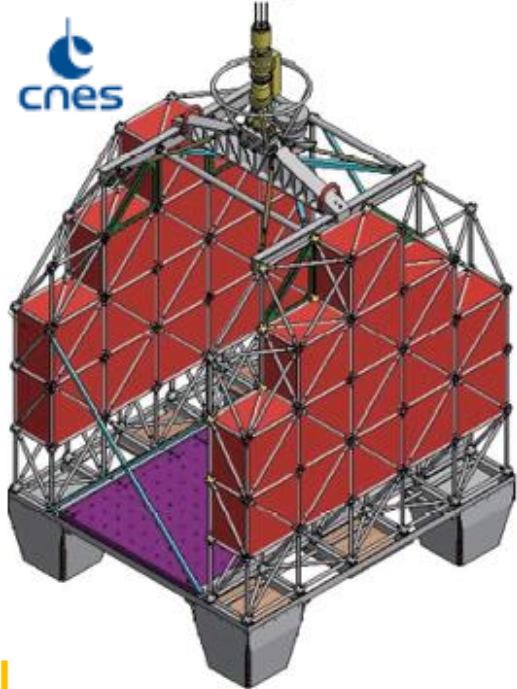
Power on each polarisation (x,y) of each detector (L,R) (with dual-polarised detectors)

if intensity only (non polarised detectors) then:
 $P_L = P_{Lx} + P_{Ly}$ and $P_R = P_{Rx} + P_{Ry}$

Instrument concept - Balloon constraints



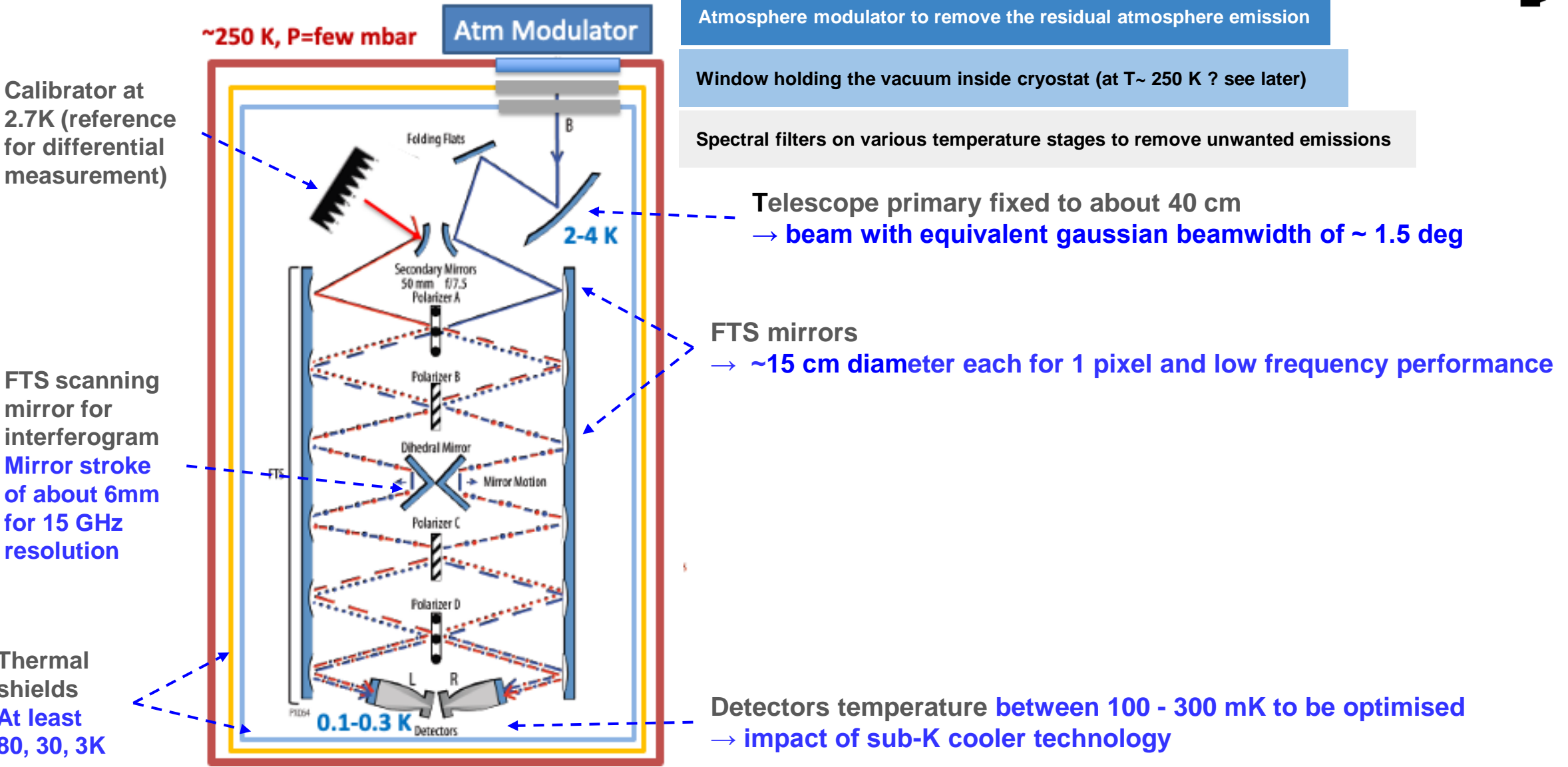
CNES "CARMEN" gondola



- Mass, Size
 - Max payload dimensions ~1.8 x 1.6 x 0.9m
 - → Telescope primary diameter of about 40 cm
- Line of sight
 - Minimum 20 deg angle of sight from zenith (balloon above)
- Limited flight time
 - Assumption of 5 days - See CNES presentation
- Residual atmosphere
 - Emission of residual atmosphere
 - Needs either a reliable model or implementing a modulator for subtraction
- Additional components
 - Cryostat window and filters
 - Measure / model their effects
- Cryogenic chain (cannot use cryocoolers)
 - Use of cryogenics → Liquid helium

CONFIGURATION	802Z CARMEN
Maximum mass at the balloon hook	1750 kg
NEV	20
Parachute	140
NSO	140
Ballast (~10%)	250
Link , ...BAX	200
Pointed Gondola with avionics and swivel	390
Remaining mass for payload units + power supply	610 kg

Instrument: measurement principle in a balloon

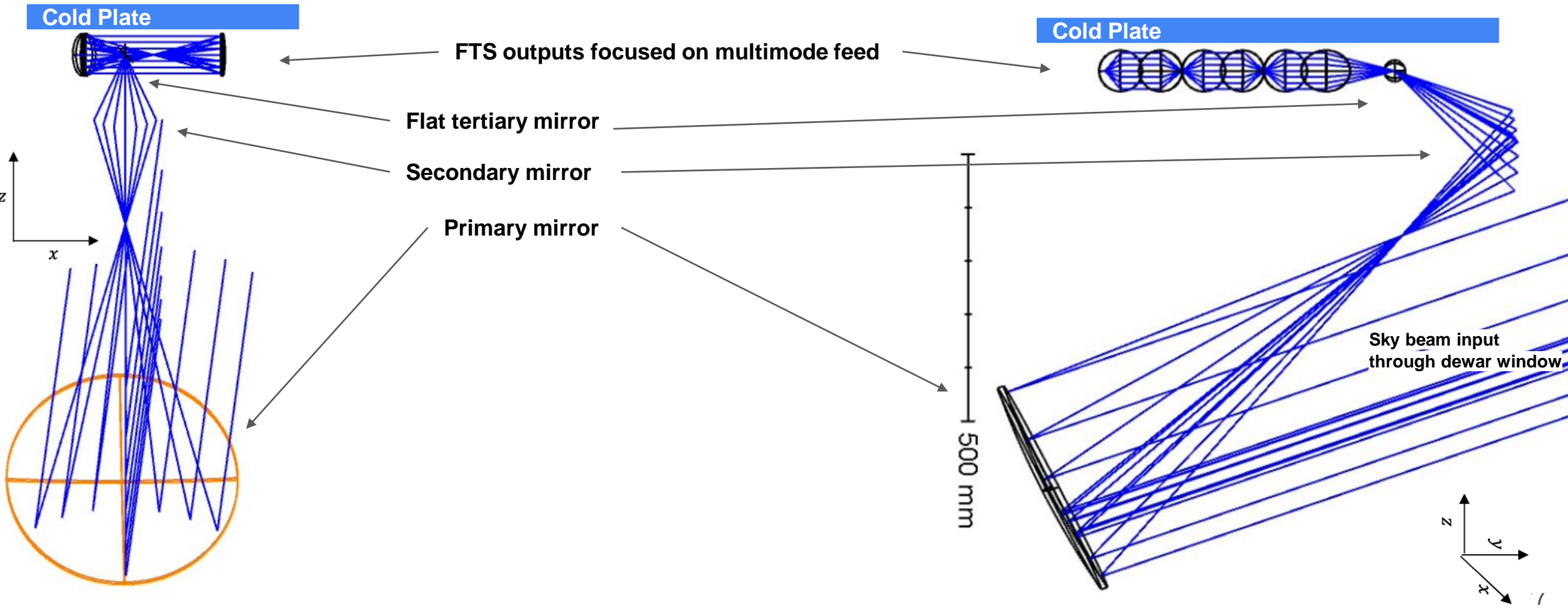


Cryostat external structure

Optics



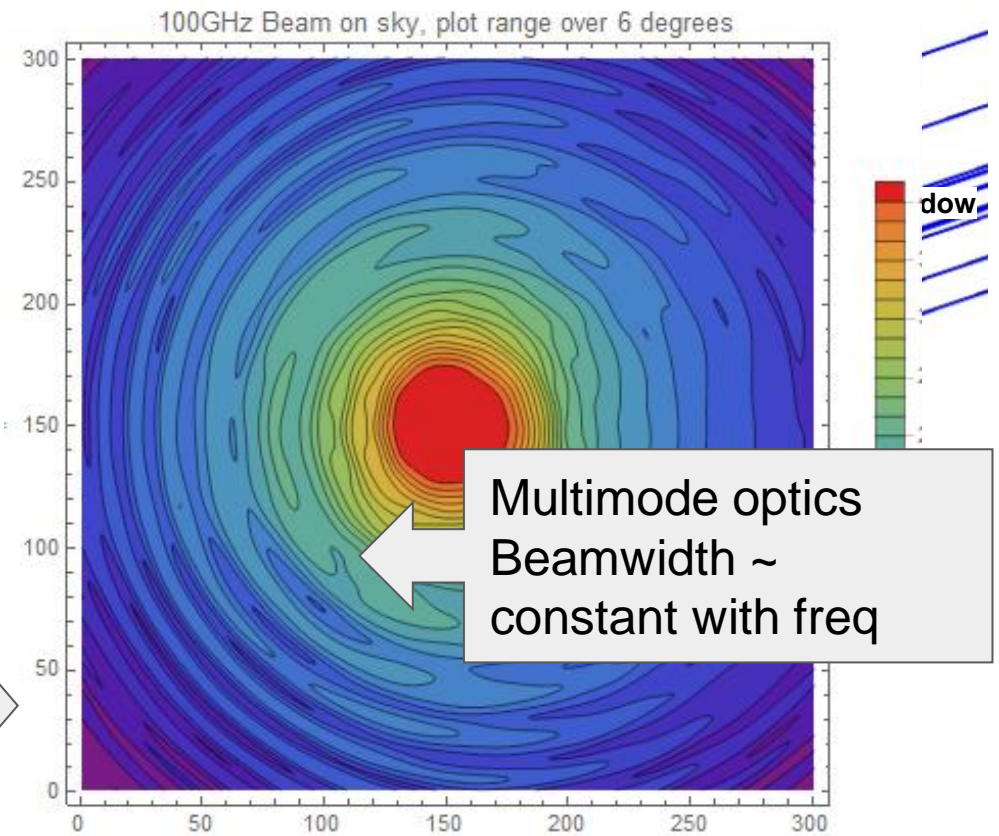
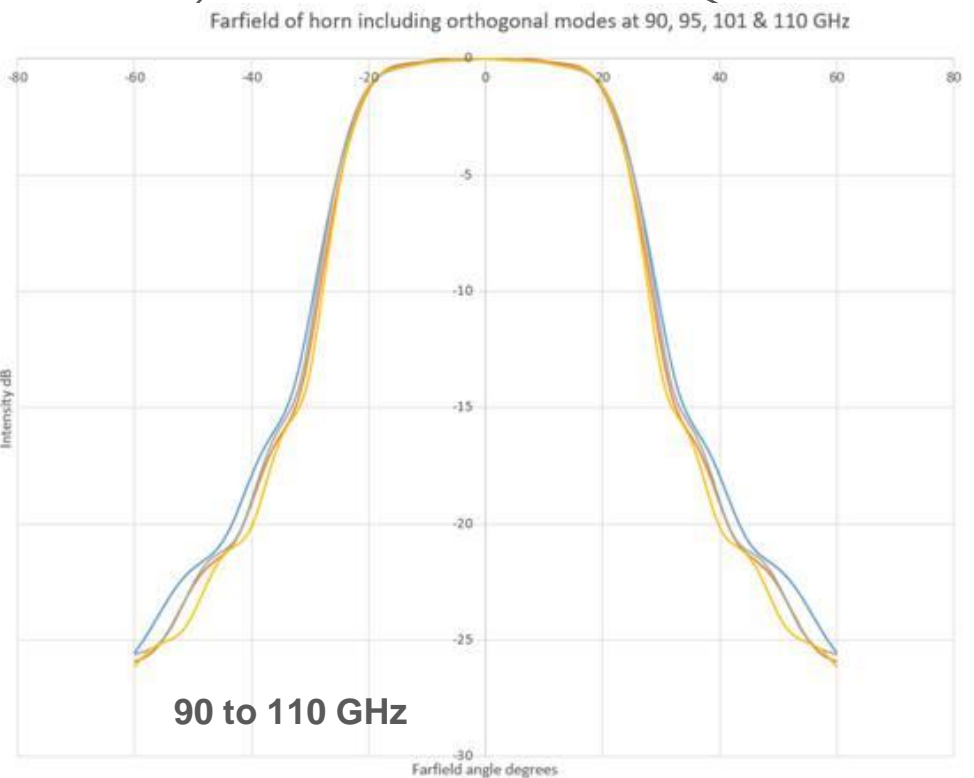
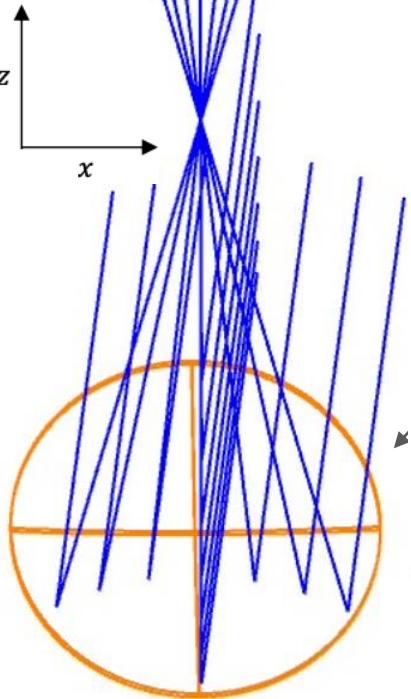
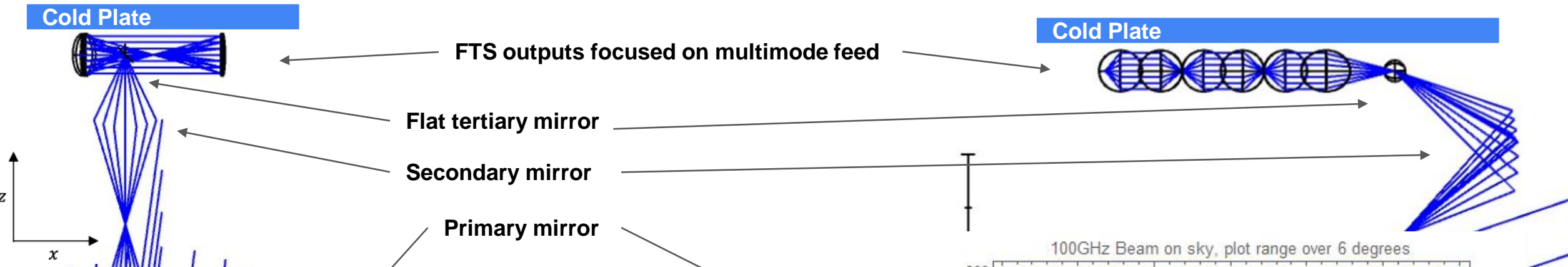
- off-axis dual mirror telescope
- + flat tertiary to redirect sky beam towards first FTS mirror
- 2nd FTS input (fixed calibrator) not shown here



Optics

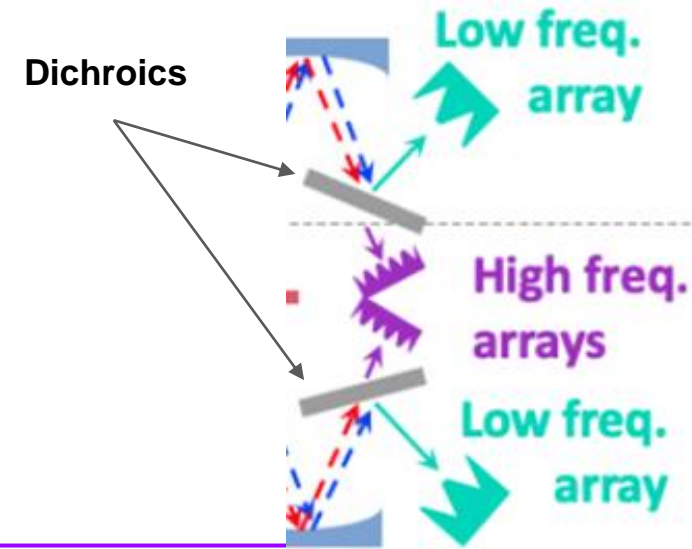


- off-axis dual mirror telescope
- + flat tertiary to redirect sky beam towards first FTS mirror
- 2nd FTS input (fixed calibrator) not shown here



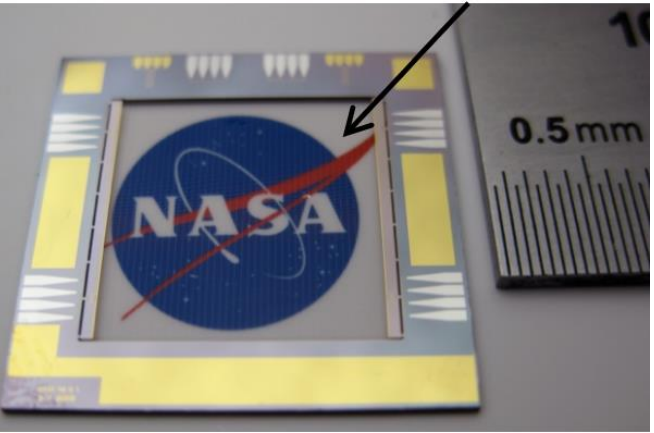
Focal planes / Detectors

- Investigation of splitting the full spectrum into 2 bands to optimise the sensitivity
 - Split around 500 GHz
 - Leading to 4 FPU: 2 per band, 2 per FTS output
- $NEP_{det} < \text{few } 10^{-16} \text{ W.Hz}^{-0.5}$ enough
 - Baseline: resistive bolometers from NASA-GSFC
 - KIDs technology would need some development



Resistive bolometers developed for *PIXIE* could be used across the whole frequency range (Kogut et al, 2011)

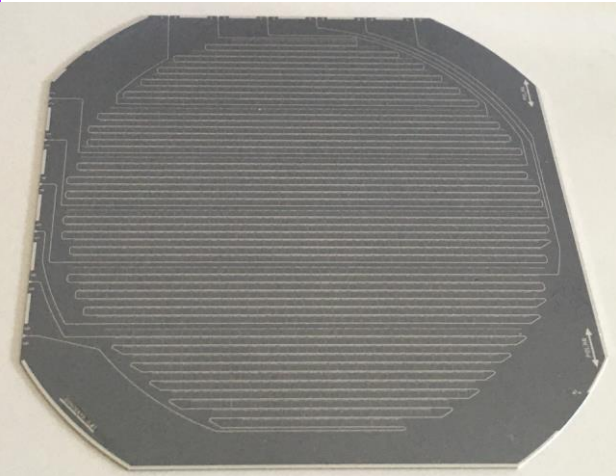
30x collecting area as Planck bolometers



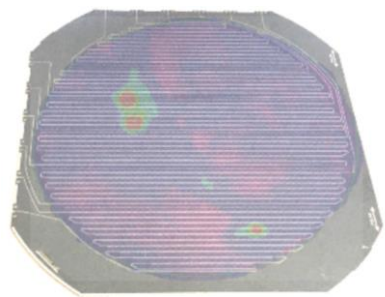
Kogut A.

PIXIE polarization-sensitive bolometer

KIDs array from Institut Néel / LPSC
2152 pixels, 6 readout lines



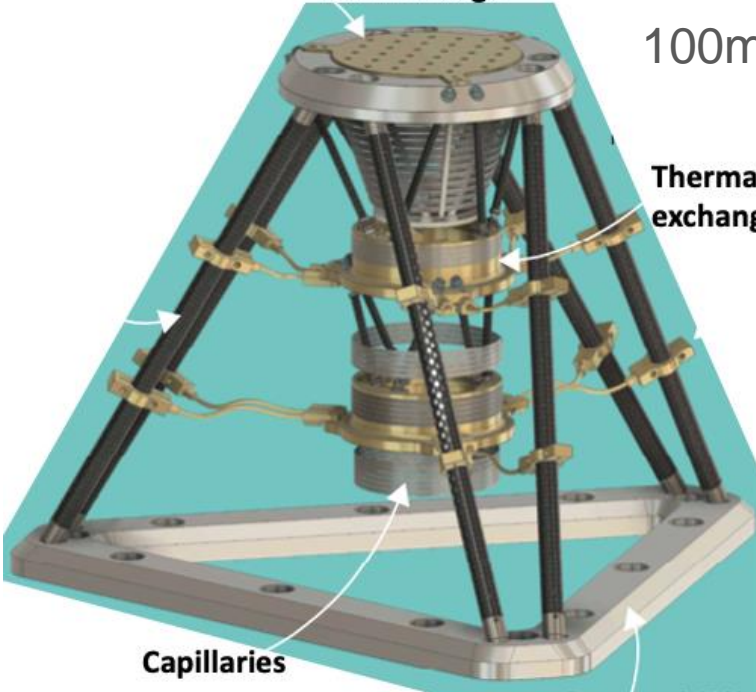
130 - 270 GHz
195 - 310 GHz



Courtesy of the CONCERTO collaboration

Cryogenic Chain

- Cooling system based on cryogenics
 - Most probably a fully liquid helium based dewar down to 2 K (such as PILOT)
 - Maybe a first stage with liquid nitrogen to provide a 77K stage
 - Use less helium, could make use of the nitrogen gas output to cool window



100 mK stage

If detector temperature $100\text{mK} < T_{\text{det}} < 260 \text{ mK}$

Thermal exchanger

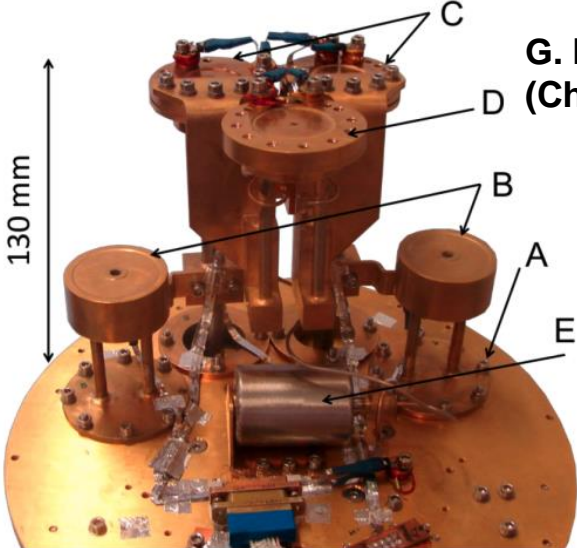
Capillaries

Base at 1.7 K

CCDR (Closed Cycle Dilution Refrigerator)
V. Sauvage et al, SPIE conf, July 2022

If detector temperature $T_{\text{det}} > 260 \text{ mK}$

- “Classic” recyclable ^3He sorption cooler (PRONAOS, PILOT) from 1.8 K
- Continuous 300mK sorption coolers from 4K



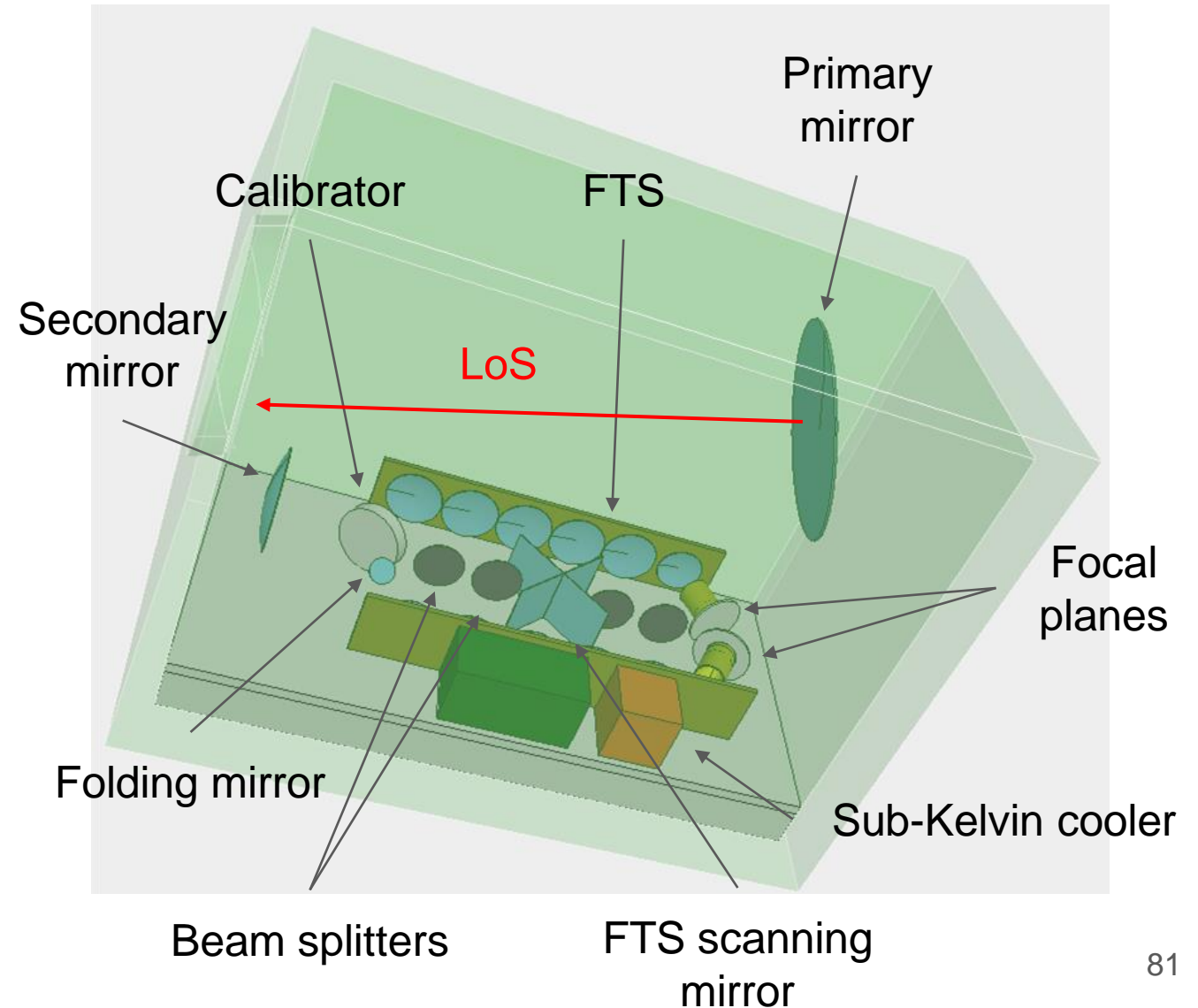
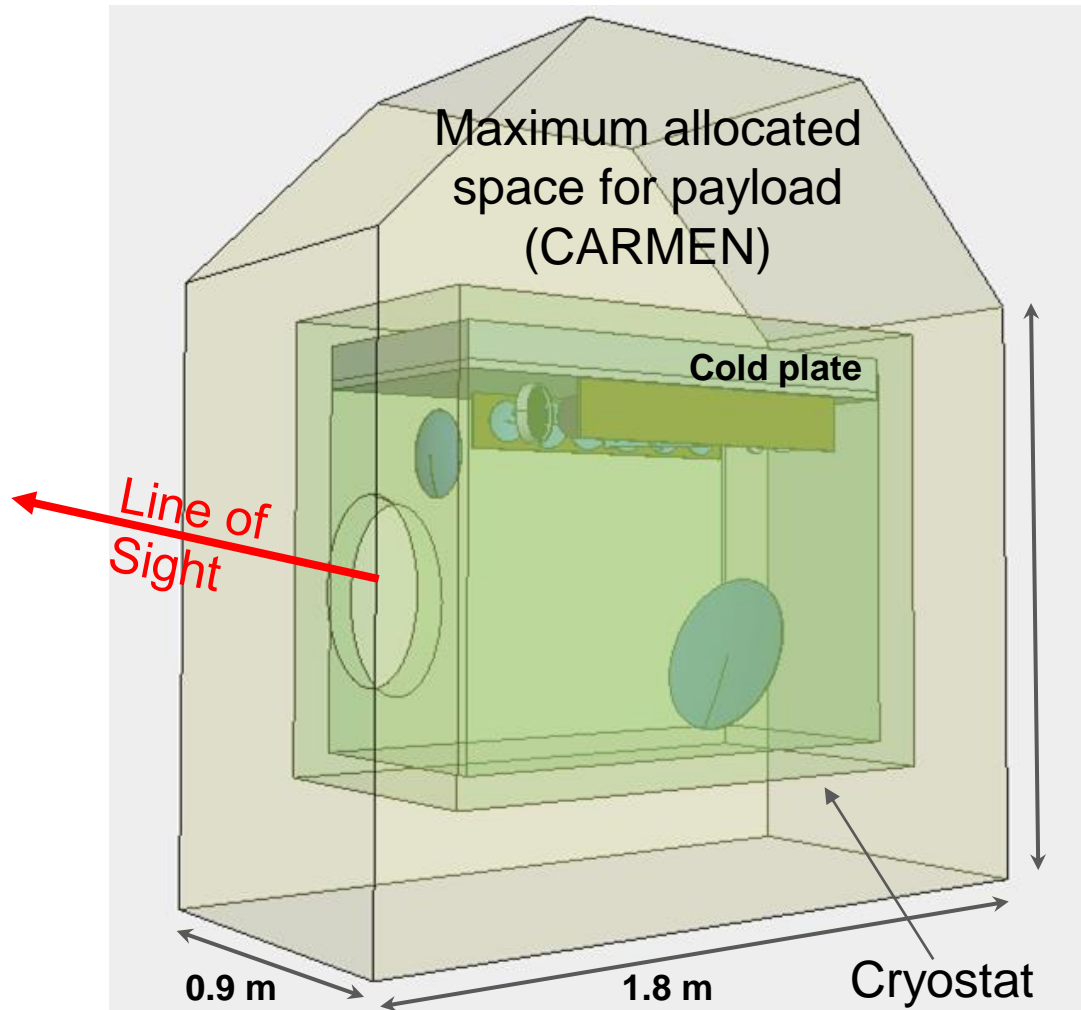
130 mm

A, B, C, D, E

G. M. Klemencic et al, 2016
(Chase Research Cryogenics)

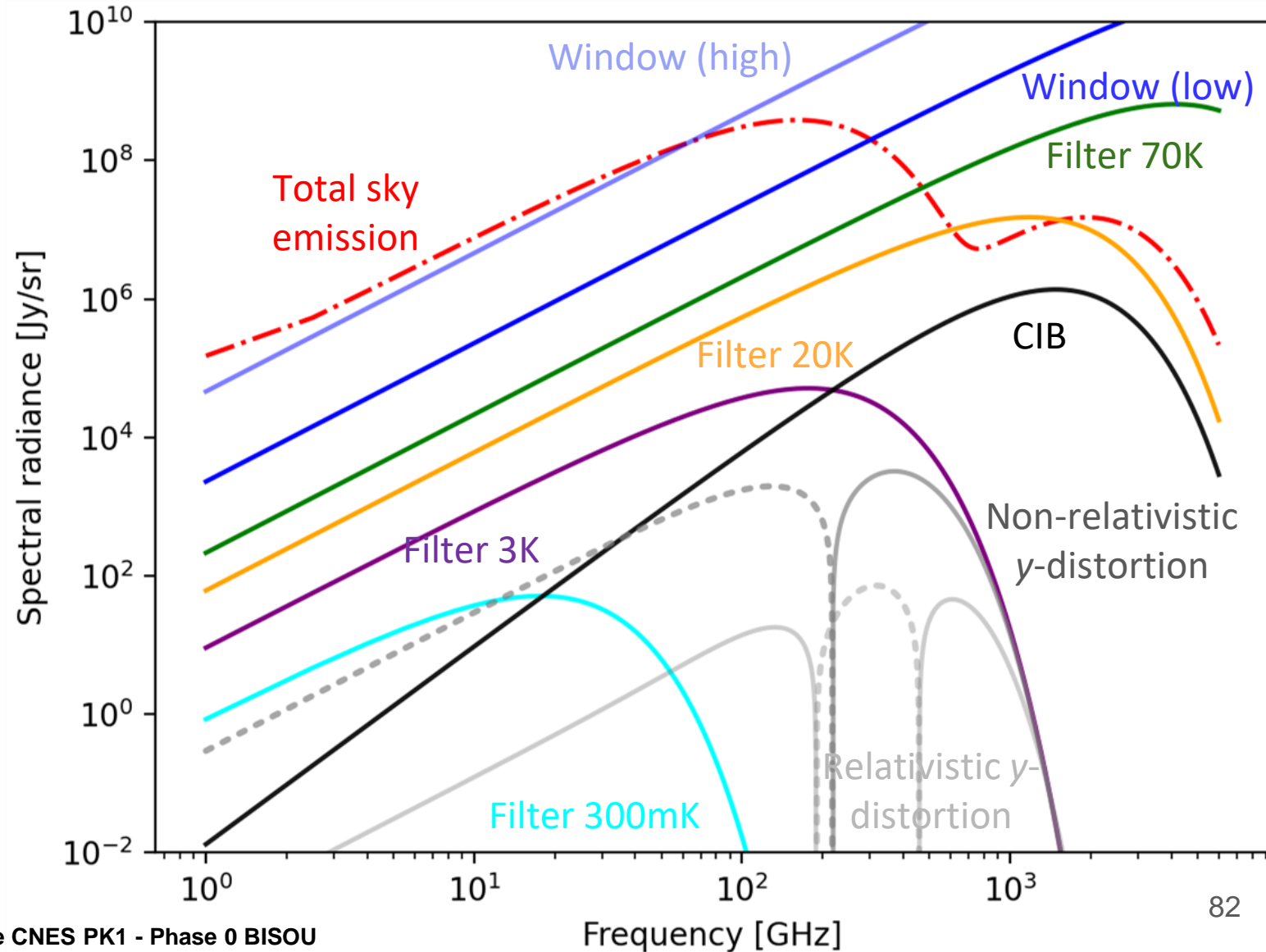
Sub-K cooler

Instrument concept - IDM model



Science Goals: Modeling the instrument

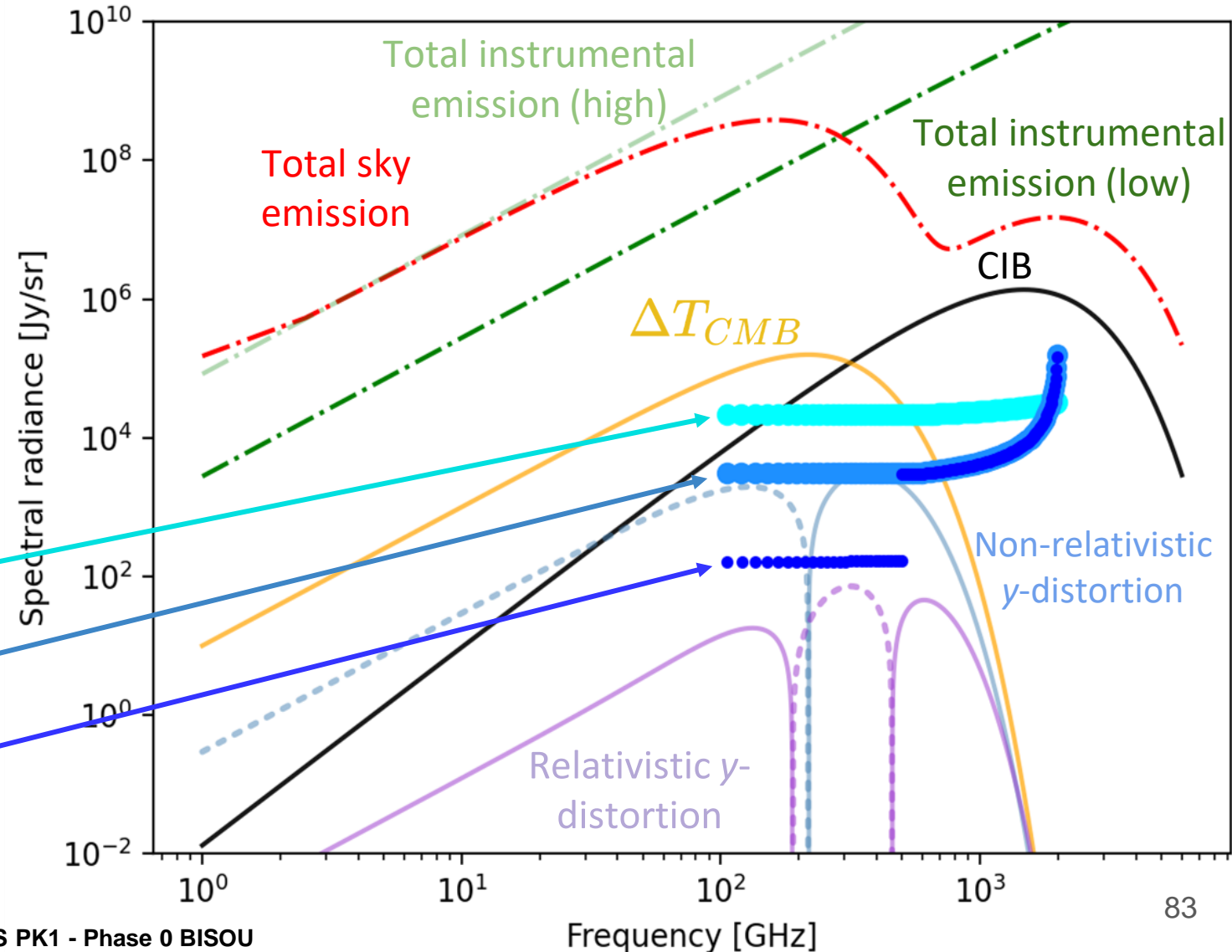
- 1 window:
 - Temperature 270K
- 4 filters:
 - Temperature 70, 20, 3K, and 300mK
 - Emissivity
 - High ~ 1%
 - Low ~ 0.1%
- Option: dichroic



Science Goals: Sensitivity



- Frequency range 90GHz - 2THz
- 5 days flight
- 75% observing time
- **No atmosphere**
- 1 window (@270K)
- 4 filters (@70, 20, 3K, 300mK) & emissivity 0.1%
- **1 detector**
 - High emissivity window + tapered filtering from 600GHz
 - Low emissivity window
 - Low emissivity window + dichroic at 500GHz



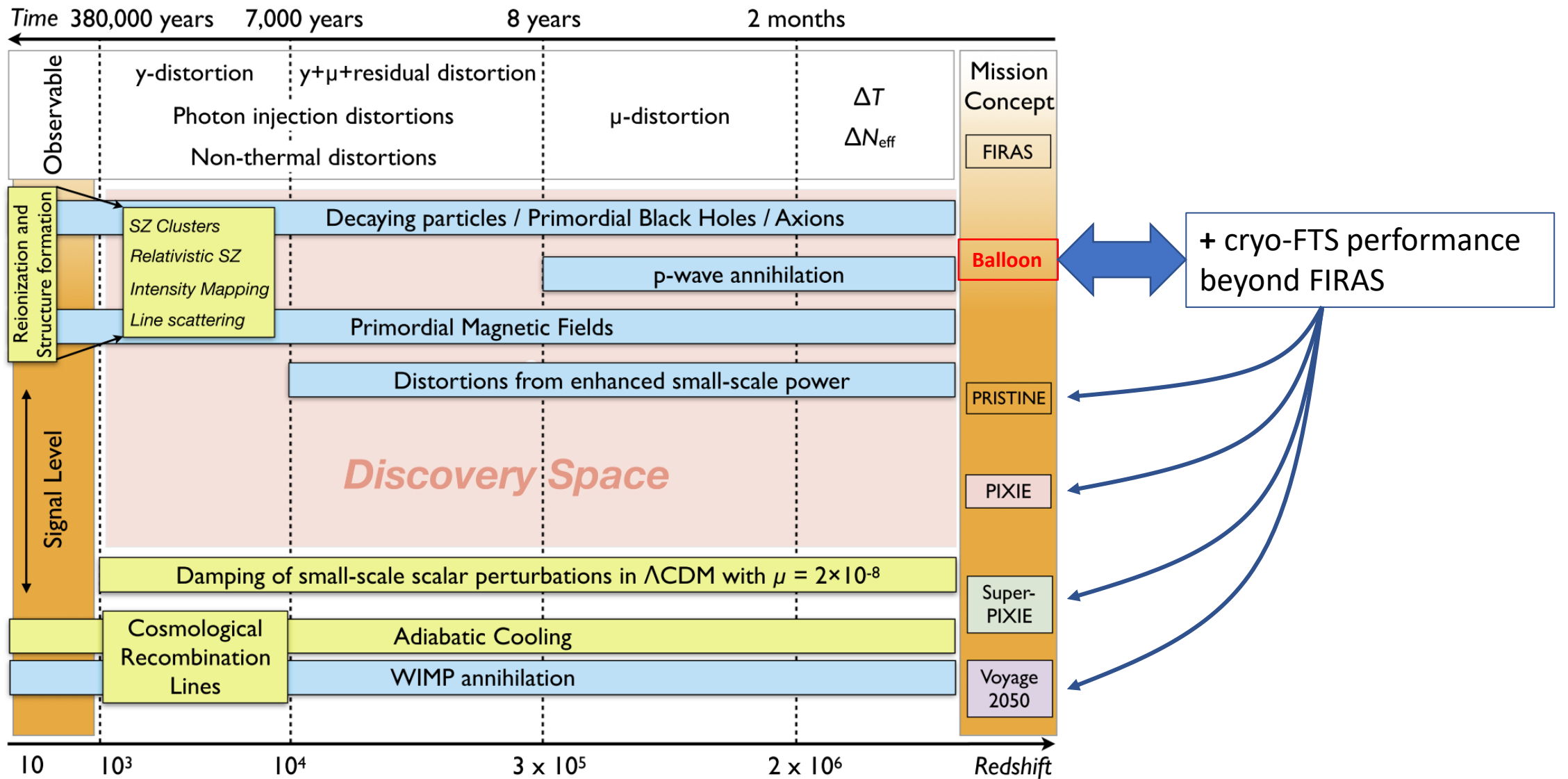


Fig. 11 Science thresholds and mission concepts of increasing sensitivity. Guaranteed sources of distortions and their expected signal levels are shown in yellow), while non-standard processes with possible signal levels are presented in turquoise. Spectral distortions could open a new window to the pre-recombination Universe with a vast *discovery space* to new physics that is accessible on the path towards a detection and characterization of the μ -distortion from the dissipation of small-scale acoustic modes set by inflation and the cosmological recombination radiation

Conclusions

- CMB research is expanding towards large and global experiments, with very high discovery potential
- Stratospheric balloons offer a great deal of opportunities for CMB research, covering the high-frequency range of CMB measurements and dust-related polarized foregrounds.
- Balloon-borne **Stokes Polarimeters will produce essential polarization data (large scales, high frequencies) and** represent very useful pathfinders for the measurement solutions of LiteBIRD:
 - Polarization Modulator Unit (rotation and optical performance)
 - Detectors in close to representative environment
- Balloon-borne **spectrometers** (differential and absolute) represent a way to investigate LIM and spectral distortions, opening new windows on the early universe, and paving the way to dedicated satellite missions.